

## ABSTRACT

Title of Document: MULTI-DIGIT MANIPULATION OF  
A CIRCULAR OBJECT

Junfeng Huang, Doctor of Philosophy, 2012

Directed By: Associate Professor, Jae Kun Shim  
Department of Kinesiology

Multi-digit prehension tasks are commonly encountered in our daily activities. Previous studies investigated behavioral characteristics and neuromuscular mechanisms during manipulation actions. The purpose of this dissertation is to investigate hand-digit control and coordination during multi-digit circular object manipulation. In particular, the dissertation focuses on peak torque, force distribution, safety margin, force regularity, and multi-digit synergy in static and dynamic manipulation. In a series of experiments, subjects grasped a customized circular handle with a precision grip, i.e. without palm contact, and performed isometric maximum/submaximal, or repetitive torque production tasks under visual feedback. The factors studied include wrist position, torque direction, and initial grasping force level in the static tasks, movement frequency and moment of inertia in the dynamic task. The findings are: (1) in the maximum voluntary contraction task, it was found that peak torque in the counterclockwise direction was greater than the clockwise direction; (2) in submaximal tasks, a large initial grasping force slowed down the subsequent torque producing process and resulted in a large safety margin; the thumb and ulnar fingers (ring and little finger) generated more torque in the clockwise direction, while radial fingers (index and middle finger) produced more torque in the counterclockwise direction; the modulation gain between normal

force and tangential force was larger in the torque increase direction than in the torque decrease direction; (3) in the repetitive dynamic task, the modulation gain increased with movement frequency and moment of inertia; within-cycle and between-cycle force regularity increased with moment of inertia, but was not affected by movement frequency; multi-digit synergy was found in the isometric task, but not in the repetitive dynamic task. In summary, this dissertation provides experiment evidence that in manipulation of circular objects, various task constraints have characteristic influence on motor output in task-specific manner, which can be understood from the perspectives of biomechanics and anatomy.

MULTI-DIGIT MANIPULATION OF A CIRCULAR OBJECT

By

Junfeng Huang

Dissertation submitted to the Faculty of the Graduate School of the  
University of Maryland, College Park, in partial fulfillment  
of the requirements for the degree of  
Doctor of Philosophy  
2012

Advisory Committee:

Professor Jae Kun Shim, Chair  
Professor John Jeka  
Professor Adam Hsieh  
Professor Avis Cohen  
Dr. Mark Hallett

© Copyright by  
Junfeng Huang  
2012

# TABLE OF CONTENTS

TABLE OF CONTENTS.....	ii
LIST OF FIGURES.....	v
Chapter 1 Introduction .....	1
1.1 Problem statement.....	1
1.2 Study objective.....	3
1.3 Dissertation organization.....	11
Chapter 2 Literature review.....	13
2.1 Constraints in multi-finger prehension .....	14
2.1.1 Extrinsic and intrinsic object properties .....	14
2.1.2 Physical constraints and task constraints.....	16
2.1.3 Grip force-load force coupling.....	17
2.1.4 Individuated digit movement and muscle synergy .....	20
2.2 Coordination patterns in multi-digit tasks .....	23
2.2.1 Finger enslaving effect.....	23
2.2.2 Uncontrolled manifold hypothesis.....	25
2.2.3 Multi-digit synergy .....	28
2.2.4 Computational models of multi-digit synergy .....	33
2.3 Manipulation of circular objects .....	36
Chapter 3 Multi-digit maximal torque production task on a circular object .....	38
3.1 Introduction .....	39
3.2 Methods.....	40
3.2.1 Subjects .....	40
3.2.2 Equipment.....	41
3.2.3 Procedure.....	42
3.2.4 Data Processing .....	45
3.2.5 Statistics.....	47
3.3 Results.....	48
3.3.1 Digit normal forces .....	48
3.3.2 Individual digit tangential forces and their moments.....	49
3.3.3 Internal and Resultant forces.....	50

3.3.4 Safety margins of normal forces and force angles.....	51
3.4. Discussion.....	53
3.4.1 Sharing of normal forces and moments of tangential forces .....	53
3.4.2 Total moments in opening and closing directions .....	54
3.4.3 Internal force and safety margin .....	55
3.5. Conclusion .....	56
Chapter 4 Multi-digit submaximal torque production task on a circular object .....	57
4.1 Introduction .....	59
4.2 Methods.....	61
4.2.1 Subjects .....	61
4.2.2 Apparatus.....	61
4.2.3 Procedure .....	62
4.2.4 Data Processing .....	65
4.2.5 Statistical analysis.....	66
4.3 Results.....	67
4.3.1 Total and individual digit normal forces .....	68
4.3.2 Total and individual digit tangential forces .....	69
4.3.3 Safety margin during torque production.....	71
4.4 Discussion.....	73
4.4.1 Grasping force alone and while rotating.....	73
4.4.2 Directional preference of individual digits .....	75
4.4.3 Effect of initial normal force on safety margin .....	76
4.5 Conclusion.....	77
Chapter 5 Multi-digit synergy in static manipulative task on a circular object .....	79
5.1 Introduction .....	80
5.2 Methods.....	82
5.2.1 Subjects .....	82
5.2.2 Apparatus.....	82
5.2.3 Procedure .....	83
5.2.4 Data processing .....	85
5.2.5 Statistical analysis.....	88
5.3 Results.....	89
5.3.1 Total normal force and total tangential force .....	89
5.3.2 Constant error of tangential force .....	91

5.3.3 Tangential force variance in UCM and ORT spaces .....	92
5.3.4 The relations of time variables .....	95
5.4 Discussion.....	96
5.4.1 Modulation of the direction of tangential force change .....	97
5.4.2 Multi-digit synergy .....	98
5.4.3 Force error in accurate torque production .....	100
5.5 Conclusion.....	100
Chapter 6 Multi-digit coordination in a repetitive rotating task on a circular object .....	101
6.1 Introduction .....	102
6.2 Methods.....	104
6.2.1 Subjects .....	104
6.2.2 Equipment .....	104
6.2.3 Procedure .....	106
6.2.4 Data processing .....	107
6.2.5 Statistical analysis .....	111
6.3 Results.....	111
6.3.1 The relationship between handle angle, normal and tangential force .....	112
6.3.2 Force hysteresis of normal and tangential force .....	114
6.3.3 Approximate entropy of normal and tangential force .....	116
6.3.4 Force variability in UCM and ORT space.....	117
6.4 Discussion.....	119
6.4.1 The effect of movement frequency on modulation of normal and tangential force in a cyclic movement .....	120
6.4.2 Force-angle relationship .....	121
6.4.3 The dependence of multi-digit synergy on frequency.....	122
6.5 Conclusion.....	123
Chapter 7 Conclusion.....	124
7.1 Summary .....	124
7.2 Future research.....	125
Bibliography .....	127

## LIST OF FIGURES

Figure 2-1 Illustration of (a) power grasp and (b) precision grasp. ....	13
Figure 2-2 Time profiles of grip force and load force. The task was to lift an instrumented object off the table, hold it for a while, and replace it back. Grip/load force ratio is always higher than the critical value, determined by smoothness of a material, i.e. smooth material has larger slip ratio, and requires greater grip force, as compared to rough material. The bottom are typical firing patterns of four kinds of mechanoreceptors. Adapted from (Johansson and Cole 1994) .....	19
Figure 2-3 (a) Musculoskeletal structure of a finger and the biomechanical outcome of some major muscles (adopted from Netter’s anatomy); (b) deep muscles of the hand and wrist (anterior view, flexor digitorum profundus is painted blue), adapted from Grey’s anatomy. .	22
Figure 2-4 Illustration for uncontrolled manifold hypothesis: (a) constant total force task; (b) torque cancellation task, assuming moment arm $r_1$ equals moment arm $r_2$ .....	26
Figure 2-5 A typical time profile of delta variance (DV) in a ramp-up, hold, then ramp-down task. Total force is shown in black on top of a force plate. It takes a few hundred milliseconds for DV to become positive after force starts to increase; however, the difference between the onset of force decrease and the moment DV becomes negative is very small. Adapted from (Shim, Olafsdottir et al. 2005) .....	30
Figure 3-1 Schematic illustration of an aluminum handle (black circle with a large hollow inside) and six-component sensors (white rectangles) at digit contacts.....	42
Figure 3-2 Schematic top view of a subject posture during maximum moment production about antero-posterior (AP) or medio-lateral (ML) axes in opening (OP) and closing (CL) directions. A customized plastic wrist-forearm brace with two sets of Velcro straps were used to secure the forearm. The handle was mounted on top of a heavy tripod which is not shown in the figure.....	43
Figure 3-3 Detailed schematic illustration of the little finger producing a force at a contact. $O_G$ : origin of the global reference system of coordinates (GRS), X: X-axis in GRS, Y: Y-axis in GRS (Z-axis is not shown in the figures, but its positive direction follows the right-handed coordinate system and its positive direction is from paper to the reader), $O_L$ : origin of local reference system of coordinates (LRS) of the little finger sensor, $x_i$ : x-axis in LRS of little finger sensor, $y_i$ : y-axis in LRS of the little finger sensor, $m_z^l$ : moment about z-axis in LRS of little finger sensor (z-axis in LRS for each sensor is parallel to Z-axes in GRS), $F^l$ : little finger force, $F_n^l$ : little finger normal force, $F_t^l$ : little finger tangential force, $F_{\mu,n}^l$ : required normal force to avoid slipping of little finger with $F_t^l$ and friction coefficient ( $\mu =1.5$ ) of the contact surface, $F_s^l$ : safety margin of normal force ( $F_n^l - F_{\mu,n}^l$ ), $d_o^l$ : position of LRS origin in GRS, $r_o^l$ : position of little finger center of pressure (CoP) in GRS, $\theta_o^l$ : angular position of $d_o^l$ in GRS. $\alpha^l$ : angle between $F_t^l$ and $F^l$ , $\alpha_\mu^l$ : angle between $F_t^l$ and $F_\mu^l$ , and $\alpha_s^l$ : safety margin of angle ( $\alpha^l - \alpha_\mu^l$ ) for little finger force. The LRS origin ( $O_L$ ) was fixed to the center of the contact surface of the sensor and a cap (shown gray) was fixed on the sensor surface. The distance between the apex of the cap and $O_L$ was $\sim 0.81$ mm.....	44



Figure 3-4 (a) Individual digit normal forces and (b) sharing at the time of maximum resultant moment about antero-posterior (AP) and medio-lateral (ML) axes in opening (OP) and closing (CL) directions. T, I, M, R, and L, respectively, represent thumb, index, middle, ring, and little fingers. Mean±S.E. across subjects are presented. ....48

Figure 3-5 (a) Moments of individual digit tangential forces and (b) their sharing at the time of maximum resultant moment about antero-posterior (AP) and medio-lateral (ML) axes in opening (OP) and closing (CL) directions. T, I, M, R, and L, respectively, represent thumb, index, middle, ring, and little fingers. Mean±S.E. across subjects are presented. ....49

Figure 3-6 (a) Internal force and (b) resultant force at the maximum moment production in opening (OP) and closing (CL) tasks about the antero-posterior (AP) and medio-lateral (ML) axes. Mean±S.E. across subjects are reported for each task condition. ....50

Figure 3-7 Safety margins of individual finger normal forces and force angles about the antero-posterior (AP) and medio-lateral (ML) axes in opening (OP) and closing (CL) tasks. The normal and tangential forces are shown as horizontal and vertical arrow, respectively. The mean and S.E. values of the safety margin of normal force and force angle across all subjects are shown next to each force vector diagram for each digit in each task condition. The mean and S.E. values of the safety margin of normal force are respectively shown as the length and thickness of a solid arrow while the mean and S.E. values of safety margins of force angle are respectively shown as the angles and their thickness. ....52

Figure 4-1 (a) The grasp plane including the circular handle and five digit tips viewed from the subject side. The thick black circle was the circular handle, and the dotted one represented the circular contour after mounting sensors. Global reference frame was defined as X: pointing to the right side of subjects; Y: upward; Z: pointing towards palm. (b) subject watched the visual feedback in a computer monitor during *Submaximal* task. The torque template was comprised of three segments, i.e. GRASP: no torque (subjects adjusted the normal/grasping force); RAMP: increase torque linearly; HOLD: keep the torque constant at 20%. ....63

Figure 4-2 An example of labeling notion in this study. Global and local reference systems ( $O_G$  and  $O_L$ ) were represented by capital letters and lowercase letters, respectively.  $r$  is the radius of the circular contour (4.5cm) and  $d$  is the distance from the center of the handle to the center of top surface of one sensor (about 4.3cm). Grey area is the spherical rubber cap.  $F_n^L$ ,  $F_t^L$ ,  $F^L$ ,  $F_{SP}^L$ ,  $F_\mu^L$ ,  $F_{SM}^L$  represent normal force, tangential force, total force, minimal normal force, critical total force and safety margin of the little finger, respectively. ....64

Figure 4-3 Time profiles of (a) total normal forces and (b) tangential forces from a representative subject in the ML/CCW condition. The subjects reached a certain normal force level first (GRASP phase: left), then controlled the torque/tangential force by following the template (RAMP and HOLD phase, right). All forces were normalized by  $F^{\max}$  and  $T^{\max}$ , respectively. ....67

Figure 4-4 Total normal force in (a) MVT task and (b) HOLD phase in sub-MAX task. ....68

Figure 4-5 Normal force sharing by individual digits in the HOLD phase. Each digit was shown in the angular position it occupied during the experiment. Filled circles were averaged values in CCW conditions while empty ones were from CW conditions. ....69

Figure 4-6 Maximum tangential force under different conditions of *Axis* and *Direction*. ....70

Figure 4-7 Tangential forces of individual digits in the GRASP phase. Different initial conditions are shown along the circumference of the contours. ....70

Figure 4-8 Tangential force sharing by individual digits in the HOLD phase. Each digit is shown in the angular position it occupied during the experiment. Filled circles are averaged values in CCW conditions while empty ones are from CW conditions. ....71

Figure 4-9 Time profiles of safety margins from a representative subject. Note that safety margin in the 0% trial had large oscillation around  $t = 4s$  due to adjustment upon initial contact. Therefore, no fitting was performed for this condition. ....72

Figure 4-10 (a) Safety margin in the HOLD phase; (b) decay coefficient  $b$  of safety margin during RAMP phase. ....73

Figure 5-1 The schematic diagram of the handle. Global reference frame is defined as X: pointing to the right side of subjects; Y: upward; Z: pointing towards subjects. (a) The plane shown here is referred to as “grasp plane” in this study. (b) Subject watch the visual feedback while manipulating the handle on the ir right hands. ....84

Figure 5-2 Samples of torque profile. Blue line and black solid line was the template and the actual torque from a trial in CW-CCW condition; while red line and black dash line was from a trial in CCW-CW condition. The four phases labeled were for CW-CCW condition (blue) based on  $t_0$ .  $t_1$  and  $t_2$  indicated the initiation and the termination of the transition phase. ....85

Figure 5-3 An example of labeling notion in this study. Lowercase letters indicate variables in local reference frame, and capital letters indicate variables in global reference frame.  $r$  is the radius of the circular contour (4.5cm) and  $d$  is the distance from the center of the handle to the center of top surface of any sensor (about 4.3cm).  $j$  represents a specific digit, L for little finger.  $F_n^L$ ,  $F_t^L$ ,  $F^L$ ,  $F_{SP}^L$ ,  $F_{\mu}^L$ ,  $F_{SM}^L$  represents normal force, tangential force, total force, critical normal force, critical total force and safety margin of the little finger, respectively. .86

Figure 5-4 Tangential force (solid line) and normal force (dashed line) from a typical subject in 12 trials when the wrist was in ML position (left) and in AP position (right). The initial torque direction is CW for the top two panels and CCW for the bottom two panels. Shaded areas represent one standard error. Transitions occurred between 4~10s. ....90

Figure 5-5 Linear regressions for decreasing and increasing phases. (a) Demonstration of normal force vs. tangential force in two trials with opposite initial directions. The solid line represents the CCW-CW condition, and the dotted line represents the CW-CCW condition. Black arrows represent the decreasing phases, and white arrows represent the increasing phases; (b) the ratio of normal force vs. tangential force (significance level was set at 0.05 for \*, 0.01 for \*\*). ....91

Figure 5-6 One-second time window average of CE during S1, S2, and  $t_0$ . Paired  $t$ -test results within each *Axis x Direction* condition are also shown. ....92

Figure 5-7 Variance in ORT (top) and UCM (bottom) subspace. One-second window averages are drawn from one second before to one second after the transition phase, i.e. [3~11s]. The two conditions from the same wrist position are shown together. ....93

Figure 5-8 Delta variance from a representative subject in ML/CCW-CW condition. Mean and one SD of tangential force from the 12 trials were shown on the secondary axis. ....94

Figure 5-9 Delta variance at S1,  $t_0$ , and S2 as well as minimum DV. ....95

Figure 5-10 Temporal relationship of CEmax and DVmin with respect to  $t_0$ . A positive value means an earlier occurrence, and a negative value means a later occurrence. ....96

Figure 6-1 Schematic view of the handle. Global reference frame is defined as X: pointing to the right side of subjects; Y: upward; Z: pointing towards the palm. The plane shown here is

called “grasp plane” in this study. (b) subject rotated the handle on their right hands under auditory signal paced by a metronome. Each beep was accompanied by a 45 ° deviation of the wrist to radial or ulnar direction. (c) the structure of the handle, the beam and two masses. 105

Figure 6-2 An example of labeling notion in this study. Lowercase letters indicate variables in local reference frame, and capital letters indicate variables in global reference frame.  $r$  is the radius of the circular contour (4.5cm) and  $d$  is the distance from the center of the handle to the center of top surface of any sensor (about 4.3cm).  $j$  represents a specific digit, L for little finger.  $F_n^L, F_t^L, F^L, F_{SP}^L, F_\mu^L, F_{SM}^L$  represents normal force, tangential force, total force, critical normal force, critical total force and safety margin of the little finger, respectively. 108

Figure 6-3 A section of angle, total tangential force, and total normal force from a representative subject. The task frequency was 120bpm (1Hz). The circles in the top figure showed the end positions of the oscillation movement. Their timing was used to slice the tangential force and normal force into epochs, as shown by the dashed vertical lines in the lower two figures. ... 109

Figure 6-4 (a) Normal force and (b) tangential force over time averaged across subjects ( $Freq: 0.5Hz, MOI: 7$ ). The time profile of handle angle was superposed on each figure as dashed lines and labeled on the right. .... 112

Figure 6-5 (a) maximal normal forces, (b) maximal tangential forces, (c) slopes, and (d) intercepts of linear regression versus MOI at three frequencies. The standard deviations were too small compared to the force magnitude and thereby omitted. .... 113

Figure 6-6 (a) Normal force and (b) tangential force versus handle angle averaged across subjects (the same condition as in Figure 6-4, only the averaged trajectories are shown). Red arrows indicate the direction of  $F_n$  and  $F_t$  in a cycle. A and B are the minima of  $F_n$  in the direction of PRO-SUP and SUP-PRO respectively. .... 114

Figure 6-7 Hysteresis of normal force (a) and tangential force (b) versus MOI, normalized hysteresis of normal force (c) and tangential force (d). Regression lines are shown for three frequencies with equations and goodness of fit. The rest of the chapter will use the same pattern to present the results. .... 115

Figure 6-8 Approximate entropy (ApEn) of (a) total normal force and (b) total tangential force versus MOI. .... 117

Figure 6-9 The variability of normal and tangential force in UCM and ORT space. The values were normalized by  $(F_n^{\max})^2$  and  $(F_t^{\max})^2$ , followed by a natural logarithm. Note that the actual variances were smaller than 1 after normalization, therefore were negative on the ordinate. .... 118

Figure 6-10 Delta variance for normal force (a) and tangential force (b). .... 119

# Chapter 1

## Introduction

### 1.1 Problem statement

Human hand is a complex apparatus we use every day to explore and interact with external physical world. Dexterous hands make human distinct from other primates. Although some species of primates have the ability to perform some basic manipulation tasks, such as pinching with thumb and long finger and using simple tools (Pouydebat, Gorce et al. 2009), the overall dexterity of their hands is by no means comparable to that of human hands. The difference seems to be contributed by, at least partially, greater independency among fingers or more dissociation of the thumb and fingers<sup>1</sup> in humans (Hager-Ross and Schieber 2000; Reilly and Hammond 2000; Schieber 1991). Anatomically, there are around 30 degrees of freedom (DOFs) in the unilateral hand and forearm musculoskeletal system, which provide sufficient flexibility and stability for various object manipulation actions. Meanwhile the extra DOFs also create the “notorious” motor redundancy problem for the control and coordination of hand and finger movements (Bernstein 1967; d'Avella, Saltiel et al. 2003; Latash, Scholz et al. 2002; Santello and Soechting 2000; Shim, Latash et al. 2005). For example, when holding an object still in the air with the thumb and index finger, there are totally 12 force and torque<sup>2</sup> components (3 forces and 3 free torques from each digit) to be controlled by the central nervous system while only 6 equilibrium equations (3 translational, 3 rotational) are mechanically necessitated. Similarly, when pointing to an arbitrary point in the space (three spatial coordinate components), a serial chain of 6 joints and 12 DOFs,

---

<sup>1</sup> In this dissertation, the definition of “finger” is referred as the second to fifth finger, i.e. index, middle, ring, and little finger; while the definition of “digit” includes the thumb and four fingers.

<sup>2</sup> Torque is defined as the vector product of the displacement from the point of application of force to rotation axis, and force vector. In some literature, it is termed as moment of force, or moment. Torque is adopted in this dissertation to avoid confusion with some other concepts, like moment of inertia.

along finger, wrist, elbow, and shoulder, allows a solution chosen from a vast repertoire of movement candidates. On the other hand, it has been found that some DOFs are not completely independent. For example, flexion of proximal interphalangeal joint (PIP) also causes flexion of distal interphalangeal joint (DIP) (Ingram, Kording et al. 2008). Motion or exertion of force by one finger brings motion or exertion of force by neighboring fingers (Hager-Ross and Schieber 2000; Zatsiorsky, Li et al. 1998). Moreover, the involuntary movement can be seen in the fingers in the non-task hand (Addamo, Farrow et al. 2007; Shim, Karol et al. 2008). The phenomenon, termed as motor overflow, is absent or particular weak in patients without corpus callosum when performing arm movements (Sternad, Wei et al. 2007). And patients with focal hand dystonia have higher contralateral and ipsilateral overflow scores than normal population (Sitburana, Wu et al. 2009). Therefore, the coupling is speculated to rise from both central and peripheral constraints (Schieber and Santello 2004).

Many researchers have investigated multi-digit coordination during manipulation of objects of various geometry shapes, such as rectangular, trapezoidal, cylindrical, and spherical objects (Gentilucci, Caselli et al. 2003; Hore, Watts et al. 2001; Kleinholdermann, Brenner et al. 2007; Seo and Armstrong 2008; Shim, Latash et al. 2004). Objects of a specific geometry shape, i.e. circular objects, have received relatively less attention (Kinoshita, Murase et al. 1996), although they are commonly encountered both in daily activities, e.g. opening jar lids, opening door knobs, adjusting audio volume, and in industry jobs, e.g. feeding raw materials for machining, or rotating valves. In these tasks, it is required to produce either maximum or precise rotating torque while maintaining enough grip force to ensure stable grasping. A distinctive feature of circular grasp is that mechanical outcomes of normal force and tangential force<sup>3</sup> are decoupled, i.e. stabilizing the

---

<sup>3</sup> Three force components are defined for circular object manipulation in this dissertation. Longitudinal tangential force acts against gravity of the object, normal force/grasping force/grip force is radial force for grasping the object, and tangential force/load force produces the torque in the tasks. Sometimes tangential

grasp action and rotating the object, respectively. In contrast, in rectangular object manipulation, torque is comprised of two components: torque by normal forces and torque by tangential forces (Latash, Shim et al. 2004). Previous studies on objects of circular shape or curvature focused on force components in translational movement only, i.e. grip force and load force in vertical direction (Baud-Bovy and Soechting 2002). It is not yet clear how individual digit normal forces and tangential forces might differ in rotational movement.

Oscillatory rotational action, as often seen in screwdriver usage, requires continuous regulation of magnitudes, direction, application points, and timing of individual digit forces in synchronous with movement phase. Previous studies suggested that rhythm movements involve a central mechanism that is different from discrete movements (Hogan and Sternad 2007). There exist abundant literature on cyclic finger tapping, abduction/adduction, pressing and wrist flexion/extension tasks (Aoki, Francis et al. 2003; Friedman, Skm et al. 2009; Schoner and Kelso 1988). In these tasks, change in task frequency will lead to distinctive system behavior. For example, in bimanual abduction/adduction task, movement pattern of index fingers changes from anti-phase to in-phase with increasing frequency (Schoner and Kelso 1988). Whether changing movement frequency will result in different coordination strategy in multi-digit circular object manipulation is investigated in this dissertation.

## **1.2 Study objective**

The goal of this dissertation is to investigate the control and coordination adopted by the central nervous system during multi-digit manipulation of a circular object (mechanically fixed or free) as a function of neuromechanical constraints. Manipulation of circular objects, such as turning

---

force and torque is interchangeable because their linear relationship due to the circular geometry shape (torque is tangential force multiplied by the radius of the handle in global reference system).

doorknobs and opening jar lids, comprises an important portion of human daily activities. Yet few studies have examined the characteristics of hand and digits in such fine-motor manipulative motor tasks. This dissertation systematically studies kinetic aspects of circular object manipulation by utilizing a customized handle and miniature force/torque sensors. Paradigms are developed to test specific hypotheses on neuromechanical constraints of hand digit control in circular object manipulation.

---

**SPECIFIC AIM 1: To characterize the effects of wrist position and torque direction on peak torque and individual digit contribution during isometric maximum voluntary torque (MVT) production on a circular object.**

Anatomical constraints on multi-digit manipulation involve different groups of joints, muscles and tendons. Extrinsic muscles, including some multi-articulate multi-tendon muscles, are muscles in the forearm and cross the wrist to produce simultaneous movements of wrist and digits in sagittal plane and/or frontal plane. Intrinsic muscles are the ones inside the hand and act on individual digits only. Changes in wrist position result in reconfiguration of carpal complex and modification of moment arms of extrinsic muscles. And rotating an object in different torque direction involves separate extrinsic/intrinsic muscle groups, e.g. palmar interossei for finger adduction and dorsal interossei for finger abduction. Therefore wrist position and torque direction are speculated to affect maximal capability of torque production of each digit as well as the hand as a whole. A previous study showed that grasping force contribution by individual fingers varied in flexion/extension and ulnar/radial deviation in a forceful grip (Li 2002). It is not known how sharing of torque by individual digits will be affected by wrist position as well as torque direction. Specific aim 1 of this dissertation is to investigate the effects of wrist position and torque direction on maximum torque production and torque sharing pattern.

**Hypothesis 1.1: The maximum voluntary torque in counterclockwise direction is greater than in clockwise direction.**

It has been shown that in neutral position, the wrist can produce larger torque in supination direction than in pronation direction (Kapandji 2001). As compared to power grasp in those studies, it is assumed that the difference in peak torque production ability will be more prominent in five-digit circular precision grasp due to the reduced ability of thumb to produce torque in pronation direction.

**Hypothesis 1.2: Torque sharing pattern by individual digits during multi-digit maximum voluntary torque production about anterior-posterior axis (pronation/supination) is different from medial-lateral axis (radial/ulnar deviation).**

Extrinsic and intrinsic muscles are differentially activated at the two wrist positions. Furthermore, tendon excursions due to wrist flexion/extension are also different (Li, Zatsiorsky et al. 2000). It is expected that different wrist positions will result in changed contribution by individual digits to the total maximum torque.

**Hypothesis 1.3: Torque contributions by individual digits during maximum voluntary torque production on a circular object follow the anatomical order from radial to ulnar digits.**

In grasping tasks, the strength of radial fingers is greater than that of ulnar fingers (Freund, Toivonen et al. 2002). And the thumb contributes about half of grasping force in prismatic grasp in order to act against the combined force of the other four fingers (Zatsiorsky, Gregory et al. 2002). It is hypothesized that the same anatomical order from radial to ulnar digits will be present for tangential force contribution during maximum torque production task on a circular object.



---

**SPECIFIC AIM 2: To determine safety margin during submaximal torque production task.**

Safety margin is the extra grasping force that prevents objects from slipping off hands during grasping (Johansson and Cole 1994). In accurate grasping action, safety margin is essential for individual digits to prevent fingertip sliding along contact surface. Safety margin is related to the stability of grasping action and it depends on both physical friction on contact surface and other factors. For example, anxiety and fear will both generate unnecessary grasping force and excessive safety margin, which might break crispy objects and result in hand fatigue or even injury. In contrast, careless manipulation or unexpected sudden load increase can accompany negative safety margin, i.e. grasping force insufficient to get hold of the object. This problem is particularly important in industry safety procedure. Therefore many researchers examined how safety margin is effected by human factors, e.g. grasp postures and hand size (Seo 2009), and working environment, e.g. workbench height and physical work demands.

Previous studies on precision grip have shown that there is a strong coupling between grip force and load force (Baud-Bovy and Soechting 2002; Burstedt, Flanagan et al. 1999; Johansson and Cole 1994; Westling and Johansson 1984). In those tasks, subjects grasped instrumented objects with thumb and one/two fingers and produced load force to lift up, hold, and replace it back. Safety margin was kept at a level relatively constant and well above zero. However, it is not yet known how grip force relates to tangential force, the function of which is rotating an object. For example, when a person grasps a glass of water and tilts it to drink, accurate magnitude and timing control of the net torque on the glass is required in order to mediate appropriate angular speed as well as to stop at a comfortable position for drinking. It has been speculated that grasping force before initiation of torque production will alter dynamics of the process because of the increased joint stiffness in metacarpophalangeal (MCP) joints (Werner, Kozin et al. 2003).

For the same reason as in maximum voluntary torque experiment, wrist position and torque direction is expected to affect the relation between normal force and tangential force, and consequently, safety margin. Specific aim 2 of this dissertation is to investigate the safety margin in submaximal torque production tasks.

**Hypothesis 2.1: Wrist position and torque direction affect the force sharing patterns of normal forces and tangential forces of individual digits.**

Wrist positions result in different muscle lengths and tendon excursions. Active or passive force or both might be affected by varying wrist positions. The effect of torque direction has been verified in maximum torque production task. It is expected that the force sharing patterns of normal forces and tangential forces of individual digits are affected by wrist position and torque direction.

**Hypothesis 2.2: The initial grasping force level affects the dynamic process during the transition and the final safety margin in the hold phase.**

For effective manipulation, a certain amount of grasping force is often required to hold the object steadily. This initial grasping force leads to alteration of the biomechanical properties of joints and muscles (Sancho-Bru, Perez-Gonzalez et al. 2003), as well as the coordination of both grasping forces and tangential forces of individual digits (Niu, Latash et al. 2009). It is therefore hypothesized that changing initial grasping force level will modify the dynamic process during the transition and result in a different safety margin in the constant torque production phase.

---

**SPECIFIC AIM 3: To characterize multi-digit coordination during STATIC submaximal torque production task.**

To investigate the problem of “motor redundancy”, experimental and theoretical frameworks have been built based on the concept of motor synergy (reviewed in Latash 2008). According to the notion of synergy, it is assumed that “the neural controller organizes variables produced by elements of a system in a task-specific way that reduces variability of certain potential important variables” (Latash and Zatsiorsky 2009). Previous studies have shown that motor synergies are observed in standing, locomotion, speech, and skiing (Balasubramaniam, Riley et al. 2000; Gracco and Abbs 1986; Vereijken, Whiting et al. 1992; Winter 1989). An analytical method, called uncontrolled manifold (UCM) analysis, has been created to dissociate the trial-by-trial variability in the motor system into two parts, one related to the task goal and the other unrelated (Scholz, Danion et al. 2002). It is hypothesized that the central controller compresses the variability in the space related to the task goal, while allows sufficient variability in the unrelated space to explore abundant DOFs (see Literature Review for details).

Two multi-digit kinetic synergies have been identified in four-finger pressing tasks and prismatic grasp tasks, i.e. force stabilizing synergy and torque stabilizing synergy (Li, Latash et al. 1998; Santello and Soechting 2000; Shim, Latash 2005; Shim, Latash et al. 2004). However, circular grasp differs from prismatic grasp in that torque in prismatic grasp is the sum of torques by both normal force and tangential force, while torque in circular grasp is produced by tangential force only. It is currently unknown if either synergy will exist in multi-digit circular object manipulation. If it does, how does it change with the direction of torque change? Specific aim 3 of this dissertation is to identify multi-digit synergy on circular object manipulation in a submaximal torque production task.

**Hypothesis 3: Torque-stabilizing synergy disappears when torque decreases and reappears when torque increases again.**

In a five-digit pressing task, positive covariation between digit forces occurred within 600 ms after the onset of decreasing phase while negative covariation appeared about 600-800 ms after the onset of increasing phase (Shim, Olafsdottir 2005). Therefore, the authors suggested that the central controller takes a fixed time to construct or destroy a force-stabilizing synergy. For submaximal torque production task, it is expected that a torque-stabilizing synergy will disappear when torque decreases and reappear when torque increases again. The latencies for each event, however, are hypothesized to be different from pressing task.

---

**SPECIFIC AIM 4: To characterize multi-digit synergy during repetitive dynamic torque production task.**

Repetitive movement, in practice, is often decomposed into a sequence of discrete movements for analysis. However, it is still widely debated whether these two movements are associated with the same neural structures (Hogan and Sternad 2007; Sternad, Dean et al. 2000). One hypothesis is that repetitive movement is planned as a limit cycle attractor by the CNS and parameters are minimally adjusted, as minor disturbance will be suppressed. Many researchers studied repetitive finger abduction/adduction, tapping, and pressing, with dynamic system theory and neural network modeling (Aoki, Francis 2003; Friedman, Skm 2009; Schoner and Kelso 1988). As compared to self-paced oscillation tasks, if the oscillation is synchronized by external cues, such as metronome beeps, the CNS needs to integrate sensory feedback and generate motor commands for subsequent movement in advance. Movement frequency was shown to alter dynamic behavioral pattern, e.g. transforming from anti-phase to in-phase with faster pace in bimanual index fingers abduction/adduction task (Schoner and Kelso 1988).

For circular object manipulation, will torque coordination pattern be different in repetitive dynamic movement from in discrete static movement as in Experiment 3? How will task condition (movement frequency) and object property (moment of inertia) affect multi-digit synergy? Specific aim 4 answers these questions by analyzing the time profile of digit forces and hand-held object kinematics in an external-cued repetitive torque production task on a circular object.

**Hypothesis 4.1: The within-cycle regularity of tangential force decreases with movement frequency and moment of inertia, while the between-cycle regularity increases with either factor.**

Regularity of within-cycle and between-cycle force output will be characterized by hysteresis index and approximate entropy, respectively (Gao, Ren et al. 2011; Pincus 1991). Researchers found that hysteresis index is positively associated with joint stiffness during ankle stretching. If force requirement increases by modifying either factor, we expect to see greater hysteresis index, or less within-cycle regularity, as the result of a stiffness increase in the wrist joint. In contrast, between-cycle regularity increased with force level in an isometric index finger abduction task (Hong, Lee et al. 2007). It is hypothesized that the between-cycle regularity in a dynamic task also increases with movement frequency and moment of inertia.

**Hypothesis 4.2: Torque-stabilizing synergy is reduced with faster rotational movement and larger moment of inertia of the circular handle.**

Positive covariation, i.e. in-phase synchronization, of digit tangential forces should occur with higher frequency, similar to the bimanual index finger abduction/adduction experiment (Schoner and Kelso 1988). Therefore, multi-digit synergy is expected to reduce or even diminish with higher frequency. On the other hand, with larger moment of inertia, the torque requirement is increased in order to maintain the same pace. The increase in tangential force is expected to

increase the variance not related to the performance variable, while have less impact on the variance related to the performance variable (Latash, Scholz et al. 2002), leading to a reduced synergy index.

### **1.3 Dissertation organization**

This dissertation is organized into seven chapters. The first two chapters offer problem statement and literature review relevant to this dissertation. Then four experiments, each corresponding to a specific aim, are presented in Chapter 3 to 6. The last chapter summarizes the results in previous chapters and discusses future direction.

Chapter 1 serves as an introduction to the research problems. Significance of the research is demonstrated. Four specific aims are proposed from views of biomechanics, ergonomics, and motor control. Each study is provided with a brief background summary and several hypotheses are formed.

Chapter 2 elaborates current knowledge foundation in biomechanical and neurophysiological aspects of hand and digits. It explains phenomena of multi-digit coupling and coordination. Both experimental evidence and theoretical frameworks are presented. In the end, current research progress on circular object manipulation is reviewed and unsolved problems are introduced.

Chapter 3 studies the peak capability of torque production on a circular object. Maximum voluntary torque is compared across different wrist positions and torque directions. Force sharing patterns by individual digits are examined. Explanation and comparison from other studies are offered.

Chapter 4 inspects force sharing pattern and safety margins in submaximal torque production task. The effects of wrist position, torque direction, and initial grip force is investigated in detail. The results are discussed from the perspectives of hand and wrist biomechanics and anatomy.

In chapter 5, multi-digit synergy is investigated in a static torque ramp-down, ramp-up task. Time profiles of torque stabilizing synergy and its decomposition to two subspaces are evaluated. The dependency of multi-digit synergy on wrist positions and torque directions is examined.

In chapter 6, a repetitive dynamic circular displacement task is performed. Multi-digit synergy is compared with that in the previous chapter on a static task. The influence of movement frequency and moment of inertia of the circular handle on torque coordination pattern is investigated.

Chapter 7 concludes the studies of previous chapters. Results are compared with each study and discussion will be provided. In the end, future research directions are discussed.

## Chapter 2

### Literature review

Prehensile manipulation with hands is the primary means humans use in order to interact with the external world. Numerous studies have targeted this problem from various grounds. Two principal categories, power grasp and precision grasp, are defined based on grasping posture (Cutkosky and Howe 1990; Naiper 1956). Depending on the shapes and sizes of manipulated objects, each category is further divided into sub-categories. This section addresses only the researches relevant to precision grasp, i.e. with distal and intermediate phalanges of the fingers opposing the thumb and no direct touch of palm with objects.

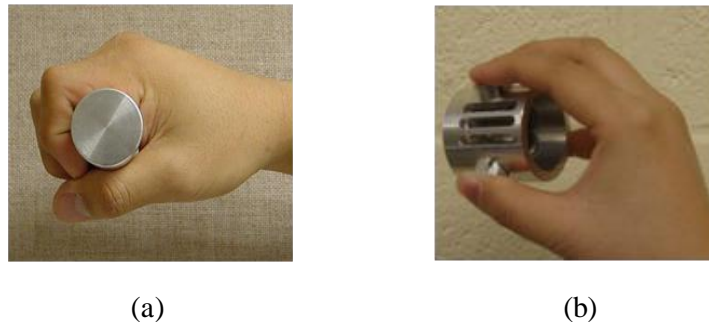


Figure 2-1 Illustration of (a) power grasp and (b) precision grasp.

First of all, biomechanical and neurophysiological factors affecting the prehension performance will be presented. These factors include extrinsic and intrinsic properties of manipulated object, task and equilibrium requirements, and constraints by central nervous system and peripheral musculotendinous structure of hand. Subsequently, recent efforts in characterizing the coordination in multi-digit prehension will be discussed. Concepts such as finger enslaving and synergy are introduced to quantify digit independency. Last, researches on circular object manipulation are reviewed. How they are related to this dissertation is also discussed.



## **2.1 Constraints in multi-finger prehension**

### **2.1.1 Extrinsic and intrinsic object properties**

When holding an object with the thumb and the opposing fingers, people choose from a repertoire of hand postures according to mechanical characteristics of the manipulated object. Before contact, visual cues about the object, such as size and shape, will affect both kinematic and kinetic aspects of grasping. For example, subjects decided the aperture of the hand during the reaching movement based on the size information (Gordon, Forssberg et al. 1991; Gordon, Forssberg et al. 1992). For grasping of a cylindrical object, the optimal diameter was found to be about 4~5cm, determined by lowest EMG signal and number of repetitions before fatigue initiation (Amis 1987; Ayoub and Presti 1971). However, Freund found that the relative contribution of pressing forces by individual fingers is irrelevant to the diameter (Freund, Toivonen 2002). This result can be extended to when the diameter gets infinite large, i.e. when pressing the hand against a flat surface (Li, Latash et al. 1998).

Object weight, estimated from the size information, is taken into consideration as well. People tend to use more digits and produce higher fingertip force for heavier objects for stable grasping action. However, when two equal weight objects were lifted, the smaller object is perceived to be heavier but grip force exerted on the larger object is larger (Gordon, Forssberg 1991), the so-called “size-weight illusion”. An explanation comes from internal model theory (Wolpert and Ghahramani 2000), stating that the illusion comes from the discrepancy between expected and actual sensory feedback. Smaller objects are expected to be lighter and therefore larger mismatch. This illusion persists even after trials of alternating lifts but subjects can learn to scale fingertip force correctly, implicating a dissociation of sensorimotor integration and perception process (Flanagan and Beltzner 2000).

Depending on the shape or the contour of external surface, a grasp trajectory is planned. In an experiment, subjects were asked to reach and grasp an object, whose shape was manipulated to be convex, flat, or concave. It was found that the hand aperture reached maximum at the half way although the information about hand conformation to the task object continued to increase until it was grasped (Santello and Soechting 1998).

Information about center of mass (CM) of objects also has an effect on motor planning before reaching. In an experiment, when the center of mass of an object was changed to right, left, or center, subjects used distinct spatial distribution of digits instead of a default placement of contact points for all positions (Lukos, Ansuini et al. 2007).

Once contact is established, the friction condition between the fingertip and contact surface are utilized for an appropriate grasping force. Friction is affected by physiological properties in the glabrous fingertip pads. For example, sweating will increase the friction by raising the viscous damping effect. A hypothesis suggests that the moisture level of fingertip pad is optimally regulated to minimize grasping force (Andre, Lefevre et al. 2010). On the other hand, friction is also modified by textural characteristics of contact surface. For instance, sandpaper has greater friction (“rougher”) than silk because of finer gratings. In this dissertation, the difference of individual skin in friction condition is neglected as subjects washed and dried their hands before the experiments. With this assumption friction is considered only material-specific.

Static coefficient of friction<sup>4</sup> is used to quantify the friction condition of contact surface. It is defined as the maximum possible tangential/load force with unit normal force with no relative sliding movement. This parameter defines a cone at the point of contact, within which a force

---

<sup>4</sup> Static coefficient of friction is slightly larger than dynamic coefficient of friction, which is used when sliding occurs. In this dissertation, static coefficient of friction is simply used when no confusion happens.

vector should be located inside for a stable grasp. Hence, in order to prevent the object from slipping, normal force should satisfy the following restraint.

$$F_n \geq F_{SP} = \frac{F_t}{\mu} \quad (2-1)$$

$F_n$ ,  $F_{SP}$  and  $F_t$  are normal force, critical normal force and tangential force, respectively.  $\mu$  is the static coefficient of friction. If  $F_n$  is smaller than  $F_{SP}$ , slip will occur. Safety margin (SM), an index of grasping stability, is defined as the extra normal force.

$$SM = F_n - F_{SP} \quad (2-2)$$

To reflect individual strength difference, SM is sometimes normalized by the normal force itself.

$$SM = \frac{F_n - F_{SP}}{F_n} \quad (2-3)$$

### 2.1.2 Physical constraints and task constraints

During a manipulative task, the forces exerted by all explicitly involved digits need to satisfy physical constraints and task constraints. Physical constraints include principles governing how an object is translated or rotated in a physical world. For example, when holding a free object in equilibrium state (stationary or translating in a constant velocity), three constraints are applied based on Laws of Newton:

- 1) The resultant horizontal force is zero;
- 2) The resultant vertical force is equal to the object weight;
- 3) The total moment of force (or torque) is zero.

The task constraints include task goals in daily life, such as holding a mug level or tilting it slowly to drink, and requirements imposed by the experiments, such as matching the resultant force to a predefined template or resisting a perturbation.

Wrist position is also included as a task constraint in this dissertation because subtasks with different wrist positions were tested. It has been shown to affect both maximum force and force sharing pattern in a forceful grip task (Li 2002). Maximum force was found with the wrist at 20 degrees in extension and 5 degrees in ulnar deviation. The authors explained that major muscles responsible for flexion have optimal lengths in this position or longest moments of arm with respect to finger joints. Deviation from this position results in different reduction in individual finger forces, possibly due to excursions of tendons from extrinsic muscles. However, a recent EMG study found that activity of intrinsic muscles was also modulated accordingly (Poston, Danna-Dos Santos et al. 2010), which implies that central nervous system might coordinate the excitation of both intrinsic and extrinsic muscles (Johnston, Bobich et al. 2010).

### **2.1.3 Grip force-load force coupling**

In a series of studies done by Johansson and his colleagues, subjects lifted an instrumented object from a support, held it in the air, and replaced it back, using a precision grip with thumb and the index finger (Johansson and Westling 1984; Westling and Johansson 1984). It was found that once contact was established between the digits and contact surface, there was a brief period of grip force increase, followed by the rising of load force. Grip force and load force then increased in parallel until the object was lifted off the support. The force ratio,  $F_n / F_t$  remained stable and above the slip ratio  $1 / \mu$ . When two digits contacted different surfaces (silk vs. sandpaper), instead of generating equal load force and sufficient grip force for both digits, the digit contacting more slippery surface (larger slip ratio) would produce less load force, while the other digit (smaller slip ratio) would produce more load force. Both force ratios  $F_n / F_t$  were well above

their slip ratios (Westling and Johansson 1984). If a slip occurred at the digit with more slippery surface, the force ratio of the nonslipping digit would have a ditch about 70ms due to compensatory raise of load force before restoring to previous level. Hence the authors suggest that each digit be independently controlled with one single parameter, the force ratio (Edin, Westling et al. 1992; Hager-Ross, Cole et al. 1996; Johansson and Cole 1994).

They also investigated the sensory mechanism and found evidence in support of the hypothesis.

There are four types of functional distinct tactile sensors underneath glabrous digit pad. They respond to mechanical deformation caused by stress and shear and are called mechanoreceptors.

According to their dynamic response, they are named as fast-adapting type I (FA I, Meissner) and fast-adapting type II (FA II, Pacini), slow-adapting type I (SA I, Merkel), and slow-adapting type II (SA II, Ruffini) sensors. Because muscle proprioception is insensitive to fingertip deformation (Dimitriou and Edin 2008; Macefield and Johansson 1996), these mechanoreceptors are hypothesized to encode the mechanical events in fingertip, such as forming and breaking contact with objects (Johansson and Flanagan 2009).

For example, both FA II and SA I sensors will be activated the moment fingertips contact and leave an object. When lifting an object lighter than anticipated, brief bursts of action potentials are elicited in FA II sensors to signal the early lift off, which leads to an abrupt termination of load force. Similarly, when lifting an object heavier than anticipated, the absence of action potentials in FA II sensors will trigger a series of small increases in load force, “probing” the appropriate level of load force until the object is lifted (Johansson and Cole 1992).

With the above experiment findings, two types of control policies, predictive control and reactive control, have been formed on the basis of internal model theory. Predictive control acts in two time ranges. On an extended time range, subjects scale appropriate grip force and load force based on the visual and haptic cue information, incorporated with previous experience with the

same or similar objects. Proper motor commands are generated through an inverse dynamics process. On a shorter time range, subjects predict the upcoming perturbation (self-generated movement or predictable external perturbation) and adjust performance parameters accordingly. An efference copy, or corollary discharge, of motor command is sent to a neuronal representation, “feed forward model”, of the object to predict the anticipated output. If sensory feedback does not match the expectation, online adjustment is required and the neural representation is updated,

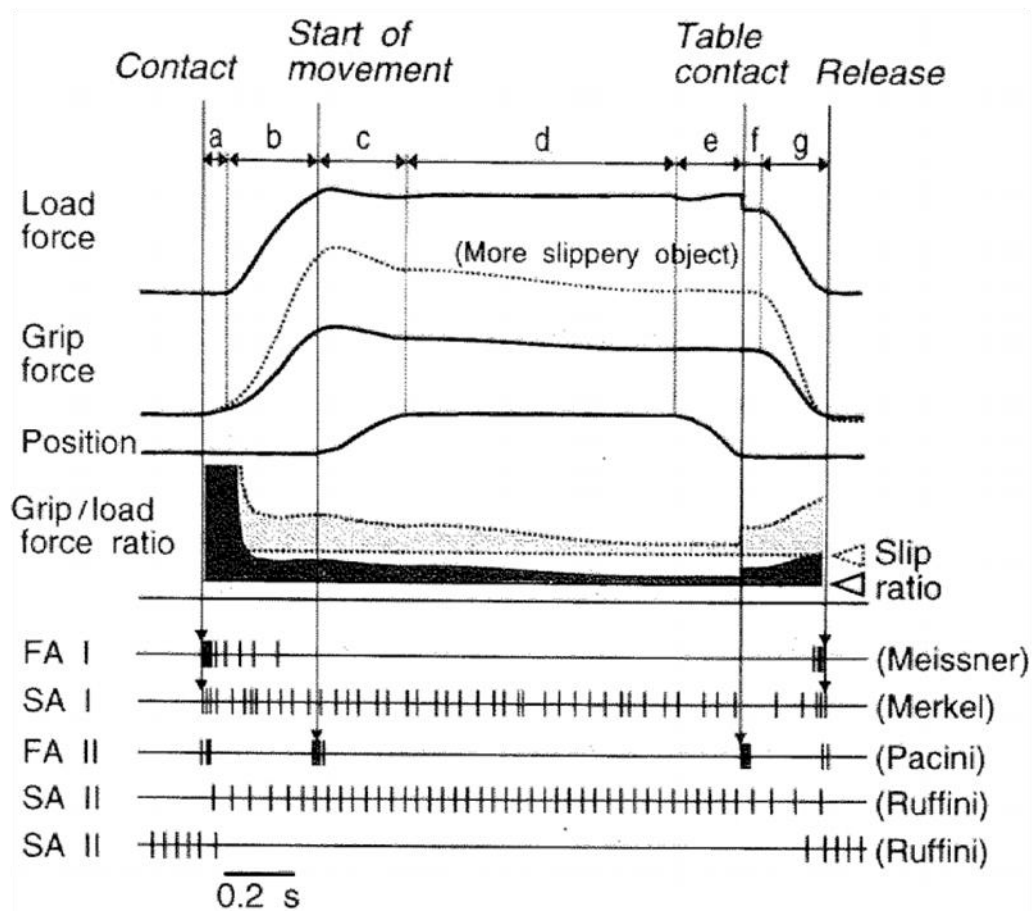


Figure 2-2 Time profiles of grip force and load force. The task was to lift an instrumented object off the table, hold it for a while, and replace it back. Grip/load force ratio is always higher than the critical value, determined by smoothness of a material, i.e. smooth material has larger slip ratio, and requires greater grip force, as compared to rough material. The bottom are typical firing patterns of four kinds of mechanoreceptors. Adapted from (Johansson and Cole 1994)

“feedback model”. On the other hand, when the perturbation is unpredictable, a reactive grip force increment and a phasic EMG response of 60~100ms delay, the so-called “catch-up” response, will be elicited to prevent the object from slipping. This automatic reflex-like response is a multisynaptic long-latency response, driven by dynamic skin deformation and excitation of the mechanoreceptors, but not by intrinsic or extrinsic muscle afferents (Macefield, Hagerross et al. 1996; Macefield and Johansson 1996).

The coordination of manipulative forces is altered in patients with Parkinson’s disease (PD) (Gordon, Ingvarsson et al. 1997; Muratori, McIsaac et al. 2008). Two features are evident: a prolonged initiation of object lift-off and tremor-like oscillatory development of the rate of grip force. However, patients still can scale grip force according to object weight, predict object weight from visual cue, and respond to self-initiated load change, indicating intact sensorimotor integration and anticipatory control. Post-operative medication will induce bradykinesia and excessive grip force. Deep brain stimulation of subthalamic nucleus can improve movement initiation and rates of force development, but its effect on grip force regulation is still ambiguous (Fellows, Kronenburger et al. 2006; Nowak, Topka et al. 2005).

#### **2.1.4 Individuated digit movement and muscle synergy**

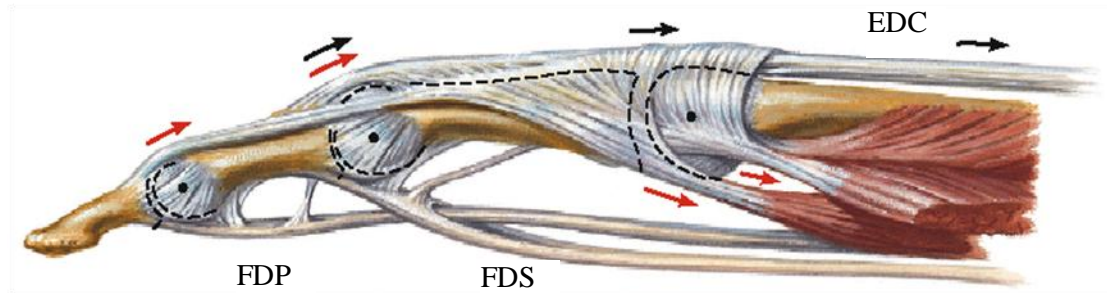
In the studies mentioned above, an implication is that digits can be controlled by independent neural network (Burstedt, Edin et al. 1997; Smeets and Brenner 1999; Smeets and Brenner 2001). Indeed, the tight coupling between grip force and load force coincides with the labeled line hypothesis, which assumes that each digit is controlled by a pair of agonist and antagonist muscles (flexor and extensor), and these muscle pairs are in turn driven by separated areas in the cortex. The hypothesis originates from the classic homunculus map discovered by Canadian surgeon Penfield (Penfield and Boldrey 1937; Penfield and Flanigin 1950). They found that electrical stimulation of body surface, e.g. arms or legs, triggered response in areas in

contralateral somatosensory cortex. Similarly, stimulation of a site in motor cortex evoked movement of a specific body part. The somatotopic map is arranged with face on the lateral side, lower extremity on the medial side, and upper extremity in between. It is speculated that individual digits might be segregated in motor and somatosensory cortex as well. Although this is roughly true for the somatosensory cortex, neural representation in the primary motor cortex (M1) is found to be widely distributed and overlapped within hand area (Schieber and Hibbard 1993). Stimulation of one area will elicit motor evoked potentials in multiple forearm muscles. And stimulation of different areas sometimes brings up the same movement of a finger. These divergent and convergent pathways between central and peripheral systems make it very difficult to find a somatotopic map in primary motor cortex as in somatosensory cortex. This situation becomes more complicated by considering intricate interconnections within motor cortex (e.g. premotor cortex and supplement motor area) and with other functional cortices (e.g. parietal cortex, basal ganglion, and cerebellum).

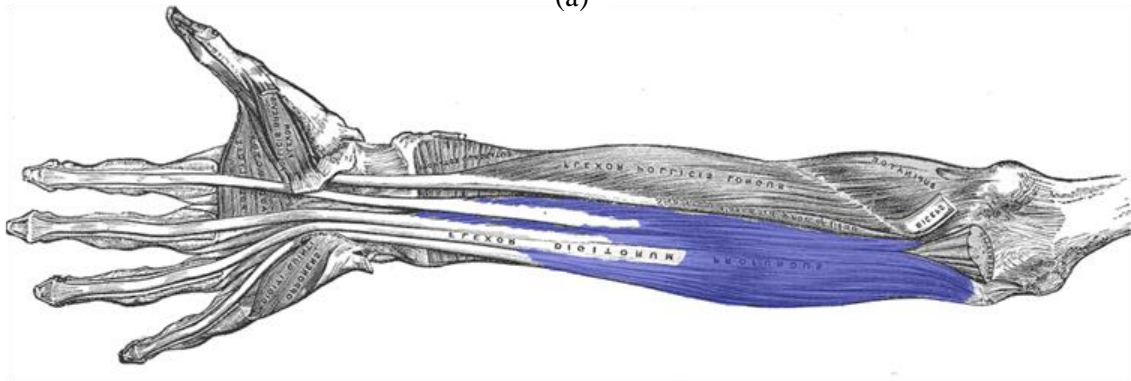
Moreover, peripheral anatomical and physiological constraints further prevent the implementation of individuated digit movement. Although index and little finger have extrinsic single tendon muscle for extension (extensor indicis proprius and extensor digiti quinti proprius, respectively), they have no such muscle for flexion. Intrinsic muscles (lumbricals, palmar and dorsal interossei) help with flexion and abduction/adduction of MCP joint and extension of PIP and DIP joint for a single finger. However, they are unable to explain individuated flexion and extension of finger movements (Landsmeer and Long 1965). On the other hand, all fingers receive parallel insertion from three long tendon muscles (flexor digitorum profundus: FDP, flexor digitorum superficialis: FDS, and extensor digitorum communis: EDC) (see Figure 2-3b). These extrinsic muscles cross wrist joint, split into four tendons and insert to the lateral or dorsal side of a given finger, fastened by the ligaments of its extensor complex. To move a single finger while maintaining other fingers still, therefore, requires coordinated activation of several muscles. For example, contraction of



FDP and FDS flexes ring finger; to prevent too much flexion on little finger, extensor digiti quinti proprius is activated. This activation of this muscle also attenuates flexion torque on the wrist and helps to maintain it still.



(a)



(b)

Figure 2-3 (a) Musculoskeletal structure of a finger and the biomechanical outcome of some major muscles (adopted from Netter's anatomy); (b) deep muscles of the hand and wrist (anterior view, flexor digitorum profundus is painted blue), adapted from Grey's anatomy.

Another hypothesis is that each of the extrinsic large muscles has compartments in their bellies for individual fingers (Danion, Li et al. 2002; Keen and Fuglevand 2004; Kilbreath and Gandevia 1992; Schieber 1991). Two subdivisions of FDP (FDPr and FDPu) was found to supply the radial and ulnar sides in a macaque's hand, respectively (Schieber 1991). However, for all three human muscles, corticomotor tracts innervate motor neurons of adjacent compartments simultaneously (Aoki, Francis 2003; McIsaac and Fuglevand 2007; Reilly, Nordstrom et al. 2004).

## 2.2 Coordination patterns in multi-digit tasks

### 2.2.1 Finger enslaving effect

Because of the multi-tendon, multi-articular muscles, both kinematic and dynamic digit movement will inevitably cause unintentional movement of all other digits. Indeed, principal component analysis of angular positions and velocities of 19 digit joints in daily activities showed that two principle components could be extracted to explain more than half of the variance (Ingram, Kording 2008). These two PCs involved simultaneous flexion and extension of all digit joints, i.e. opening and closing of the entire hand, while higher order components reflected finer adjustment of hand posture. Similarly, when subjects were instructed to produce force with only one digit, the other digits produced involuntary force as well (Li, Latash 1998; Reilly and Hammond 2000). This is called “*enslaving effect*”. The instructed fingers and non-instructed fingers are called “master” and “slave” fingers, respectively. The enslaving effect makes individuated digit movement very difficult. On the other hand it provides a simplification for the problem of motor redundancy by grouping together relevant effectors for the most frequent and important everyday activities.

In a pressing study (Li, Latash 1998), subjects were asked to produce maximal force by pressing single or multiple fingers against force sensors for a few seconds. It was found that all fingers could produce more force when it acts alone than when it has to act with other fingers. This phenomenon is called “*force deficit*”. It is speculated that the CNS might have an upper boundary limiting the capacity of simultaneous activation of multiple muscles. The neural drive has to be divided, in multi-finger tasks, to instructed fingers, resulting in less force output in individual fingers. In a subsequent task, subjects were asked to follow a visual template on screen and to produce a ramp force to several levels of submaximal force. The forces by individual fingers maintained a linear relationship throughout the entire process, i.e. a *force sharing* pattern was

created since initiation and preserved thereafter. This implies another possible control strategy by the CNS to simplify the computation process, i.e. by fixating the sharing pattern, it needs only to specify the overall activation intensity for parallel-linked multi-effector system, thereby reduce the specific detail for each output, the so-called “minimum intervention principal” (Hogan 1984).

A neural network model is proposed to explain the findings above. It assumes that force output is a combined summation of both multi-tendon and single-tendon muscles (Zatsiorsky, Li 1998).

$$\begin{pmatrix} F_I \\ F_M \\ F_R \\ F_L \end{pmatrix} = \frac{1}{n^b} \begin{pmatrix} w'_{II} & w'_{IM} & w'_{IR} & w'_{IL} \\ w'_{MI} & w'_{MM} & w'_{MR} & w'_{ML} \\ w'_{RI} & w'_{RM} & w'_{RR} & w'_{RL} \\ w'_{LI} & w'_{LM} & w'_{LR} & w'_{LL} \end{pmatrix} \begin{pmatrix} m_I \\ m_M \\ m_R \\ m_L \end{pmatrix} + \begin{pmatrix} v_{II} & 0 & 0 & 0 \\ 0 & v_{MM} & 0 & 0 \\ 0 & 0 & v_{RR} & 0 \\ 0 & 0 & 0 & v_{LL} \end{pmatrix} \begin{pmatrix} m_I \\ m_M \\ m_R \\ m_L \end{pmatrix} \quad (2-4)$$

Finger mode  $m$  is a hypothetical variable and assumed to be controlled by the CNS to set forth the force output of any single finger. For the right hand of **Error! Reference source not found.**, the first term represents the multi-tendon muscles, i.e. any mode to finger  $i$  will generate force at all fingers. The second term represents the single-tendon muscles, i.e. mode to finger  $i$  will generate force at the specific finger only.  $n$  (possible values: 1~4) is the number of instructed fingers in a task and  $b$  is a task-specific constant, found experimentally to be about 0.6 ~ 0.7 (Danion, Schoner et al. 2003). The addition of gain coefficient is to explain the force deficit phenomenon. This model has been validated by current experiment data.

In four-finger task, the two terms of equation **Error! Reference source not found.** can be combined into a single matrix  $E$  (“enslaving matrix”).

$$\begin{pmatrix} F_I \\ F_M \\ F_R \\ F_L \end{pmatrix} = E \begin{pmatrix} m_I \\ m_M \\ m_R \\ m_L \end{pmatrix} = \begin{pmatrix} w_{II} & w_{IM} & w_{IR} & w_{IL} \\ w_{MI} & w_{MM} & w_{MR} & w_{ML} \\ w_{RI} & w_{RM} & w_{RR} & w_{RL} \\ w_{LI} & w_{LM} & w_{LR} & w_{LL} \end{pmatrix} \begin{pmatrix} m_I \\ m_M \\ m_R \\ m_L \end{pmatrix} \quad (2-5)$$

Enslaving matrix  $E$  is usually full-rank (the determinant is non-zero and hence invertible). Force space and mode space has a homologous relationship, i.e. a unique force vector corresponds to a unique mode vector. By converting performance variables into a set of hypothetical central command variables, this mapping allows to avoid the consideration of complex anatomical structure and so called “spurious” effect (Latash, Scholz et al. 2001).

### 2.2.2 Uncontrolled manifold hypothesis

For multi-effector systems, a theoretical framework, called uncontrolled manifold (UCM) analysis, is developed by Scholz and Schöner to analyze the trial-by-trial variability (Scholz and Schöner 1999). By projecting the element variables into task space (orthogonal space, usually only one dimension) and its conjugate space (UCM space), the total variance of element variables can be divided into two components. Variance in orthogonal ( $V_{ORT}$ ) space will affect the performance variable, while variance in UCM space ( $V_{UCM}$ ) will not affect the performance variable. The UCM hypothesis is that humans take advantage of the variability in UCM space to explore a variety of solutions. For a given task, the first step to decompose the total variance is to define the direction for the orthogonal space. For example, when subjects perform a constant total force task with four fingers, the orthogonal space is defined along direction  $\mathbf{R}_1$ .

$$\mathbf{R}_1 = [1 \quad 1 \quad 1 \quad 1]^T \quad (2-6)$$

T stands for the transpose of a matrix or a vector. The sum of forces along direction  $\mathbf{R}_1$  should equal the target force, i.e.

$$(\mathbf{R}_1^T, \mathbf{f}) = f_I + f_M + f_R + f_L = F_{target} \quad (2-7)$$

$\mathbf{f}$  is the vector composed of individual finger forces.  $(\cdot, \cdot)$  represents inner product. A simple version when there are only two fingers is shown in Figure 2.4a. The ellipse is the envelope of all data points. Typically, the variability along vector  $\mathbf{R}_1$  (orthogonal space),  $V_{ORT}$ , should be

suppressed while the variability orthogonal to  $\mathbf{R}_1$  (UCM space),  $V_{UCM}$ , is not restrained because points moving along that line will not affect the sum of all forces.

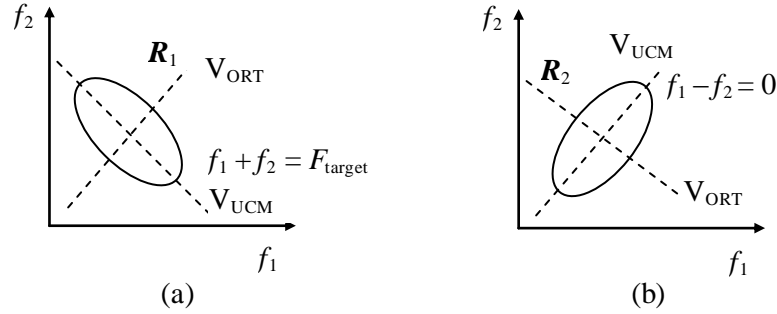


Figure 2-4 Illustration for uncontrolled manifold hypothesis: (a) constant total force task; (b) torque cancellation task, assuming moment arm  $r_1$  equals moment arm  $r_2$ .

When subjects perform a torque cancellation task, e.g. torque produced by index and middle finger is cancel by torque by ring and little finger, the orthogonal space is defined along direction  $\mathbf{R}_2$ .

$$\mathbf{R}_2 = [r_I \quad r_M \quad -r_R \quad -r_L]^T \quad (2-8)$$

$$(\mathbf{R}_2, \mathbf{f}) = f_I r_I + f_M r_M - f_R r_R - f_L r_L = 0 \quad (2-9)$$

$\mathbf{R}$  is the vector of the moment arms for individual finger force with respect to a physical or hypothetical rotation axis. In Figure 2-4(b), the two moment arms are assumed the same for simplicity. The task is to keep two forces equal. As long as the variance along  $\mathbf{R}_2$  is small, it does not matter how large both forces are, i.e. they can move along the line  $f_1 - f_2 = 0$  freely. In four-finger pressing task, the rotation axis is usually defined at the center point between middle and ring finger sensors. In rectangular object prehension task, this axis is defined as the line passing through thumb and perpendicular to the opposite plane where four fingers contact. Moment arms are defined according to the perpendicular distance from each finger to the rotation axis and can be positive or negative depending on whether the finger contributes agonist or antagonist torque.

When there are more than one performance variable simultaneously controlled, for instance a constant total force and zero total torque, the orthogonal space is spanned by  $\mathbf{R}_1$  and  $\mathbf{R}_2$ . However, it should be aware that  $\mathbf{R}_1$  and  $\mathbf{R}_2$  might not be orthogonal to each other, i.e.  $(\mathbf{R}_1, \mathbf{R}_2) \neq 0$ ; the variance along each direction might overlap and be duplicated.

Finger modes  $\mathbf{m}$ , as defined in previous subsection, are usually chosen as the set of elemental variables instead of forces. Therefore,  $\mathbf{R}$  from previous equations should be converted to another vector  $\mathbf{Q}$  by taking account of enslaving matrix  $\mathbf{E}$ .

$$\mathbf{Q} = \mathbf{R}^T \mathbf{E} \quad (2-10)$$

The projection of  $\mathbf{m}$  in the orthogonal space  $\mathbf{m}_\perp$  and in the UCM spacem  $\mathbf{m}_\parallel$  is defined as:

$$\mathbf{m}_\perp = \sum_{i=1}^{n_1} (\mathbf{m}, \mathbf{e}_i) \mathbf{e}_i \quad (2-11)$$

$$\mathbf{m}_\parallel = \sum_{i=1}^{n_2} (\mathbf{m}, \mathbf{f}_i) \mathbf{f}_i \quad (2-12)$$

$\{\mathbf{e}_i\}, \{\mathbf{f}_i\}$  and  $n_1, n_2$  are the bases and dimensions of the orthogonal space and the UCM space, respectively. And the sum of  $n_1$  and  $n_2, n$ , is the number of elemental variables.

Delta variance (DV) is defined as the difference of variance per degree of freedom in the UCM space and in the orthogonal space, normalized by total variance per degree of freedom.

$$\text{DV} = \frac{V_{\text{UCM}} / n_1 - V_{\text{ORTH}} / n_2}{(V_{\text{UCM}} + V_{\text{ORTH}}) / (n_1 + n_2)} \quad (2-13)$$

DV is an index for quantifying multi-digit coordination. If DV is greater than zero, a synergy is said to exist to stabilize the performance variable; if DV is less than zero, the synergy does not exist or is destroyed. And the greater DV is, the synergy among digits or effectors is stronger.

Note that for tasks with different number of elemental variables, the maximum (when  $V_{\text{ORTH}}$  is

zero) and minimum (when  $V_{UCM}$  is zero) will change. For example, in four-finger force pressing task,  $n$  is 4 and DV is between  $-4$  and  $4/3$ ; while in three-finger force pressing task,  $n$  is 3 and DV is between  $-3$  and  $3/2$ . Therefore, in practice, a Fisher's transformation is sometimes executed to compare DV in different tasks (Karol, Kim et al. 2010).

### 2.2.3 Multi-digit synergy

Synergy has been used to answer the notorious motor redundancy problem. Bernstein observed that when a blacksmith hit a chisel with a hammer repetitively, the variance of endpoint position was usually smaller than those of joint angles (wrist, elbow, and shoulder), i.e. the target was hit accurately despite large variation of intermediate joints each effort. Bernstein concluded that human use coordination pattern (motor synergy) to reduce or freeze extra degree of freedom (Bernstein 1967). A formal definition of synergy is that in a given task, there exist a set of motor elements that coordinate to achieve a goal on performance variable (Latash 2008). Three core rules are emphasized in this definition.

1. Sharing. All elements should contribute to the performance variable.
2. Error compensation or flexibility/stability. If an unexpected perturbation occurs to one element, other elements should be adjusted automatically to reduce the variance of performance variable.
3. Task specificity. Different combinations can be chosen on the same set of elements for various tasks<sup>5</sup>.

Multi-digit synergy can be quantitatively characterized by delta variance (DV) introduced in the previous subsection. So far two kinetic synergies have been identified from experiment data,

---

<sup>5</sup> This rule is essential because it can be proven that even an unanimated object can exhibit the first two features [109] Latash, M.L., Shim, J.K., *et al.* A central back-coupling hypothesis on the organization of motor synergies: a physical metaphor and a neural model. *Biol Cybern*, 2005. **92**(3): p. 186-91.

namely force-stabilizing synergy and torque-stabilizing synergy (Li, Latash 1998; Santello and Soechting 2000; Zhang, Zatsiorsky et al. 2006). Their functions, as the names suggest, are to keep total force and total torque stable, respectively.

In a pressing task, subjects were asked to produce a ramp total force with four fingers for a consecutive 10 trials (Li, Latash 1998). It was found that the variance of total force was smaller than the sum of variance of individual finger forces, implicating an error compensation mechanism among them to stabilize the total force. This force-stabilizing synergy does not appear as soon as the ramp starts (Shim, Latash et al. 2003). Instead, negative DV of a period of 600~800 milliseconds proceeded before DV switched to positive values. This period of time did not depend on ramp time and was suggested to reflect the minimum amount of time for the CNS to assemble finger forces into a synergy.

Similarly, when subjects were asked to generate a ramp total torque with respect to the longitudinal line through the middle point of middle and ring finger, the torque stabilizing synergy appeared (Zhang, Zatsiorsky 2006). In fact, even in the first task where only force production was explicitly specified, subjects unconsciously utilized a torque-stabilizing synergy to minimize the rotation effect. In contrast, there was no secondary synergy for force control in torque production task. Therefore, it was suggested that torque stabilizing synergy is implemented by default to keep the wrist still. An alternative explanation is principle of mechanical advantage, i.e. effectors with greater moment arm will contribute more. As compared to middle and ring fingers, index and little fingers are farther from the rotation axis and produce more force, therefore generate more force.



*Relationship of variances in UCM and orthogonal space with force magnitude and force rate*

It has been well documented that the standard deviation of a force is linearly correlated with its magnitude (Newell, Carlton et al. 1984; Newell and Carlton 1988). However, this relationship is established on the single effector and does not apply to multi-effector system where multi-digit synergy exists to compensate each other's error, resulting in a much smaller variance of total

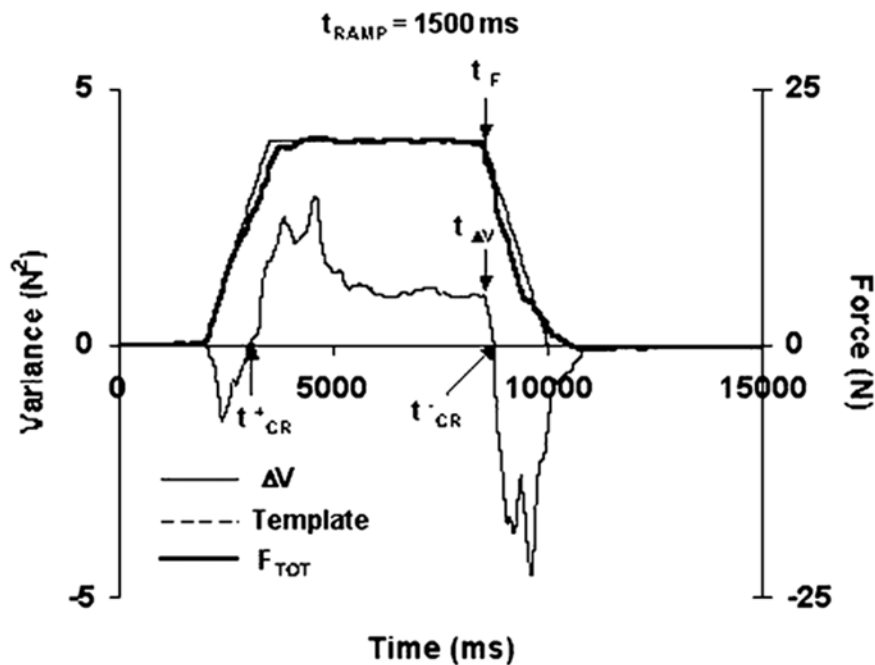


Figure 2-5 A typical time profile of delta variance (DV) in a ramp-up, hold, then ramp-down task. Total force is shown in black on top of a force plate. It takes a few hundred milliseconds for DV to become positive after force starts to increase; however, the difference between the onset of force decrease and the moment DV becomes negative is very small. Adapted from (Shim, force  $V_{ORT}$ . Further investigation found that  $V_{UCM}$  changed linearly with the magnitude of target force, while  $V_{ORT}$  showed a strong dependence on the rate of force production (Latash, Scholz 2001; Latash, Scholz 2002). As a result, the force control feature was salient only when  $V_{UCM}$  is greater than  $V_{ORT}$ . A single-joint kinematic model (Gutman, Latash et al. 1993) was extended to

explain this phenomenon. It assumes that pattern of motor variability is determined by variation of two scaling parameters: the amplitude and duration of the motor output. Variance in UCM space is caused by the amplitude parameter; while variance in the orthogonal space is mediated by the duration scaling parameter. A recent experiment, however, could not find the modulation effect of frequency on variance in the orthogonal space across trials (Friedman, Skm 2009). Instead, the coefficient of variation of the duration scaling parameter was found to decrease with increased frequency. As a result, the effect of force rate increase caused by increased frequency was diminished by the decrease of variance of the parameter

#### *Principle of superposition*

In a prismatic grasping task, subjects grasped a rectangular handle with six components (three forces and three torques in space) sensor for each digit and sustained it against an external torque (Latash, Shim 2004). The normal forces, vertical tangential forces and free moments from all digits were segregated into two sets. One set of variables was responsible to act against the gravity of the handle, while the other set was to maintain the rotational equilibrium against external load. In contrast with Li's experiment in which torque requirement was not explicitly specified, both force and torque goals in this experiment were interpreted to subjects in plain language, i.e. *hold the handle and keep it still in the air*.

The discovery coincides with a control strategy in robotic research, i.e. the principle of superposition (Arimoto, Tahara et al. 2001). This theory hypothesizes that for a pair of robotic fingers, the design of force and torque feedback can be decoupled so that position and posture of the object can be controlled separately. Indeed, of the two sets of variables, there is high

correlation within each set and almost zero correlation between. Chain reaction<sup>6</sup> has been hypothesized to account for the physics constraints in these tasks (Shim, Latash et al. 2005).

### *Principle of hierarchy*

In multi-digit prehension tasks involving the thumb and some or all fingers, it is typical to perform UCM analysis on a hierarchical two-level. The upper level (VF-TH level) includes the thumb and the “virtual finger”, which has the same resultant wrench, i.e. force and torque vectors, as the combination of fingers. The lower level (IF level) comprises individual fingers. Synergies have distinct characteristics at two levels. At upper level, forces and torques by the thumb and the virtual finger need to meet physical constraints. A positive correlation is usually expected for normal forces. At lower level, however, individual fingers should compensate the variation of other fingers to maintain a relatively stable value of the virtual finger, i.e. negative correlation or reciprocal activity (Santello and Soechting 2000). When holding a rectangular object in the air with a prismatic grip, it was found that force stabilizing synergy exists at both VF-TH and IF levels for tangential force, and only at VF-TH level for normal force; while torque stabilizing synergy exists at only IF level for torque by tangential force, at only VF-TH level for torque by normal force. The absence of synergy for normal force and its torque at IF level is, as the authors argued, because an increase in UCM variance at VF-TH level will increase the variance of VF, which should have been suppressed at IF level to achieve a synergy of element fingers (Gorniak, Zatsiorsky et al. 2009).

---

<sup>6</sup> Note that the phrase “chain reaction” does not imply casual relation among variables in each set. They are constrained only by physical principles.

### *Effects of neuromuscular training and fatigue on multi-digit synergy*

Muscular apparatus of the hand can be altered by intervention as well as by acute or chronic neuromuscular diseases. How the CNS corresponds to peripheral changes and adapts multi-digit coordination pattern might provide valuable information for both rehabilitation and physical exercise. Strength training and fatigue can be viewed as opposite directions to modify the neuromuscular system, i.e. strengthening and weakening, respectively.

In a strength training study (Shim, Hsu et al. 2008), three groups of subjects went through different isokinetic training protocols: all fingers training together, single finger training with self-restricted motion of other fingers, and single finger training without self-restricted motion of other fingers. As compared to control group, subjects from all three groups had increased maximum force, decreased force error and finger independence. Torque stabilizing synergy emerged only in the group training four fingers together, while force stabilizing synergy emerged only in the group training single finger with self-restricted motion of other fingers.

Peripheral fatigue can be induced by single finger and multiple finger exercises. In single finger exercise, effects of fatigue were transferred to non-involved fingers, reducing their maximum forces (Danion, Latash et al. 2001). Force sharing pattern was also adjusted to compensate the declination of the finger. However, the variance of total force remained unchanged. The ability of error compensation by non-involved fingers diminished after four-finger fatigue exercise (Kruger, Hoopes et al. 2007). Further analysis using UCM found that during fatigue, more dexterous finger, e.g. index finger was used more than less dexterous fingers, i.e. ring and little fingers (in preparation).

#### **2.2.4 Computational models of multi-digit synergy**

Numerous modeling studies have been conducted to investigate neuromuscular mechanisms underlying multi-digit synergy, on the basis of a variety of behavioral and neurophysiological

evidence (Burstedt, Edin 1997; Goodman and Latash 2006; Mussa Ivaldi, Morasso et al. 1988). For simplicity, only computational models related to UCM hypothesis will be discussed here. Principle of optimality is incorporated because other than task constraints and performance variables, it is believed that there are implicit biomechanical or physiological goals human try to optimize during movement planning (Nelson 1983). The criteria include minimal jerk (the rate of change of acceleration) (Hogan 1984), minimal energy consumption (e.g. squared sum of force, mode, or kinematic variables) (Hershkovitz, Tasch et al. 1997), minimal entropy function (Hershkovitz, Tasch et al. 1995) and minimal torque change (Uno, Kawato et al. 1989). Pataky hypothesized that at a given tangential force, the deformation of soft tissue of fingertip pad is minimized by varying normal force: strain energy minimization (Pataky 2005). The simulation results of finite element method partially matched the observation of safety margin in previous experiments.

Two categories of computational models have been extensively studied, i.e. feedback model and feedforward model. Each model can be successfully applied to explain part of current experiment findings and they are not mutually exclusive. From the perspective of pure control theory, a feedforward model can be viewed as a feedback model with feedback gain of zero; while a feedback model can be regarded as a feedforward model with the feedback loop wrapped into a black box.

In feedback models, the CNS monitors sensory feedback (visual, proprioception, or tactile) and makes adjustment to motor commands. Note it is not necessary for sensory feedback to be continuous, as seen in discrete-event, sensor-driven control (Johansson and Cole 1994), in which tactile information is updated only at specific moments signaling contacting, leaving the support, and restoring contact. Among various models, optimal feedback control has received extra attention (Todorov and Jordan 2002; Todorov 2004). It is based on principle of minimal intervention, an idea similar to UCM hypothesis. By the assumption, the controller does not

respond unless the output of multi-effect system deteriorates the performance. Therefore, the criterion includes not only the performance variable but a penalty term for the input from upper boundary. Properties such as motor synergy emerge as a consequence of this dynamic model. However, it has some drawbacks. For example, sensory delay in this model is simply regarded as larger noise; some parameters will result in self-excitation. Another model is called central back coupling control, i.e. motor neurons project through interneurons to inhibit surrounding motor neurons (Latash, Shim 2005). Renshaw cells are introduced as the interneurons because of their role in recurrent inhibition. Time delay and threshold control are incorporated in this model and some non-trivial characteristics of multi-digit synergy, such as a switching from positive to negative co-variation between finger forces at a critical time, and simultaneous appearance of force stabilizing synergy and torque stabilizing synergy, can be reproduced. Since the feedback in the second model is mediated by interneurons, the question about the role of sensory feedback is raised, i.e. is it possible for an open-loop system to exhibit multi-digit synergy, without explicit reliance on sensorimotor integration?

In feedforward models, the CNS plans movement parameters, e.g. moving trajectory or time profile of force, in advance and executes the motor commands, as compared to parallel and intermingled planning and execution processes in feedback models. The feedforward models do not require sensory signals for online control, although it may be still essential to update inverse dynamics, which is speculated to be computed in cerebellum (Hatze 2000). Without explicit sensory feedback, feedforward models can predict certain behaviors requiring quick movement. However, this feature also makes feedforward models vulnerable to noise, i.e. unable to achieve the task goal under external perturbation or intrinsic parameter deviation. This is partially avoided by a model proposed by Goodman and colleagues. It assumes that a central controller receives three inputs: ideal time profile of a performance variable (theoretically can be approximated by average of infinite trials), deviation from the ideal profile in a single trial, and an input unrelated

to the task goal (Goodman and Latash 2006). Variability in the second input will affect performance while variability in the third input will not and may be chosen from arbitrary function or some optimization criteria. Jacobian of the plant can be learned or updated from sensory information but unavailable for online correction of motor commands. This model can reproduce results like multi-digit synergy and its learning effect.

### **2.3 Manipulation of circular objects**

A number of everyday tasks involve manipulation of objects with circular shapes, like cups, screwdrivers, and doorknobs. A lot of researchers have investigated kinematics and dynamics aspects when people hold cylindrical objects, especially in industry ergonomics for better designs to reduce work-related fatigue and injuries (Armstrong, Fine et al. 1987; Friden 2001; Kao 2003; Silverstein, Fine et al. 1986). In these studies, subject usually grasp instrumented or ordinary objects with power grasp, i.e. closing the object with both thumb and fingers, and pressing them against the palm. In industry, a common occupational disease, called hand-arm vibration syndrome, may rise from long-term use of vibration tools held with power grasp.

Another category, however, has received relatively less attention, i.e. precision grasp of circular objects. This kind of grasp is commonly seen in our daily activities, such as turning discs, assembling circular parts, and handling round-shaped fruits. In some extent, it is similar to the prismatic grasp discussed above (Gorniak, Zatsiorsky et al. 2009; Li, Latash 1998; Shim, Latash 2005). Both have a grasp plane, a plane connecting the fingertips of the thumb and fingers, parallel to the palm. Grasp action has to satisfy the same friction constraint between digit pads and contact surface to prevent slipping. However, in circular grasp, all digits are placed on a circular contour and only tangential force contribute to the resultant torque; while in prismatic grasp, both normal force and tangential force generate torque orthogonal to the grasp plane .

Some preliminary results have been published about circular object manipulation (Kinoshita, Murase 1996). Kinoshita studied the effects of various anthropometric factors (hand length, hand width, wrist width, and digit lengths), diameter and weight of object, and number of digits on grip force production and individual digit contribution. Among three tested sizes, optimal diameter was found to be 7.5cm with minimal grip force. Larger diameter handle (10cm) leads to extension of digits and adds passive tension of flexor muscles on grip force, while smaller diameter handle (5cm) causes more flexion of DIP joints and extra grip force. For the same load, usage of more digits is associated with smaller grip force, possibly due to psychological easiness or more contact area for friction. Thumb contributes the most part of grip force, about 30% to 40%, followed by ring finger, while index finger contributes the least. It is hypothesized that the optimal position for grip force production is in opposition to the thumb, where ring finger is in five-digit grasp. When the diameter of the handle increases, both middle and little finger move close to the ring finger, raising the contribution from these two fingers.



## Chapter 3

### Multi-digit maximal torque production task on a circular object<sup>1</sup>

#### Abstract

Individual digit-tip forces and moments during torque production on a mechanically fixed circular object were studied. For the experiments, subjects positioned each digit on 3-dimensional force/moment sensors attached to a circular aluminum handle and produced the maximum voluntary torque on the handle. The torque direction and the orientation of the torque axis were varied for different conditions. It was found that (1) the maximum torque in the closing (clockwise) direction was larger than in the opening (counterclockwise) direction, (2) the thumb and little finger, respectively, had the largest and the smallest sharing of both total normal force and total moment, (3) the sharing of individual digit moments was not affected by the orientation of the torque axis or the torque direction while the sharing of individual digit normal forces changed due to the torque direction, and (4) the normal force safety margins had the largest and smallest values in the thumb and little finger, respectively.

Keywords: *finger; torque; circular object; safety margin*

---

<sup>1</sup> This chapter contains the following original paper reprinted by the permission from Taylor & Francis  
Jae Kun Shim, Junfeng Huang *et al.* Multi-digit maximum voluntary torque production on a circular object.  
*Ergonomics*, 2007, 50(5): 660-75.

### 3.1 Introduction

Manipulation of circular objects, such as opening a jar lid, twisting a valve, or rotating a door knob is a part of everyday activities. These activities usually involve a torque production (a twisting action) on a grasped object and are commonly taken for granted. However, they may present serious problems for elderly people, stroke patients, people operating hand prostheses, or control of robotic hands. Repetitive and forceful performance of such tasks in job conditions increase the risk of injury and motor disorders, such as carpal tunnel syndrome (Kao 2003; Kutluhan, Akhan et al. 2001; Wei, Huang et al. 2003).

As in any multi-finger manipulation, the studied task is mechanically redundant [in five-digit grasps, the digits exert 30 force and moment components on the grasped object while the object, if rigid, has maximally six degrees of freedom (Shim, Latash et al. 2005; Shim, Latash et al. 2005)] and the same object manipulation can be performed in many different ways. In particular, due to the grasp redundancy, the sharing of the total force among the individual digits cannot be predicted from pure mechanical considerations. The torque production on mechanically constrained objects differs from manipulation of the objects in the air (Shim, Latash 2004). When a hand-held object is mechanically free, the performer is allowed to exert only those forces and moments that satisfy the equilibrium requirements, e. g. the vertical forces should equal the object weight. In contrast, when an object is affixed to an external support, the forces exerted on the object can be of any value. The only mechanical constraint is that the normal digit forces should be sufficiently large to prevent slipping at digit contact.

In the literature, studies of multi-digit prehension—in particular the studies on the total force sharing among individual fingers—have been mainly limited to a prismatic precision grip, i.e. the grip by the tips of the digits in which the thumb and the fingers oppose each other (reviewed in Zatsiorsky, Latash 2004). In such a prehension, the fingers act in parallel and the forces acting on the object are easier to analyze and comprehend (Rearick and Santello 2002; Santello and

Soechting 2000; Shim, Latash et al. 2003; Shim, Latash 2004; Shim, Lay et al. 2004; Shim, Latash 2005; Shim, Latash 2005; Zatsiorsky, Gregory 2002). While several previous studies have addressed the manipulation of circular objects (Amis 1987; Fowler and Nicol 1999; Kinoshita, Murase et al. 1996; Lee and Rim 1991; Radhakrishnan and Nagaravindra 1993; Shih and Wang 1997), they mainly focused on the resultant force/moment (Fowler and Nicol 1999; Voorbij and Steenbekkers 2002), one digit force exerted on the object (Fowler and Nicol 1999), or on the force production without twisting actions (Kinoshita, Murase 1996).

This study focuses on the individual digit-tip forces and moments during a torque production on a mechanically fixed circular object. Two independent variables, the torque direction and the orientation of the axis of rotation with respect to the subject's body, have been systematically varied. The goal of the study was to investigate (a) the magnitudes of total force and moment under different torque directions and axes, (b) the relative contributions of individual digit force/moment to the total force/moment, and (c) the relations between normal and tangential forces at individual digit contacts.

## **3.2 Methods**

### **3.2.1 Subjects**

Ten right-handed males participated in this study as subjects, Table 1. The hand lengths were measured as the shortest distance between the distal crease of the wrist and the middle finger tip when a subject positioned the palm side of the right hand and the lower arm on a table with all finger joints being extended. The hand width was measured between the radial side of the index finger metacarpal joint and the ulnar side of the little finger metacarpal joint. The preferred angular positions of digit tips were measured during an all-digit natural prehension of a wooden

circular object of 4.5 cm radius. The relative angular positions of fingers measured with respect to the thumb position ( $0^\circ$ ) were averaged across all subjects for later equipment settings, Figure 1A. All subjects gave informed consent according to the protocol approved by the Internal Review Board (IRB) of University of Maryland.

Table 3-1 Age and anthropometric data of subjects (n=10).

Age (yrs)		26.2 $\pm$ 3.7
Weight (kg)		70.1 $\pm$ 2.1
Height (cm)		176.3 $\pm$ 4.7
Hand length (cm)		19.9 $\pm$ 1.9
Hand width (cm)		9.1 $\pm$ 0.9
Digit position ( $^\circ$ )	Index	109.0 $\pm$ 12.6
	Middle	156.3 $\pm$ 11.2
	Ring	187.0 $\pm$ 8.2
	Little	240.8 $\pm$ 15.4

Mean $\pm$ S.D. across subjects are reported.

### 3.2.2 Equipment

Five six-component sensors (Nano-17, ATI Industrial Automation, Garner, NC) were attached to a circular aluminum handle whose centers were positioned at the averaged relative angular positions of fingers, Figure 1A. Aluminum caps were attached to the surface of each sensor. The bottom of the cap was flat and mounted on the surface of a sensor while the top part was round (the curvature  $k = 0.222 \text{ cm}^{-1}$ ) to accommodate the curvature of the circle shown as a dotted circle in Figure 1A. Sandpaper [100-grit; static friction coefficients between the digit tip and the contact surface was 1.5; measured previously (Zatsiorsky, Gregory 2002)] was placed on the round contact surface of each cap to increase the friction between the digits and the caps. The radius from the center of the circular handle ( $O_G$ ) to the contact surface ( $r_o^l$ ) was 4.5 cm for each sensor. The force components along the three orthogonal axes and three moment components about the three axes in the local reference system (LRS) for each sensor were recorded, Figure 1B. The whole circular handle with the sensors was mechanically fixed to the head of a heavy tripod (Husky, Quick Set Inc., Smokie, IL). The position of the handle could be adjusted by adjusting

the tripod head while three 15 Kg barbells were loaded on each leg of the tripod to prevent tripod movement during force/torque exertions to the circular handle. The sensors were aligned in the X-Y plane. The plane spanned by the X- and Y-axes will be referred to as the grasp plane (Shim, Latash 2005; Shim, Latash 2005).

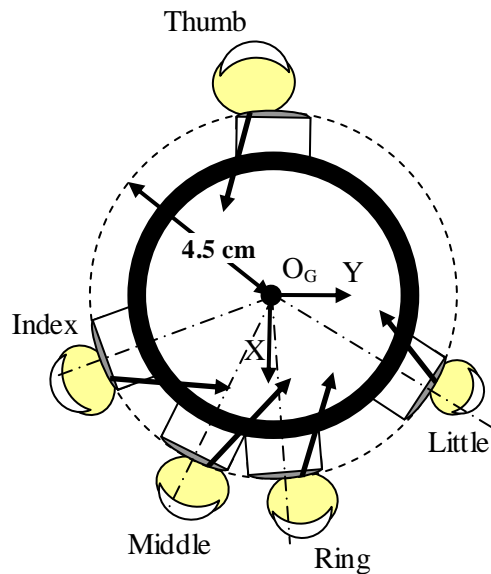


Figure 3-1 Schematic illustration of an aluminum handle (black circle with a large hollow inside) and six-component sensors (white rectangles) at digit contacts.

A total of 30 analog signals from the sensors were routed to two synchronized 12-bit analog-digital converters (PCI-6031 and PCI-6033, National Instrument, Austin, TX) and processed and saved in a customized LabVIEW program (LabVIEW 7.1, National Instrument, Austin, TX) on a desktop computer (Dell Dimension E510, Austin, TX). The sampling frequency was set at 100 Hz.

### 3.2.3 Procedure

Subjects washed their hands with soap and warm water to normalize the skin condition of the hands. The subjects sat on a chair and placed their right upper arm in a forearm brace that was fixed on a table, Figure 2. The forearm was secured with a couple of Velcro straps. The upper

arm was abducted  $\sim 45^\circ$  in the frontal plane and flexed  $\sim 45^\circ$  in the sagittal plane. The forearm was aligned parallel to the sagittal axis of the subject. Two moment axes and two moment directions were used for four task conditions ( $2 \times 2 = 4$ ). Two moment axes were respectively parallel to the anterior-posterior (AP) axis and to the medio-lateral (ML) axis, and the two directions were respectively opening (OP) and closing (CL). The subjects grasped the handle with each digit positioned on the round part of the cap of the designated sensor. Subjects were required to turn the handle 'as hard as possible' for a few seconds for AP-OP (i.e., moment production about the AP axis in OP direction), AP-CL, ML-OP, and ML-CL. The order of conditions was balanced across subjects.

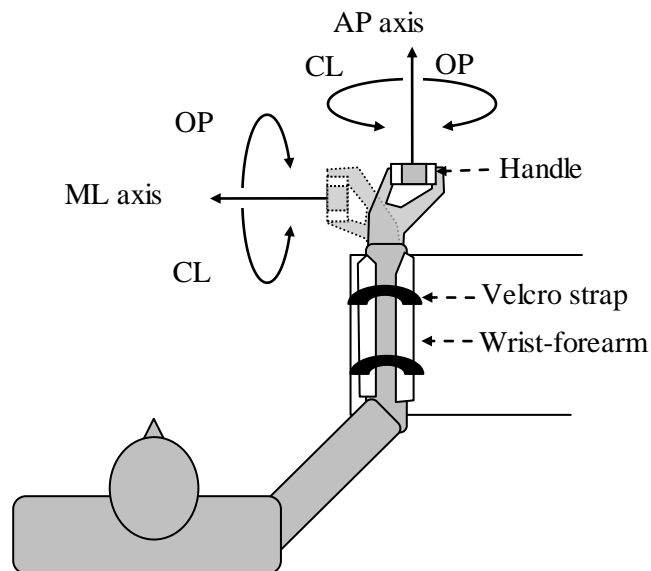


Figure 3-2 Schematic top view of a subject posture during maximum moment production about antero-posterior (AP) or medio-lateral (ML) axes in opening (OP) and closing (CL) directions. A customized plastic wrist-forearm brace with two sets of Velcro straps were used to secure the forearm. The handle was mounted on top of a heavy tripod which is not shown in the figure.

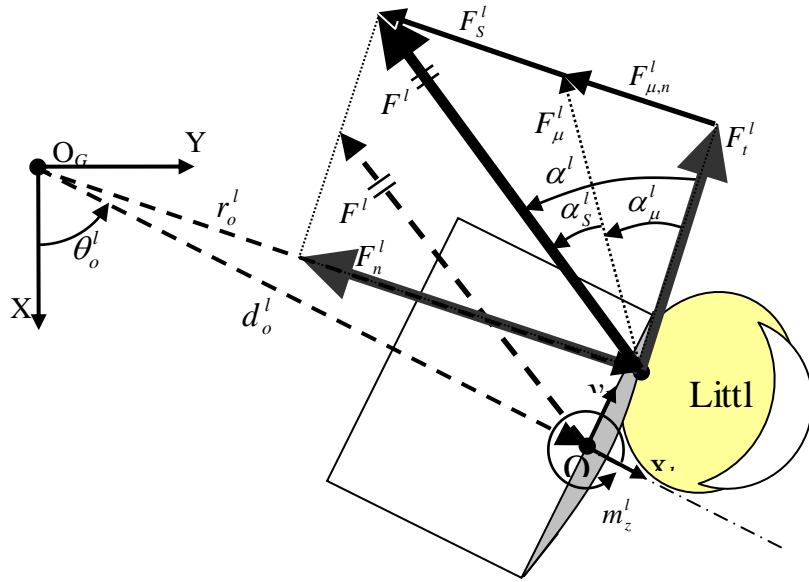


Figure 3-3 Detailed schematic illustration of the little finger producing a force at a contact.  $O_G$ : origin of the global reference system of coordinates (GRS), X: X-axis in GRS, Y: Y-axis in GRS (Z-axis is not shown in the figures, but its positive direction follows the right-handed coordinate system and its positive direction is from paper to the reader),  $O_L$ : origin of local reference system of coordinates (LRS) of the little finger sensor,  $x_i$ : x-axis in LRS of little finger sensor,  $y_i$ : y-axis in LRS of the little finger sensor,  $m_z^l$ : moment about z-axis in LRS of little finger sensor (z-axis in LRS for each sensor is parallel to Z-axes in GRS),  $F^l$ : little finger force,  $F_n^l$ : little finger normal force,  $F_t^l$ : little finger tangential force,  $F_{\mu,n}^l$ : required normal force to avoid slipping of little finger with  $F_t^l$  and friction coefficient ( $\mu = 1.5$ ) of the contact surface,  $F_s^l$ : safety margin of normal force ( $F_n^l - F_{\mu,n}^l$ ),  $d_o^l$ : position of LRS origin in GRS,  $r_o^l$ : position of little finger center of pressure (CoP) in GRS,  $\theta_o^l$ : angular position of  $d_o^l$  in GRS.  $\alpha^l$ : angle between  $F_t^l$  and  $F^l$ ,  $\alpha_\mu^l$ : angle between  $F_t^l$  and  $F_\mu^l$ , and  $\alpha_s^l$ : safety margin of angle ( $\alpha^l - \alpha_\mu^l$ ) for little finger force. The LRS origin ( $O_L$ ) was fixed to the center of the contact surface of the sensor and a cap (shown gray) was fixed on the sensor surface. The distance between the apex of the cap and  $O_L$  was  $\sim 0.81$  mm.

### 3.2.4 Data Processing

Since planar tasks in the grasp plane were employed in this experiment, we focused on individual digit forces in the plane and moments of these forces orthogonal to the plane. Since sticking a digit tip to the contact surface was not allowed in this experiment [so-called ‘soft contact model’ (Arimoto, Tahara 2001; Mason and Salisbury 1985; Nguyen and Arimoto 2002; Shimoga and Goldenberg 1996)], a free moment (Shim, Latash 2005; Shim, Latash 2005; Zatsiorsky 2002) about the direction of a normal force was possible only due to the friction between the digit tip and the contact surface. However, we will not consider this component because the magnitude of this component recorded was ignorable and it does not contribute to the task moment about Z-axis. The moment produced by each digit about Z-axis could be expressed as the sum of the moment produced by the force along y-axis in LRS ( $F_y^j$ ; directly recorded from the sensor) and moment about z-axis at the center of sensor surface ( $m_z^j$ ), Equation 1. In the present experiment, the digit was not in direct contact with the sensor, but rather in contact with the sensor cap. The moment  $m_z^j$  is due to the distance from the LRS origin ( $O_L$ ) where  $m_z^j$  was measured to the point on the sensor cap where the digit force was applied.

The force components measured in LRS origin ( $O_L$ ) were converted into the components in GRS using the direction cosines, Equation 2. These components and the moment about the Z-axis in GRS ( $M_z^j$ ) values computed from Equation 1 were then used to compute the tangential force components ( $F_r^j$ ) at the digit contact on the cap, Equation 3. The normal force component was calculated from Equation 3. Note that the force measured at LRS origin is equivalent to the force produced by the digit in terms of its magnitude and direction.

$$M_z^j = m_z^j + d_o^j \times F_y^j \quad (3-1)$$



$$\begin{bmatrix} F_x^j \\ F_y^j \end{bmatrix} = \begin{bmatrix} \cos \theta_o^j & -\sin \theta_o^j \\ \sin \theta_o^j & \cos \theta_o^j \end{bmatrix} \begin{bmatrix} F_x^j \\ F_y^j \end{bmatrix} \quad (3-2)$$

$$F_t^j = M_z^j / r_o^l \quad \text{and} \quad F_n^j = \sqrt{(F_x^j)^2 + (F_y^j)^2 - (F_t^j)^2} \quad (3-3)$$

$j$  is one of the five digits, i.e. thumb, index, middle ring, little.

The safety margin of normal force ( $F_s^l$ ) was calculated as the magnitude difference between the normal force ( $F_n^j$ ) calculated from Equation 3 and the minimal normal force ( $F_{\mu,n}^l$ ) required to avoid slipping of a digit tip on the contact surface with the given friction coefficient  $\mu$ , Equation 4 (Kinoshita, Murase 1996; Pataky, Latash et al. 2004; Westling and Johansson 1984). The relative safety margin was expressed as the ratio of  $F_s^l$  to  $F_n^l$ . The safety margin of force angle ( $\alpha_s^l$ ) was calculated as the difference between the recorded force angle ( $\alpha^l$ ) and the minimum angle of force ( $\alpha_{\mu}^l$ ) required to avoid slipping of digit tip with a given tangential force, Equation 5.

$$F_s^l = F_n^l - F_{\mu,n}^l \quad (3-4)$$

$$\alpha_s^l = \alpha^l - \alpha_{\mu,n}^l \quad (3-5)$$

Resultant force ( $F^{re}$ ) is the force that could have caused a translational effect of the handle if the handle had not been mechanically fixed to the tripod. This force is also known in the literature as the manipulation force (Gao, Latash et al. 2005). Internal force ( $F^{in}$ ) is a set of forces that cancel out due to oppositions of digit forces. Thus, it does not cause a translational effect, even on a free handle.  $F^{re}$  and  $F^{in}$  were calculated along X- and Y-axes, Equations 6 and 7.

$$\begin{bmatrix} F_X^{re} \\ F_Y^{re} \end{bmatrix} = \begin{bmatrix} \sum_{j=1}^5 F_X^j \\ \sum_{j=1}^5 F_Y^j \end{bmatrix} \quad (3-6)$$

$$\begin{bmatrix} F_X^{in} \\ F_Y^{in} \end{bmatrix} = \begin{bmatrix} \sum_{j=1}^5 |F_X^j| - |F_X^{re}| \\ \sum_{j=1}^5 |F_Y^j| - |F_Y^{re}| \end{bmatrix} \quad (3-7)$$

Equation 7 yields the total internal force, i.e. the sum of magnitudes of force components acting in X and Y directions that cancel each other. This value is different from the usually determined grip or pinch force. We explain the difference with an example: suppose that a grip force recorded at rest equals is 10 N. This means that both the thumb and the opposing finger each exert a 10 N force. Equation 7 in such a case would yield an internal force of 20 N. We used this method of internal force computation rather than determining an average internal force per digit (i.e. dividing the total force by five) because in the circular grasps the individual normal digit forces act in different, but not necessarily opposite, directions. We do not address an internal moment, i.e. a set of local moments in opposite directions that cancel each other (Gao, Latash 2005) because in the present experiment the moments produced by each digit were always in the same direction of the task moments.

### 3.2.5 Statistics

Standard descriptive statistics and repeated-measures ANOVA with the within-subject factors of DIGIT [5 levels: thumb (T), index (I), middle (M), ring (R), and little (L)], AXIS [2 levels: antero-posterior (AP) and meteo-lateral (ML) axes], DIRECTION [2 levels: opening (OP) and closing (CL) directions], and COORDINATE (2 levels: X-axis and Y-axis) were performed. The level of significance was set at  $p = .05$ . Although the safety margin of angle ( $\alpha_s^l$ ) has a circular

nature (Rao and Sengupta 2001), it was treated as a linear variable because  $\alpha_s^l$  values formed a data cluster in the same quadrant. The Kolmogorov-Smirnov test and Shapiro-Wilk test were used to test violation of the normal distribution assumption, and Levene's homogeneity test to test the assumption of variance homogeneity. The data in figures are presented as group means and standard errors (S.E.).

### 3.3 Results

#### 3.3.1 Digit normal forces

At the time of maximum resultant moment production, subjects produced the largest normal force with a thumb and the smallest with a little finger ( $T > R = M = I > L$  and  $R = I$ ), Figure 3A. This finding was supported by three-way ANOVA with the factors of DIGIT, AXIS, and DIRECTION, which showed a significant effect of DIGIT [ $F(4,36)=162.5, p<.001$ ]. On average, the sharing of

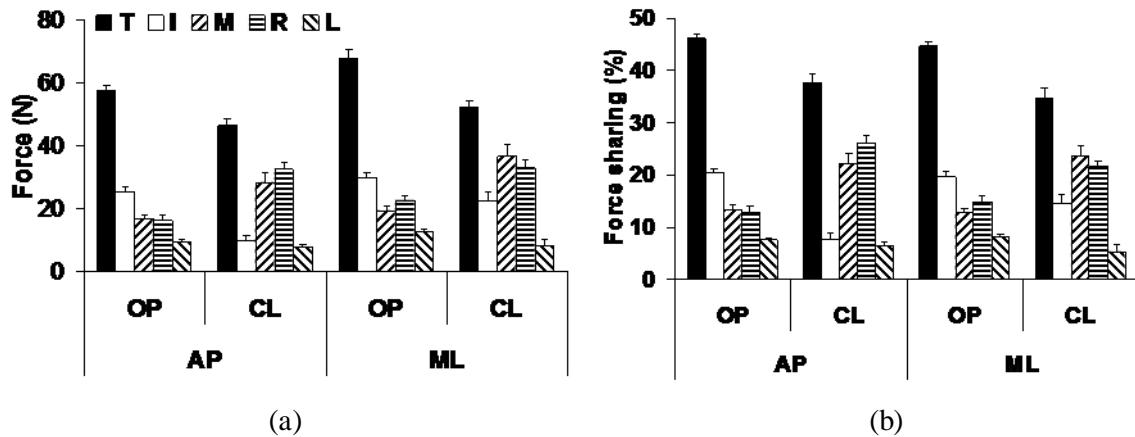


Figure 3-4 (a) Individual digit normal forces and (b) sharing at the time of maximum resultant moment about antero-posterior (AP) and medio-lateral (ML) axes in opening (OP) and closing (CL) directions. T, I, M, R, and L, respectively, represent thumb, index, middle, ring, and little fingers. Mean  $\pm$  S.E. across subjects are presented.

the total normal force by individual digits was in the order of T (40.8%), R (18.8%), M (18.0%), I (15.5%), and L (6.9%), Figure 3B. There was no significant AXIS effect found.

### 3.3.2 Individual digit tangential forces and their moments

Due to the perfect linear relation between the individual digit tangential forces and individual digit moments ( $F_t^j = M_Z^j / r_o^l$ ;  $r_o^l$  is a constant), and the same expected results for statistical analysis, we will discuss only the individual digit moments. Subjects produced the largest moment by the thumb and the smallest moment by the little finger and it was in the order of anatomical digit alignments from the thumb to the little finger [T (thumb) > I (index) > M (middle) = R (ring) > L (little);  $F(4,36)=76.2, p<.001$ ], Figure 4A. The subjects produced the larger total moment in CL direction than in OP direction (AP-OP:  $2.01 \pm 0.12$ , AP-CL:  $2.82 \pm 0.34$ , ML-OP:  $2.12 \pm 0.16$ , and ML-CL:  $2.47 \pm 0.26$ ), which was reflected by a significant effect of DIRECTION [CL > OP;  $F(1,9)=10.19, p<.01$ ]. The sharing of the total moment by the digits was

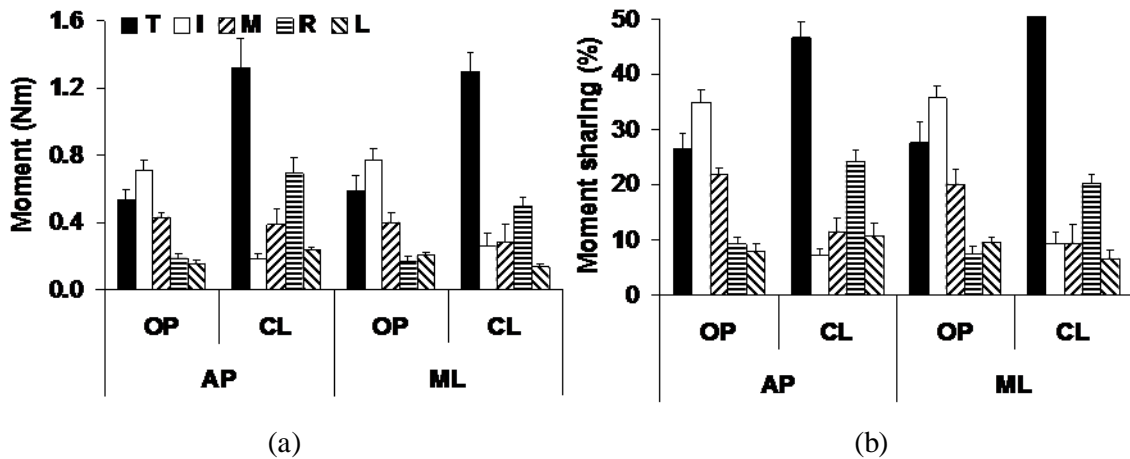


Figure 3-5 (a) Moments of individual digit tangential forces and (b) their sharing at the time of maximum resultant moment about antero-posterior (AP) and medio-lateral (ML) axes in opening (OP) and closing (CL) directions. T, I, M, R, and L, respectively, represent thumb, index, middle, ring, and little fingers. Mean  $\pm$  S.E. across subjects are presented.

T (38.8%), I (21.8%), M (15.6%), R (15.2%), and L (8.6%). There was no significant AXIS effect found.

### 3.3.3 Internal and Resultant forces

Subjects produced about twice as large an internal forces along the X-axis than the Y-axis [X-axis > Y-axis;  $F(1,9)=279.0$ ,  $p<.001$ ], Figure 5. This reflects that the internal force was larger in the direction of thumb normal force than in the direction orthogonal to it. The internal force was 14% larger for ML axis than AP axis [ML > AP;  $F(1,9)=11.39$ ,  $p<.01$ ] and 20% larger in CL than in OP [CL > OP;  $F(1,9)=17.44$ ,  $p<.01$ ].

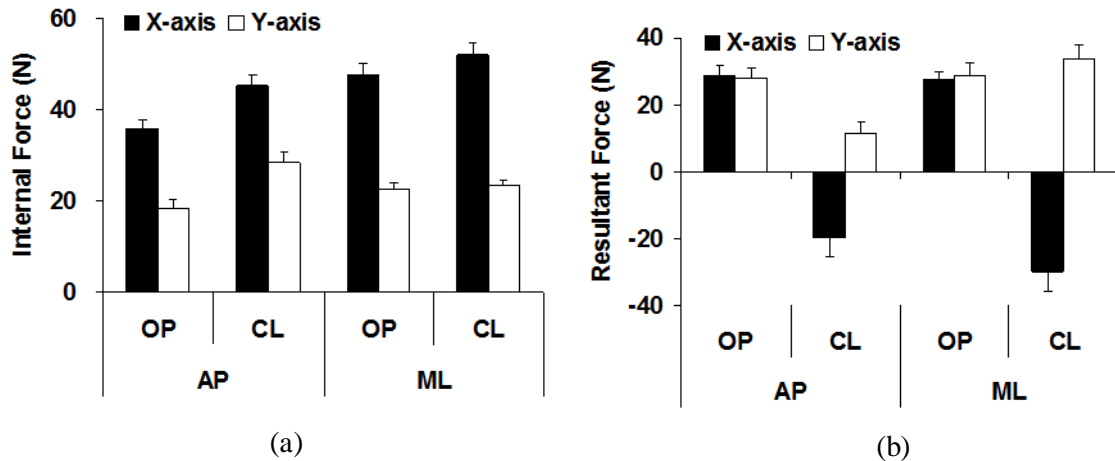


Figure 3-6 (a) Internal force and (b) resultant force at the maximum moment production in opening (OP) and closing (CL) tasks about the antero-posterior (AP) and medio-lateral (ML) axes. Mean  $\pm$  S.E. across subjects are reported for each task condition.

The resultant forces along X-axis during moment production in CL direction were negative for all subjects while the resultant forces for other conditions were all positive. In other words, the thumb force along X-axis was smaller than the resultant force of fingers along X-axis for CL direction, but larger for OP direction. However, when three-way ANOVA was run on the magnitudes of resultant forces, the resultant forces did not show any effects of AXIS,

DIRECTION, or COORDINATE. Significant interactions in resultant force magnitudes were found in AXIS X DIRECTION [F(1,9)=13.2,  $p < .01$ ] and AXIS X DIRECTION X COORDINATE [F(1,9)=7.2,  $p < .05$ ].

### **3.3.4 Safety margins of normal forces and force angles**

The thumb and little fingers showed the largest and smallest safety margins of normal forces, respectively. On average, they were in the order of T (41.8 N), R (20.2 N), M (19.4 N), I (14.3 N), and L (6.8 N) [T > R = M = I > L and R > I; F(4,36)=91.9;  $p < .001$ ], Figure 6. The safety margin for ML axis was larger than AP axis [ML > AP; F(1,9)=56.4;  $p < .001$ ]. No significant DIRECTION effect was found while a significant effect of DIGIT x DIRECTION [F(1,9)=42.2;  $p < .001$ ] was observed. The relative values of the safety margins (% of the exerted normal forces) showed the largest and smallest values in the thumb and index finger, respectively [T (72.2%) > R (79.1%) > M (73.2%) > L (67.9%) > I (61.6%); F(4,36)=9.5;  $p < .001$ ]. There were significant effects of AXIS [ML > AP; F(1,9)=24.0;  $p < .005$ ] and all factor interactions, but no significant effect of DIRECTION [F(1,9)=3.9;  $p = .078$ ].

Compared to the force safety margins, the safety margins of the individual digit force angles showed somewhat different results: the largest in the ring finger [R (38.8 °) > M (35.2 °) = T (34.7 °) = L (31.5 °) > I (28.6 °), M = L, M > I, and T = I; F(4,36)=9.93;  $p < .001$ ]. The safety margins of force angles were larger for ML axis than AP axis [ML > AP; F(1,9)=20.76;  $p < .01$ ]. A significant DIRECTION effect was not found while there were significant effects of all factor interactions.

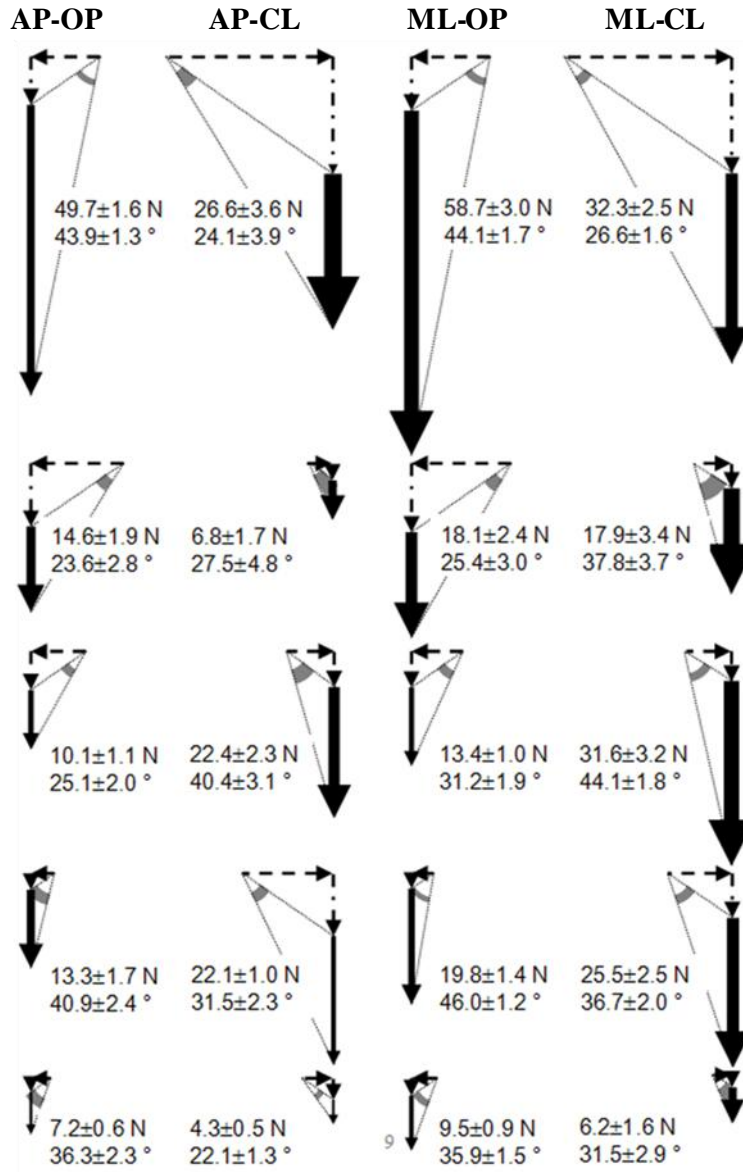


Figure 3-7 Safety margins of individual finger normal forces and force angles about the antero-posterior (AP) and medio-lateral (ML) axes in opening (OP) and closing (CL) tasks. The normal and tangential forces are shown as horizontal and vertical arrow, respectively. The mean and S.E. values of the safety margin of normal force and force angle across all subjects are shown next to each force vector diagram for each digit in each task condition. The mean and S.E. values of the safety margin of normal force are respectively shown as the length and thickness of a solid arrow while the mean and S.E. values of safety margins of force angle are respectively shown as the angles and their thickness.

### **3.4. Discussion**

#### **3.4.1 Sharing of normal forces and moments of tangential forces**

During the moment production on a circular object in this study, individual digit normal and tangential forces were not evenly distributed. Their sharing pattern was similar to that of previously reported individual MVC forces during digit-tip pressing (Olafsdottir, Zatsiorsky et al. 2005), i.e. among all five digits, the thumb contributes the largest sharing while little finger has the smallest sharing. In a study on forceful grasping of a circular object, Kinoshita et al. (1996) showed that the sharing pattern of the individual digit normal forces was consistent regardless of the weight of the object. Although our study was different from Kinoshita's in terms of the task (moment production vs. force production), our study also showed that the sharing pattern of normal forces during moment production was not affected by such task conditions as the wrist position or the direction of the moment.

It has been known that the finger forces during the tasks of grasping force production or grasping moment production are affected by the wrist positions (Fong and Ng 2001; Hazelton, Smidt et al. 1975; Jung and Hallbeck 2002; Li 2002). In particular, Dumont et al. (2005) recently performed an experiment of repetitive dynamic movements of wrist flexion-extension with a cylindrical handle and reported different sharing of digit-tip forces at contacts with the handle throughout the wrist movements. However, in this study the sharing of the moments of individual digit tangential forces did not depend on whether the torque was generated by the pronation-supination efforts (AP axis) or by the ab/adduction efforts (ML axis). The sharing of individual finger normal forces showed changes due to the moment directions such as opening and closing actions.

Besides the intrinsic and extrinsic muscles for grasping, the moment production tasks require pronators and supinators during moment production about the AP axis and muscles for radio-ulnar deviations during the twisting actions about the ML axis. Thus, this finding suggests that



the moment sharing patterns among individual digits are preserved regardless of the muscle groups utilized for moment productions, although the muscle groups affect the normal force sharing.

The lack of statistically significant effects of the AXIS orientation on the sharing pattern of the tangential forces or moments of tangential forces adds another fact to the discussion on whether the tangential forces of individual fingers work as active force generators or they are just passive force transmitters, similar to the fingers of robot hands and grippers (Pataky, Latash et al. 2004). In most of robotic hands, all the finger joints are simple hinges and the tangential (lateral) forces are supported by the structure and transmitted to the hand-held object via the fingers passively. In humans, the metacarpophalangeal (MCP) joints have a freedom to move in the radial-ulnar direction and hence exerting a tangential force requires a generation of the ab/adduction moment at the MCP joints. However, the passive resistance at the joint may also contribute to the moments at the MCP joints. To answer the question on the relative contribution of the active moment generation versus passive resistance to the total moment at the MCP joints, the electromyographic (EMG) recordings of the internal muscles of the hand are necessary.

### **3.4.2 Total moments in opening and closing directions**

The maximum torque (8.7 Nm) previously reported during opening actions of a 'jar' (Voorbij and Steenbekkers 2002) was four times larger than the maximum torque (2.1 Nm) found in our study. The difference could be due to (a) the difference between the diameters of the circular objects [6.6 cm in Voorbij and Steenbekkers (2002) vs. 4.5 cm in this study], (b) the different grasping configurations (two-hand power grip vs. multi-digit precision grip), and different friction coefficients of the contact surfaces (unknown coefficient of aluminum surface vs. 1.5).

The total moment was larger in closing direction than in opening direction. However, the maximum moment production capability was the same for pronation-supination (AP) and radio-

ulnar deviation (ML) actions. Thus, the currently popular design of circular valves and jar lids may cause difficulties in opening. In everyday activities, a jar lid or a circular valve closed with the maximum moment may be hard to be opened due to the smaller moment production capability in the opening direction. This difficulty may also be contributed by the difference between dynamic and static frictions during closing and opening movements, i.e. the dynamic friction during closing is usually smaller than static friction for initiation of opening (Blau 1996; Zatsiorsky 2002). Thus, a larger moment is required to open a circular valve than to close at the same angular position. Based on the directional difference in the maximum moment production capability found in this study and a previous study (Shim, Latash 2004), one could suggest a modification of the current design of circular jar caps or valves, i.e. a switched design of opening and closing directions, although a stronger suggestion on this direction switch would require studies on many other variations of moment production conditions in different subject groups such as grasping types, inclusion of female/elderly people, etc.

### **3.4.3 Internal force and safety margin**

The larger internal forces were found for radio-ulnar deviation actions of the wrist than pronation-supination action. If a large internal force is considered as an index of inefficient force use, one can suggest that the normal forces are used in a larger efficiency for pronation-supination than radio-ulnar deviations.

Due to the geometry of the circular handle, only a tangential force, not a normal force, can produce a moment around the axis orthogonal to the grasp plane. Humans usually exert a larger normal force to an object than absolutely necessary to prevent the object from slipping (Gao, Latash et al. 2005; Gordon, Westling et al. 1993; Hager-Ross, Cole 1996; Johansson and Cole 1994). In this study, we also found significantly larger individual digit normal forces than the normal forces that are mechanically required. Although the order of normal force safety margin

did not follow the anatomical order of digits, the largest and smallest safety margin values were found in the thumb and little finger, respectively.

Although the safety margin forces are considered to serve to avoid fingers from slipping at contact surfaces and to increase grasping stability (Cole and Johansson 1993; Goodwin, Jenmalm et al. 1998; Pataky, Latash et al. 2004), one can consider the safety margin as an index of normal force inefficiency because, in particular, the moment production tasks on a circular object do not require any safety margin forces. In this context, the thumb and little finger had the smallest and largest efficiencies of normal force use since they showed largest and smallest safety margins, respectively. The underlying mechanism which determines different safety margins for different digits is not yet clear and remains for further investigations.

### **3.5. Conclusion**

From the current study on five-digit moment productions on a circular object, we conclude that (1) the maximum torque in the closing direction is larger than in the opening direction, (2) the thumb and little finger, respectively, have the largest and the smallest sharing for both total normal force and total moment, (3) the sharing pattern of moments of individual digit tangential forces is not affected by the orientation of torque axis or the torque direction while the sharing of normal forces changes due to the torque direction, and (4) the normal force safety margins have the largest values in the thumb and the smallest values in the little finger.

## Chapter 4

### **Multi-digit submaximal torque production task on a circular object**

#### Abstract

This study investigated the relationship of individual digit normal forces and tangential forces during a submaximal torque production on a fixed circular object. The geometry shape makes it possible to decouple a contact force into two force components: normal force for grasping stability and tangential force for rotating action. The hypotheses are: (1) normal forces and tangential forces are modulated by wrist positions and torque directions; (2) initial normal force alters the dynamic process and the final value of safety margin. Subjects grasped a circular handle with one of the four normal force levels (0%, 10%, 20%, or 30% of maximum, GRASP phase), followed a visual template from 0% to 20% of maximum torque in 6 seconds (RAMP phase), and held the torque constant for another 4 seconds (HOLD phase). Subjects were asked to produce torque about medial-lateral or anterior-posterior axis in clockwise or counterclockwise direction. In total, each subject performed 16 conditions (2 wrist positions: (ML and AP) X 2 torque directions (CW and CCW) X 4 initial normal force levels = 16). The normal force and tangential force components at each digit contact were measured. Safety margin, the extra normal force over slip threshold, was calculated in order to quantify the relationship between normal force and tangential force. Results include: (1) in constant torque production (HOLD phase), the total normal force was changed by initial normal force and wrist position systematically, but the contribution by individual digits to the total normal force was affected only by torque direction; (2) during initial grasping (GRASP phase) when the torque was close to zero, the radial finger pair (index and middle fingers) and the ulnar finger pair (ring and little fingers) generated torques in opposite direction; (3) with higher initial normal force level, safety margin changed slower in RAMP phase and the final safety margin in HOLD phase was larger. In conclusion, this study

showed that in submaximal torque production, the action of grasping and rotating, as evidenced by normal force and tangential force respectively, were regulated by initial normal force, wrist position, and torque direction separately.

Keywords: *normal force; tangential force; torque; circular object; safety margin*

## 4.1 Introduction

Manipulation of objects with circular geometry shape like balls or discs is a common activity people engage in daily activities. A better understanding of biomechanics in circular object manipulation is beneficial to elderly people or patients with reduced strength, as well as to people in industry environment where repetitive and forceful operation of machines may induce muscle fatigue or injuries (Kuo, Chang et al. 2009; Kutluhan, Akhan 2001). Previous studies on circular object manipulation investigated the effects of handle size and number of digits involved (Kinoshita, Murase 1996), hand size and contact area (Seo and Armstrong 2008), on interphalangeal joint force (Amis 1987; Fowler and Nicol 2002) and force distribution (Freund, Toivonen 2002). These results often focus on forces perpendicular to contact surface (grasping force) or along longitudinal axis (push/pull force). Tasks involving production of torque/rotating force tangential to contact surface, like rotating a door knob or opening a jar, have not been fully studied (Long, Conrad et al. 1970; Shim, Huang et al. 2007). In our previous experiment, subjects produced maximum voluntary torque with different wrist positions and torque directions. We found that these two factors affect total normal force and resultant torque independently. In particular, normal force is larger when wrists are extended, and the maximum torque in the clockwise direction is greater than in the counterclockwise direction.

The current study investigates normal force and torque during submaximal torque production. It is important because maximum effort is often not necessary or even hazardous, as in the case of rotating a door knob. Take ball throwing as another example. In order to achieve the desired trajectory and spinning of the ball, a precise control of the magnitude and timing of torque and normal force is essential (Jinji and Sakurai 2006). In such tasks, there are infinite possible combinations of forces from individual digits, i.e. the problem of redundancy (Bernstein 1967; Latash 2000). How normal force and torque components are distributed among individual digits is one of the goals in this study. A coordination pattern of either component, if it exists, might

exhibit distinct dependency on wrist position and torque direction similar to maximum torque task.

In various grasp studies, a steady hold of objects is required before further manipulation. This implies a sufficient initial normal force to prevent objects from slipping. In fact, for a given load force or tangential force, people usually produce extra normal force, which is called safety margin (Westling and Johansson 1984). A higher safety margin leads to better capability to resist perturbation, but also increased chance of muscle fatigue and injury and less efficient use of normal force (Lin and McGorry 2009; Seo 2009). Researchers found that safety margin can be affected by object properties, e.g. surface material, fragility, geometry, and external constraints, e.g. number of digits used, subject populations of different age, psychological status, or with pathological conditions (Gorniak, Zatsiorsky et al. 2010; Westling and Johansson 1984; Winges, Eonta et al. 2009). It has been shown that a initial normal force increases not only the stiffness of finger, wrist joints (Nakazawa, Ikeura et al. 2000; Winges, Soechting et al. 2007), whole-hand grasping (Van Doren 1998), and the contact area of each digit and leads to change of viscosity and compliance of finger pad (Jindrich, Zhou et al. 2003). Therefore, we hypothesize that safety margin will be modified by changing initial normal force.

This study investigates sharing patterns of individual digit normal forces and torque as well as safety margin in an isometric submaximal torque production task. Subjects produced 20% of their maximum torque on a mechanically fixed circular handle under visual feedback. Normal forces and tangential forces of all five digits are calculated from data of 3D force/torque sensors. Three factors are systematically changed: wrist position (*Axis*), torque direction (*Direction*) and initial normal force level (*Grip*). These factors can reveal possible effects of muscle groups (pronation, supination, ulnar deviation and radial deviation) and initial normal force on the coordination pattern of normal force and torque, and the safety margin, respectively.

## **4.2 Methods**

### **4.2.1 Subjects**

Ten right handed male volunteers ( $25.4 \pm 3.2$  years old), without history of neurological disorder or injuries on the upper extremity, were recruited for this study. The average height was  $173.2 \pm 5.4$ cm and the average weight was  $68.5 \pm 5.3$ kg. The right hand length, averaged  $20.1 \pm 2.3$ cm, was measured as the distance from the midpoint of transverse wrist crease to the tip of the middle finger. The hand width, averaged  $8.9 \pm 1.8$ cm, was measured as the distance from the radial side of the index finger to the ulnar side of the little finger at the metacarpophalangeal joint level. During the preparation stage, they were asked to naturally grasp a wooden circular module of the same size as the aluminum handle used later. The angular positions of the fingers relative to the thumb were measured and averaged across subjects. All subjects provided informed consent according to the standards required by the University of Maryland's Institutional Research Board.

### **4.2.2 Apparatus**

Five 3D force/torque sensors (NANO-17, ATI Industrial Automation, Garner, NC, USA) were placed on an aluminum circular handle, with a radius of 4.5cm after installment. The relative angular positions of the sensors for the fingers with respect to the sensor for the thumb were calculated above. A spherical rubber cap was mounted on top of each sensor to conform to the circular contour (Figure 1a). Sandpaper (110-grit, with the static coefficient of friction of 1.5 measured in (Zatsiosky 2002)) was used to cover the caps to increase the friction between the digit tips and contact surface. The handle was fixed on a tripod in appropriate height and orientation.

A total of 30 analog signals from the sensors were routed to two synchronized 12-bit analog-digital converters (PCI-6031 and PCI-6033, National Instrument, Austin, TX) and processed and



saved in a customized LabVIEW program (LabVIEW 7.1, National Instrument, Austin, TX) on a desktop computer (Dell Dimension E510, Austin, TX). The sampling frequency was set at 100 Hz.

### **4.2.3 Procedure**

Before the experiment, subjects washed their hands with warm water and soap to neutralize skin condition. Subjects sat on a chair in front of a monitor screen and fixed the right upper arm in a customized plastic brace (Figure 4-1b). The upper arm was abducted about 45° in the frontal plane and flexed about 45° in the sagittal plane. The forearm was aligned parallel to the sagittal line of the subject and secured with two sets of Velcro straps. The flexion/extension angle of the wrist was adjusted and fixated. After the preparation, subjects were asked to carry out the two experiments in sequence.

#### *Experiment I (MVT task)*

Subjects were asked to produce maximum voluntary torque (MVT) in either clockwise (CW) or counterclockwise (CCW) direction, with the direction of the grasp plane (the plane enclaves the circular handle and five digit tips, see Fig4-1b) parallel to medial-lateral (ML) axis or anterior-posterior (AP) axis. Subjects performed one trial for each condition. Experimenters recorded the maximum resultant torque ( $T^{\max}$ ) and the total normal force ( $F_n^{\max}$ ) at the moment when  $T^{\max}$  was achieved for the four conditions. A 3-minute break was given between trials to avoid muscle fatigue.

#### *Experiment II (Sub-MAX task)*

In this experiment, the monitor screen was divided into left and right panels. On the left panel, the total normal force was shown as a watermark moving vertically, indicating the total normal force produced. The target line was indicated by a red bar, which was shown in one of four different

positions, i.e. 0%, 10%, 20%, and 30% of  $F_n^{\max}$ . On the right panel, the trajectory of torque generated (yellow line) was displayed on top of a torque template (black line).

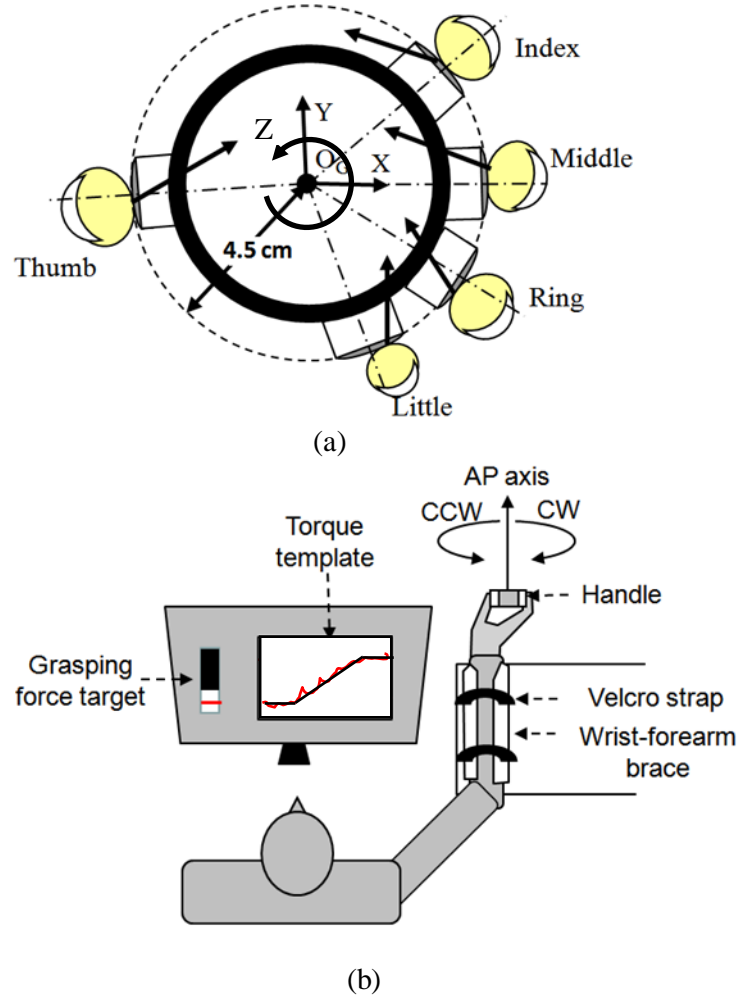


Figure 4-1 (a) The grasp plane including the circular handle and five digit tips viewed from the subject side. The thick black circle was the circular handle, and the dotted one represented the circular contour after mounting sensors. Global reference frame was defined as X: pointing to the right side of subjects; Y: upward; Z: pointing towards palm. (b) subject watched the visual feedback in a computer monitor during *Submaximal* task. The torque template was comprised of three segments, i.e. GRASP: no torque (subjects adjusted the normal/grasping force); RAMP: increase torque linearly; HOLD: keep the torque constant at 20%.

When a trial started, subjects first matched the total normal forces to one of the normal force levels for four seconds (GRASP phase in Figure 4-1b). For 0% of  $F_n^{\max}$  trials, there was no initial contact between the digits and the handle until the end of GRASP phase. Subjects then followed the template and increased the torque to 20% of  $T^{\max}$  in six seconds (RAMP phase), and held the torque constant for another four seconds (HOLD phase). For each condition, subjects practiced a few times before the experiment started. A total of 16 trials, one initial normal force level with each combination of wrist position (ML or AP) and torque direction (CW or CCW), were recorded. At least 2-minute break was given between trials. Subjects did not report any discomfort during or after the experiment.

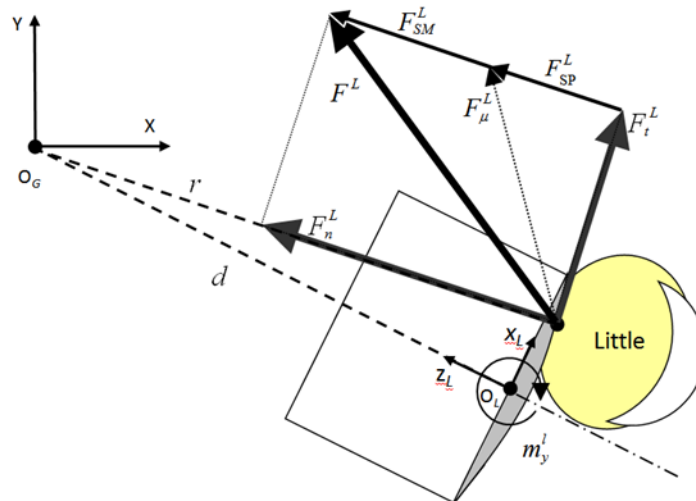


Figure 4-2 An example of labeling notion in this study. Global and local reference systems ( $O_G$  and  $O_L$ ) were represented by capital letters and lowercase letters, respectively.  $r$  is the radius of the circular contour (4.5cm) and  $d$  is the distance from the center of the handle to the center of top surface of one sensor (about 4.3cm). Grey area is the spherical rubber cap.  $F_n^L$ ,  $F_t^L$ ,  $F^L$ ,  $F_{SP}^L$ ,  $F_{\mu}^L$ ,  $F_{SM}^L$  represent normal force, tangential force, total force, minimal normal force, critical total force and safety margin of the little finger, respectively.

#### 4.2.4 Data Processing

Individual digit force and torque data were processed with a customized Matlab program (Mathworks, Netick, MA). A zero phase-shift Butterworth filter was used to remove any noise above 25Hz (Shim, Latash 2005). Because the data were recorded on the local centers of top surface of the sensors ( $O_L$ ), a transformation was performed to compute the actual forces and torques at the points of application of forces. According to the “soft finger” assumption (Arimoto, Tahara 2001; Mason and Salisbury 1985), a free moment about the direction of a normal force exists due to the rotational friction between the digit tip and the contact surface (Figure 4-2). However, we did not consider this component because it did not contribute to the task torque about the Z-axis and the magnitude of this component recorded was ignorable. Tangential force was the sole source for the torque, thereby chosen as one of the dependent variables instead. According to the principal of parallelism, this torque equaled the torque by local force  $f_x$  subtracted by the free moment  $m_y$ .

$$M_Z^{(j)} = F_t^{(j)} r = f_x^{(j)} d - m_y^{(j)} \quad (4-1)$$

See Figure 4-2 for labeling notions of each variable.  $j$  stands for a specific digit (T, I, M, R, L for thumb, index, middle, ring, and little finger). The tangential force  $F_t^{(j)}$  and normal force  $F_n^{(j)}$  of digit  $j$  on the contact surface was thereby computed as follows.

$$F_t^{(j)} = (f_x^{(j)} d - m_y^{(j)}) / r \quad (4-2)$$

$$F_n^{(j)} = \sqrt{(F_x^{(j)})^2 + (F_z^{(j)})^2 - (F_t^{(j)})^2} \quad (4-3)$$

Safety margin was defined as the difference between the actual normal force and the minimal normal force  $F_{sp}$  that was necessary to prevent the digit tip from slipping (Westling and Johansson 1984). In order to compare across conditions, it was normalized by the normal force.

$$SM = \frac{F_n - F_{SP}}{F_n} = \frac{F_n - |F_t| / \mu}{F_n} \times 100\% \quad (4-4)$$

where  $\mu$  is the static friction coefficient. The absolute of tangential force was used because the resultant torque in GRASP phase might be negative.

In this experiment, no constraint was imposed on the amount of normal force after the initial GRASP phase. Subjects often overpowered with excessive normal force, causing a quite large safety margin throughout a trial. A recent study used Fisher's transformation to adjust for the saturation effect of safety margin (Gorniak, Zatsiorsky 2010). We found, however, the final safety margin was affected by the initial normal force. Hence Fisher's transformation was not clearly defined in this case. Instead, the temporal profile during the RAMP phase was fitted with an exponential function (see Figure 4-9 in Results section for a demonstration). The decaying constant  $b$  in equation (4-5) was calculated and compared across conditions.

$$SM(t) = SM_{\text{end}} + (SM_{\text{init}} - SM_{\text{end}})e^{-b(t-t_{\text{init}})} \quad (4-5)$$

where  $t_{\text{init}} = 4\text{s}$ , and  $SM_{\text{end}}$  and  $SM_{\text{init}}$  were calculated as the average of SM over one-second window right before and after the RAMP phase.

#### 4.2.5 Statistical analysis

Repeated measures MANOVA were performed for individual and resultant normal forces and tangential forces, with the within-subject factors of torque *Direction* (counterclockwise, CCW and clockwise, CW), wrist *Axis* (medial-lateral, ML and anterior-posterior, AP) and *Grip* (0%, 10%, 20%, and 30%). For normal and tangential force sharing, the effect of *Grip* was indecisive because of insufficient residual degree of freedom. Wilk's Lambda test scores were reported when appropriate. When comparing forces before and after the RAMP phase, the 1-second time averages were computed and *Phase* was added as additional factor. Both actual and normalized values of normal forces and tangential forces were compared. Levene's homogeneity test was

used to test the assumption of variance homogeneity. Bonferroni test was used for the main effect comparison. The level of significance was set at  $p = 0.05$ . The data in figures were presented as means and standard errors.

### 4.3 Results

Figure 4-3 shows the time profiles of the total normal forces and tangential forces from a typical subject when the wrist was aligned along ML axis and the torque direction was in CCW.

Although the error of initial normal force increased with the force level ( $Grip: F(2,8) = 14.257, p = 0.002$ ), the tangential forces matched the template very well. The error of tangential force during the HOLD phase did not show any difference for any factor or interaction ( $2.0 \pm 0.1\%$ ).

When starting with an initial normal force, the normal forces tended to freeze or drop a little before rose again. The following subsections examine each variable in more detail.

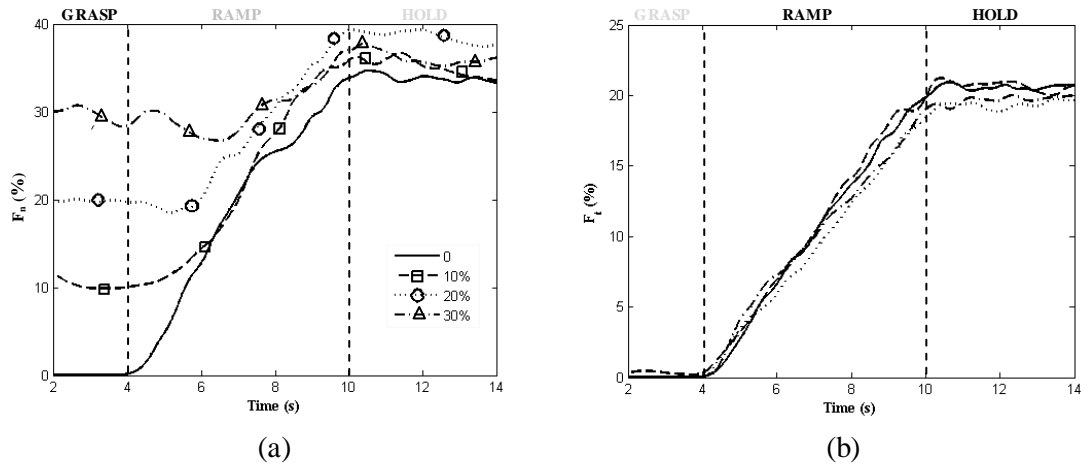


Figure 4-3 Time profiles of (a) total normal forces and (b) tangential forces from a representative subject in the ML/CCW condition. The subjects reached a certain normal force level first (GRASP phase: left), then controlled the torque/tangential force by following the template (RAMP and HOLD phase, right). All forces were normalized by  $F^{\max}$  and  $T^{\max}$ , respectively.

### 4.3.1 Total and individual digit normal forces

#### *MVT task*

Subjects produced greater normal forces along AP axis ( $155.6 \pm 3.6\text{N}$ ) than along ML axis ( $127.1 \pm 2.5\text{N}$ ) ( $F(1,9) = 40.8, p < 0.000$ ). No *Direction* effect or interaction was found.

#### *Sub-MAX task*

The total normal force should match one of the four target levels in the GRASP phase, but was not specified in the HOLD phase. As in MVT task, the total normal force was greater along ML axis (*Axis*,  $F(1,9) = 15.5, p = 0.003$ ). However, when normalized by  $F^{\text{max}}$ , there was no difference between the two wrist positions. Increasing the normal force in the initial GRASP phase led to larger normal force in the HOLD phase (44.6N, 45.4N, 49.5N, and 52.7N for 0%, 10%, 20%, and 30%, respectively;  $F(3,27) = 14.4, p < 0.000$ ) although the difference was much smaller than the initial values.

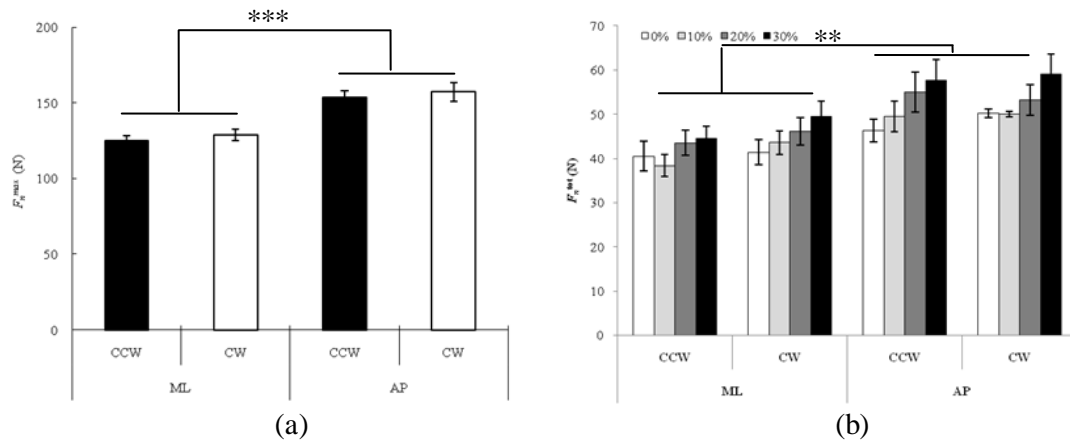


Figure 4-4 Total normal force in (a) MVT task and (b) HOLD phase in sub-MAX task.

The sharing pattern of normal force was altered only by *Axis* ( $F(5,5) = 10.8, p = 0.01$ ) in the GRASP phase. In contrast, in the HOLD phase, torque *Direction* had significant effects on all except for the little finger. More specifically, thumb and index finger contributed more in the

CCW direction, while middle and ring fingers more in the CW direction (Figure 4-5). On average, the normal force sharing was Thumb (44.3%), Ring (18.8%), Index (14.5%), Middle (13.6%), and Little (8.8%) with ( $T > R = I = M = L$ ,  $R > M$ ,  $I > L$ , the differences were significant at  $p < .05$ ).

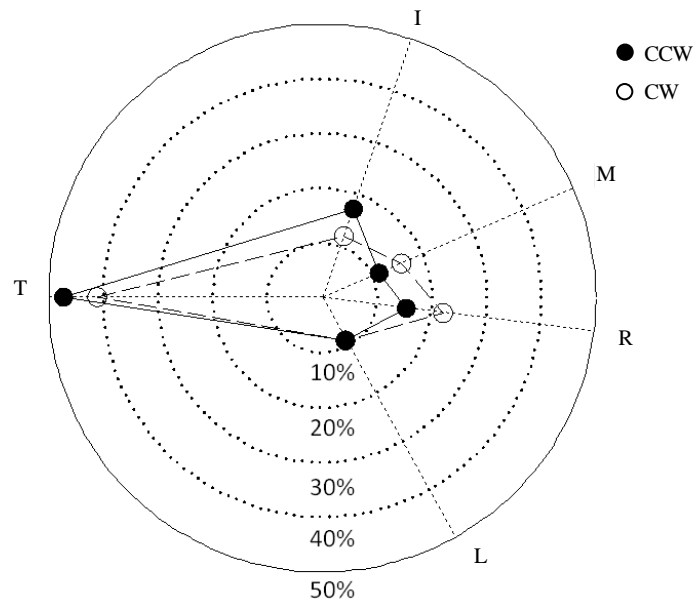


Figure 4-5 Normal force sharing by individual digits in the HOLD phase. Each digit is shown in the angular position it occupied during the experiment. Filled circles are averaged values in CCW conditions while empty ones are from CW conditions.

### 4.3.2 Total and individual digit tangential forces

#### *MVT task*

Subjects produced larger torque in CW (supination/ulnar deviation) direction than CCW direction (pronation/radial deviation) by 23% ( $F(1,9) = 11.87$ ,  $p = 0.007$ ). Wrist positions did not affect the maximum torque or tangential force.



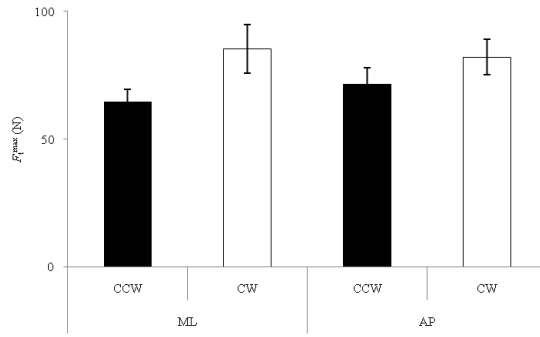


Fig. 4-6 Maximum tangential force under different conditions of *Axis* and *Direction*.

*Sub-MAX task*

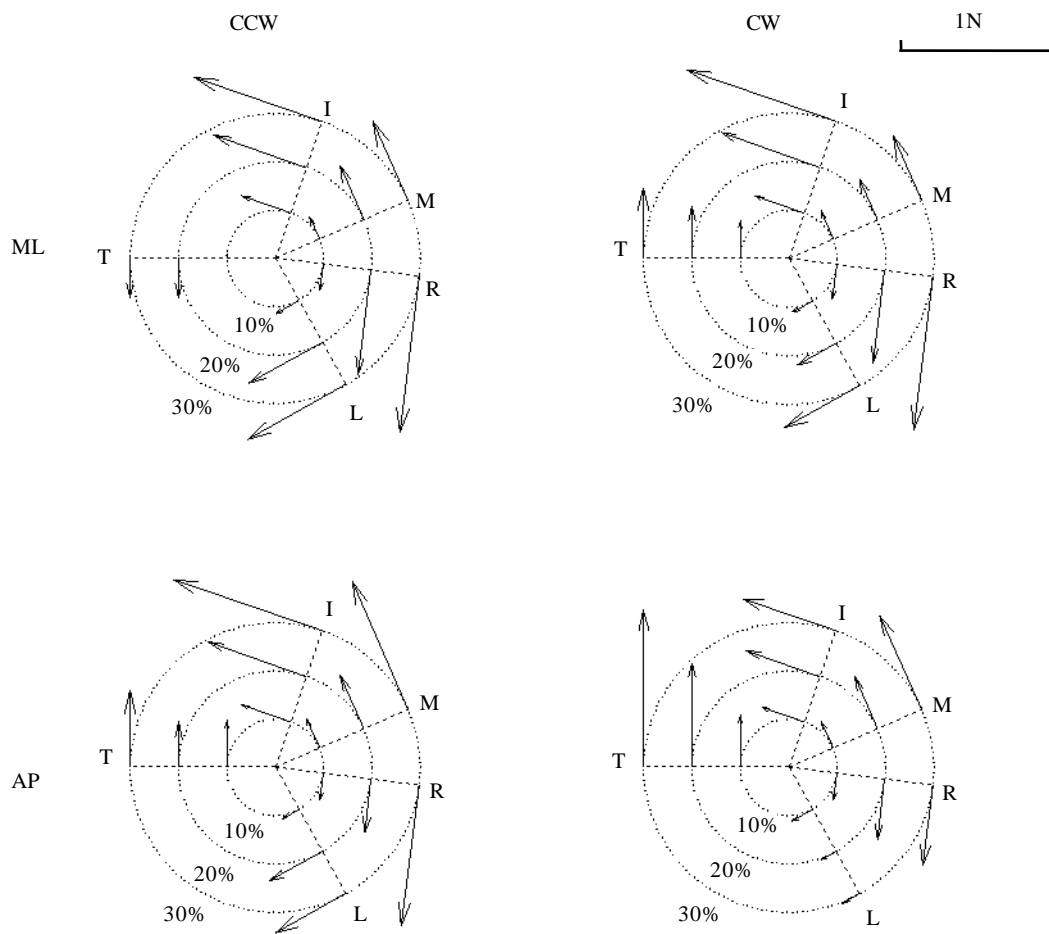


Figure 4-7 Tangential forces of individual digits in the GRASP phase. Different initial conditions are shown along the circumference of the contours.

In the GRASP phase, all digits generated small but non-zero tangential forces even though the total tangential force was close to zero (see the figure above). In particular, index and middle fingers consistently acted in CCW direction while thumb, ring and little fingers consistently acted in CW direction (except thumb in ML/CCW condition). The magnitudes of these tangential forces increased with the initial normal force levels (*Grip*,  $F(10,30) = 3.68, p = 0.003$ ).

In the HOLD phase, the sharing pattern of tangential force was affected by *Direction* ( $F(5,5) = 48.69, p < 0.000$ ) but not by *Axis*. Specifically, the thumb, ring and little fingers contributed more in CW direction, while index and middle fingers more in CCW direction (Figure 4-8).

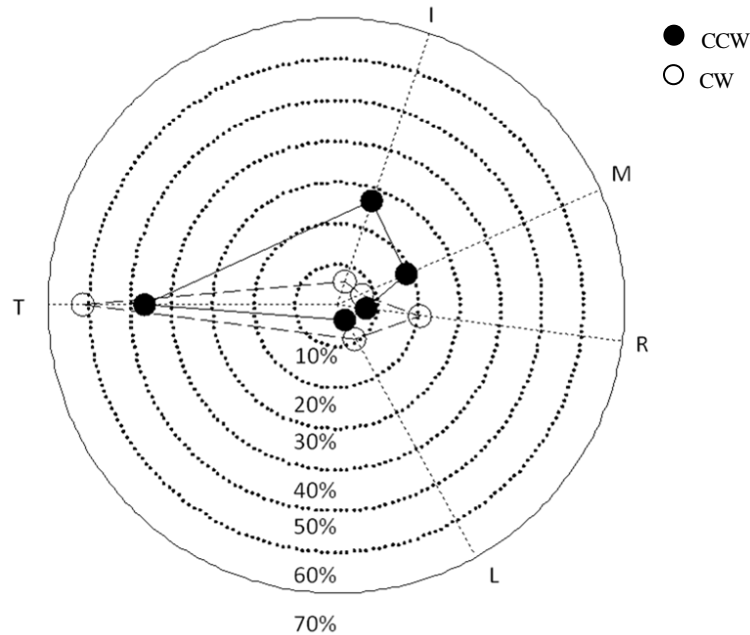


Fig. 4-8 Tangential force sharing by individual digits in the HOLD phase. Each digit is shown in the angular position it occupied during the experiment. Filled circles are averaged values in CCW conditions while empty ones are from CW conditions.

### 4.3.3 Safety margin during torque production

In the 0% normal force condition, safety margin had an oscillation for less than one second upon initial contact (see Figure 4-9). Therefore, this condition was excluded from model fitting

described in the *Method* section. Subjects adjusted the positions of digit-tips on the contact surface during this period. In contrast, a secured grasp was already established before RAMP phase for the other three *Grip* conditions, and safety margin was close to one since tangential force was neglectable (it was smaller than one due to the existence of initial tangential forces of individual digits).

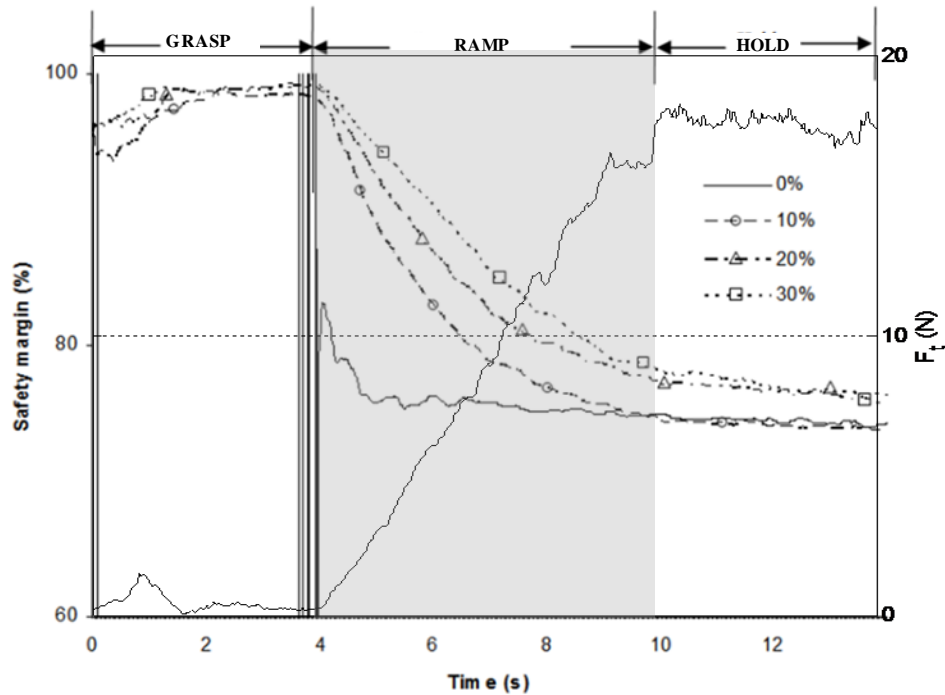


Fig. 4-9 Time profiles of safety margins from a representative subject. Note that safety margin in the 0% trial had large oscillation around  $t = 4s$  due to adjustment upon initial contact. Therefore, no fitting was performed for this condition.

Safety margins in the HOLD phase ( $SM_{end}$  in equation 4.5) showed significant main effects of all three factors (*Axis*,  $F(1,9) = 10.6$ ,  $p = 0.010$ ; *Direction*,  $F(1,9) = 11.6$ ,  $p = 0.008$ ; *Grip*,  $F(3,7) = 6.7$ ,  $p = 0.018$ ). It was larger when wrist was aligned along AP axis or the torque direction was in CCW direction. An increase in initial normal force resulted in a greater  $SM_{end}$  (see Figure 4-10(a)).

The decay coefficient  $b$  decreased with initial normal force level ( $F(2,18) = 6.65, p = 0.007$ ), indicating a slower transition of safety margin. The effects of *Axis*, *Direction* or interactions were not significant.

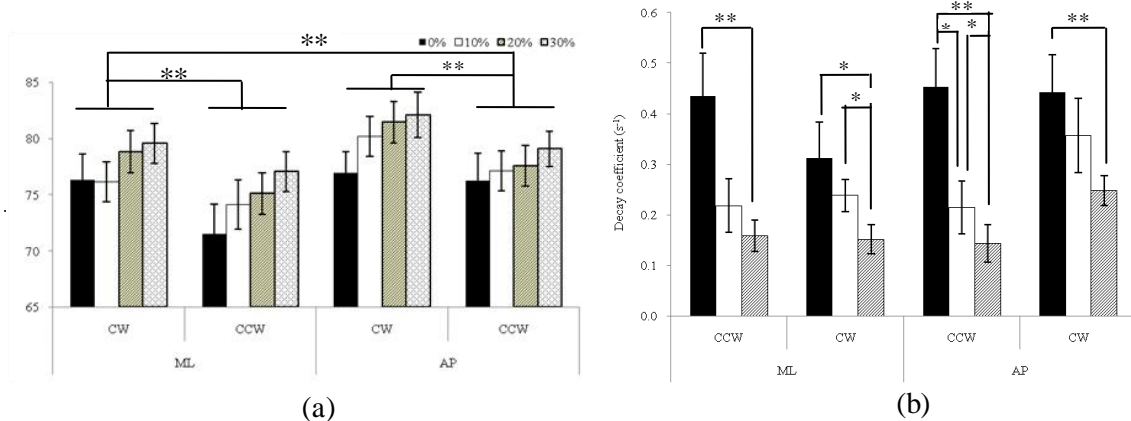


Fig. 4-10 (a) Safety margin in the HOLD phase; (b) decay coefficient  $b$  of safety margin during RAMP phase.

## 4.4 Discussion

In this paper we investigated the effects of wrist position, torque direction, and initial normal force on an isometric submaximal torque production task with a circular handle. Total and individual digits normal forces, tangential forces, and safety margins were examined. In this section we compare the results found in this experiment with several similar studies. Tentative explanation will be given from the perspectives of biomechanics and anatomy.

### 4.4.1 Grasping force alone and while rotating

The current research found a larger normal (grasp) force when generating maximum torque in AP position. This result is consistent with finger studies that examine the role of wrist position in digit tip force. For instance, Li found that subjects produced the largest static pressing force when wrists were extended around  $20^\circ$  (Li 2002). On the other hand, in a dynamic task subjects showed

a decrease of maximum grasp force with wrist flexion (Mogk and Keir 2003). One reason for the increase of normal force in extended wrist position is associated with the additional passive force in AP position due to the stretch of extrinsic flexors, e.g. flexor digitorum superficialis (FDS) and flexor digitorum profundus (FDP) that constitute 80% of finger tip normal forces (Li 2002; Tanaka, Amadio et al. 2005). Another possible factor is the shift of lateral bands of extension mechanism toward the flexion side of PIP joints, making extrinsic extensor contribute to normal force output at the finger tips (Brand and Hollister 1999; Elfenbein and Rettig 2000; Garcia-Elias, An et al. 1991).

The sharing pattern of normal force showed a dependency on wrist position as well when the total normal force was explicitly controlled at a submaximal level (GRASP phase). However, this dependency disappeared when the total tangential force was explicitly controlled (HOLD phase). Maintaining sufficient force for each and all digits became the only constraint for normal force. It is likely the increased activity from muscles that have simultaneous effects of flexion and abduction/adduction, such as flexor carpi radialis and first dorsal interosseous, and decreased activity from antagonist muscles, led to an increase in both normal force and tangential force. These muscle groups altered the sharing pattern and made it independent on wrist position. It is not clear from this study how individual muscle groups are reconfigured in response to the change of goal. A study of two-digit (thumb and index finger) pinching, however, suggested that both intrinsic and extrinsic muscles showed modulation effects with wrist angle when constant force was produced (Johnston, Bobich 2010). Also it is suggested that when comparing grasp data, anthropometric data should be taken into consideration (Pataky, Slota et al. 2012).

Examining the role of the thumb can reveal why its contribution changed with torque directions. It was found that the difference when the thumb acts in parallel and in opposition with other fingers could be as much as two fold (Olafsdottir, Zatsiorsky et al. 2005). By comparison, the change of normal force sharing by the thumb was not drastic in the current study. Nevertheless,

because all digits were allowed to roll freely on the contact surface, the actual angle between the thumb and the index finger was smaller in CCW direction than in CW direction. Therefore, the thumb acted more as an antagonist to all four fingers in CCW direction and contributed greater normal force (almost 50%) as compared to a more agonist role in CW direction.

Our findings can provide some insight to a neural network model developed for finger force production using force-mode hypothesis (Danion, Schoner 2003; Zatsiorsky, Li 1998). According to the hypothesis, it is assumed that a set of commands (“modes”) from central nervous system causes force output of other effectors due to various constraints.

$$\begin{bmatrix} \mathbf{F}_n \\ \mathbf{F}_t \end{bmatrix} = \begin{bmatrix} \mathbf{E}_{nn} & \mathbf{E}_{nt} \\ \mathbf{E}_{tn} & \mathbf{E}_{tt} \end{bmatrix} \begin{bmatrix} \mathbf{m}_n \\ \mathbf{m}_t \end{bmatrix} \quad (4-7)$$

In the grasping subtask,  $\mathbf{m}_n = 1$  and  $\mathbf{m}_t = 0$ ; while in the torque subtask,  $\mathbf{m}_t = 1$  (or -1 for CW torque direction) and  $\mathbf{m}_n > \mathbf{m}_n^{SP}$  for slippery prevention. Each component  $\{\mathbf{E}_{ij}\}$  ( $i, j = n$  or  $t$ ) in the “generalized” enslaving matrix is a task-specific time varying matrix. The diagonal matrices,  $\mathbf{E}_{nn}$  and  $\mathbf{E}_{tt}$ , represent the coupling within normal forces and tangential forces. Four-finger experiments about these coefficients have been carried out previously (Pataky, Latash 2004; Zatsiorsky, Li 1998). The non-diagonal matrices,  $\mathbf{E}_{nt}$  and  $\mathbf{E}_{tn}$ , represent the coupling between normal forces and tangential forces. It can be concluded that  $\mathbf{E}_{nn}$  is dependent on wrist position, while  $\mathbf{E}_{nt}$  is independent on wrist position. Note that this conclusion does not conflict with our previous claim that the control of normal force and torque can be decoupled (Shim and Park 2007). The “central controller” may take in account the different component matrices and plan appropriate command for a goal correspondingly.

#### 4.4.2 Directional preference of individual digits

Digits in this study showed directional preference in tangential force production. In the grasping subtask when the total tangential force was close to zero (within  $\pm 1\text{N}$ ), the radial fingers (index

and middle) generated CCW direction tangential forces while the thumb and the ulnar fingers (ring and little) generated CW direction tangential forces. The increase of these tangential forces with the normal force level implies that the activation of specific extrinsic/intrinsic muscles discussed above, i.e. flexor and abductor/adductor at the same time. In torque subtask, all digits produced tangential forces in the task direction. Nevertheless, the preference persisted, i.e. the radial fingers generated larger forces in CCW direction while the thumb and the ulnar fingers generated larger forces in CW direction. This result can be understood by considering the thumb and index/middle finger pair first. A majority of daily activities engage the thumb and radial fingers, such as holding a baseball. In such scenario, radial fingers generate CCW torque to oppose the thumb for a secure grasp. When the ulnar fingers are added, they tend to have the role of “force balancer” and act in the opposite direction. In a circular grasp, this will also lead the radial fingers to move toward the thumb (Kinoshita, Murase 1996). As in rectangular object prehension, while maintaining a rotational equilibrium without external torque load, the two pairs of fingers often act as agonist and antagonist, respectively. This arrangement is not mechanically necessitated and might be the result of passive spanning and rolling of fingertips on the contact surface. If acting against an active external load or increasing torque steadily as in this study, the antagonizing effect disappears and the two pairs of fingers will operate in the same direction.

#### **4.4.3 Effect of initial normal force on safety margin**

When manipulating an object, an initial normal force is necessary to hold it before further force or torque can be applied (Kinoshita, Backstrom et al. 1997). This is called “preloading phase” in some literature (Johansson and Cole 1994). In precision prehension, it is often automatically followed by the simultaneous increase of normal force and tangential force, called “loading phase”. The two phases are clearly separated in this study to GRASP and RAMP phases. We investigated how the initial normal force affects the continuous process of tangential force following. Safety margin was used to characterize the transient process instead of direct

normal/tangential force for normalization purpose. Since tangential force matched the template quite accurately, safety margin was closely associated with normal force, with greater normal force for a larger safety margin.

Unlike some experiments mimicking manipulation of fragile objects (Gorniak, Zatsiorsky 2010) or compliant objects (Winges, Eonta 2009), the contact surface in our experiment is solid and no restriction was imposed on the amount of normal force subjects should use after the initial GRASP phase. Nevertheless subjects generated quite large safety margins no matter what initial normal force level was. In the HOLD phase, safety margin was well above 60% even with 0% *Grip* condition. Both normal force and safety margin converged to a certain level (see Figure 4-3(a) and 4-9), suggesting a steady normal force output independent of initial value.

Another conclusion we can draw is the initial normal force does not necessarily facilitate the tangential force production. The hypothesis mentioned in the introduction assumes that the stiffness of the wrist and phalangeal joints can be increased by initial normal force, which causes a quicker response. Our study points to the opposite effect, showing the transition phase was impeded by the initial normal force. This effect is possibly due to the differential involvement of two sets of muscle groups, i.e. muscles for grasping and rotating respectively. The greater the first set of muscle group is activated, the longer it takes to transfer the duty of generating force to the second set of muscle group.

## **4.5 Conclusion**

This study investigated sharing patterns of individual digit normal forces and tangential forces in submaximal torque ramp production task on a circular object. Distribution of normal force and tangential force is modified by the direction of tangential force during rotating. Radial fingers (index and middle finger) predominantly generate tangential force of CCW direction, while the



thumb and ulnar fingers (ring and little finger) mostly tangential force of CW direction. Safety margin is affected by initial normal force. Smaller initial normal force causes faster transition process and closer to the control value.

## Chapter 5

### Multi-digit synergy in static manipulative task on a circular object

#### Abstract

Previous researches studied prehension of objects of various geometrical shapes. This study investigated multi-digit coordination in a static torque production task on a circular object. More specifically, we examined the relationship between normal/grasp force and tangential force, and multi-digit synergy, while systematically altering wrist position and torque direction. The hypotheses are: (1) the relationship between normal force and tangential force is dependent on the direction of torque change; (2) a multi-digit synergy stabilizing total torque is broken down when torque reduces and reappears when torque increases. In the experiment, subjects grasped a circular handle with the right wrist aligned along mediolateral (ML) or anteriorposterior (AP) axis. They produced 20% maximum torque in one of the two directions: clockwise (CW) or counterclockwise (CCW) (stable phase 1), decreased the torque linearly to zero (decrease phase), increased to 20% maximum in the other torque direction (increase phase), and held constant for . It was found that: (1) the magnitude of force ratio (normal force vs. tangential force) was smaller during decrease phase than increase phase; (2) maximum constant error occurred during the transition, at the wrist position of supination/ulnar deviation; (3) delta variance, an index of multi-digit synergy, dropped to a minimum during the transition process and recovered after the torque changed to the other direction.

Keywords: *torque; synergy; circular object; normal force; tangential force*

## 5.1 Introduction

Many researchers studied grasping with the thumb and index/middle or four fingers (Flanagan, Burstedt et al. 1999; Friedman, Latash et al. 2009), or on rectangular objects, in which a hand posture called “prismatic grasp” is used, i.e. thumb opposite to the other digits (Latash, Shim 2004). However, five-digit grasp on circular objects, though commonly seen on occasions such as rotating plates, door knobs, and jar lids, are most studied in the field of human factors and ergonomics (Adams and Peterson 1988; Fowler and Nicol 1999; Kong, Lowe et al. 2007; Pataky, Slota 2012; Seo, Armstrong et al. 2007). Seo and colleagues examined the normal force when producing torque on a cylindrical handle along longitudinal direction. The normal force was larger when the torque was in the direction of wrist flexion than in the opposite direction. They suggested inward torque direction causes greater flexion of distal interphalangeal joint, a position advantageous for normal force production. On the other hand, our previous study on maximal voluntary torque found that if the torque direction is tangential to the grasp plane ( an imaginative plane with all digit-tips on it), the normal force will not be affected (Shim, Huang 2007). Another factor considered in our previous study is the wrist position, on the basis that tension and moment arms for individual muscles might change under different wrist positions (Buchanan, Moniz et al. 1993; Li 2002). Indeed, we found that the total normal force is greater when the wrist is extended. However, the researches above address the maximal force production only. It is not clear if those results will hold in a submaximal force production task, in which the problem of motor redundancy will rise (Bernstein 1967). Therefore, the purpose of this study is to investigate individual normal force and tangential force while subject perform submaximal torque production task.

The relationship between normal force and tangential force has been studied quite thoroughly. In precision grip, normal force shows a modulation effect by tangential force, i.e. an increase in tangential force is accompanied by an increase in normal force. This modulation is affected by a

variety of factors, including surface friction, movement direction, subjects with impaired sensitivity, or the action of other body parts (Burstedt, Flanagan 1999; Hager-Ross, Cole 1996; Nowak and Hermsdorfer 2003; Werremeyer and Cole 1997). However, our previous study on maximal torque production showed that the normal force at the moment of maximal torque is independent of torque direction while the maximal torque (tangential force) is not, which raises the question whether normal force and tangential force in circular grasp are correlated in submaximal task.

When producing isometric force, it is observed that variability increases with force magnitude, although the relationship might vary among different force ranges (Carlton and Newell 1993; Christou, Grossman et al. 2002; Slifkin and Newell 2000). However, it is only tested with single effector or two-digit precision grip. When producing constant force with multiple digits, digits are shown to work together and compensate the error by each other. Therefore the resultant variability would be much smaller than the sum of variability by individual digits. This phenomenon is termed as multi-digit synergy and it was confirmed in many studies with equilibrium requirement, such as producing constant total force, or keeping the manipulandum still, etc (Latash, Shim 2004; Santello and Soechting 2000; Scholz, Danion 2002). In one of the experiments, subjects performed four-finger pressing force production with a paradigm of ramp-up, hold, and then ramp-down. After the force onset, negative co-variation among individual digit forces appeared after a delay of a few hundred milliseconds. The latency is suggested to be the critical time to organize a force synergy (Shim, Olafsdottir 2005). This paradigm will be used in the current study with some variation, i.e. ramp-down, then ramp-up in another direction. A hypothesis is that torque stabilizing synergy will be gradually broken down during the decrease phase and reappear during the increase phase.

This study investigates multi-digit coordination among individual digits normal forces and tangential forces in submaximal torque production task. Different combinations of wrist positions

and torque directions are tested. The purpose of this study has three folds: (1) to examine the relationship between normal force and tangential force within decrease phase and increase phase; (2) to quantify performing error under various conditions; (3) to characterize multi-digit synergies in submaximal torque production tasks.

## **5.2 Methods**

### **5.2.1 Subjects**

Ten healthy young right-handed subjects (average age:  $26 \pm 3.1$  years old; average height:  $174 \pm 9.5$  cm; average weight:  $76 \pm 10$  kg) were recruited to the study. No subjects reported previous history of neurophysiological disorder or injury on upper extremity. None of the subjects had any finger-intensive practice, such as playing music instrument, for more than 2 consecutive years. Subjects were given informed consent according to University of Maryland's Institutional Research Board.

### **5.2.2 Apparatus**

An aluminum circular handle was customized for this study. The relative angular positions of fingers with respect to thumb were measured with a wooden handle of the same size prior to the experiment. Averaged angles were used to determine the relative angular positions of five 6D sensors (NANO-17, ATI Industrial Automation, Garner, NC, USA) installed around the circumference. The radius after installment was 4.5cm. A spherical rubber cap was mounted on top of each sensor to conform to the circular contour (Figure 1a). Sandpaper (110-grit, static coefficient of friction, 1.5, measured in (Zatsiosky 2002)) was used to cover the caps to increase the friction between fingertips and contact surface. The handle was fixed on a tripod in appropriate height and orientation.

Thirty channels of data (local forces and torques in 3D space) were routed through signal amplifiers and digitized with two analog-digital converters (PCI-6031 and PCI-6033, National Instrument, Austin, TX). A customized Labview program (National Instrument) was written to collect the data and give subjects online visual feedback. Sampling frequency of 6D sensors was 100Hz.

### **5.2.3 Procedure**

Before the experiment, subjects washed their hands with warm water and soap to normalize skin condition. Subjects sat on a chair in front of a monitor screen and fixed the right upper arm in a customized plastic brace (Figure 5-1). The upper arm was abducted about 45 ° in the frontal plane and flexed about 45 ° in the sagittal plane. The forearm was aligned parallel to the sagittal line of the subject and secured with two sets of Velcro straps. The wrist was positioned so that the direction of the plane with all five digit tips (grasp plane) was parallel to the anterior-posterior (AP) or medial-lateral (ML) axis.

In a preparatory task, subjects performed a maximum voluntary torque production test (MVT) under four different combinations of wrist position (AP or ML) and torque direction (counterclockwise: CCW or clockwise: CW). Two trials were tested for each condition. The larger value of each condition was recorded. At least 1 minute of rest was given between each trial to avoid fatigue.

Before each trial, subjects grasped the handle with one of the two wrist positions (AP/ML) and relaxed. A two-second baseline was recorded and removed to eliminate the effect of gravity. Subjects first produced torque in one direction (CW/CCW) to 20% of MVT and held it constant for 4 seconds (S1 phase). Then subjects decreased the torque to zero and increased in the opposite direction (CCW/CW) to 20% of MVT (transition phase). This phase took 6 seconds.

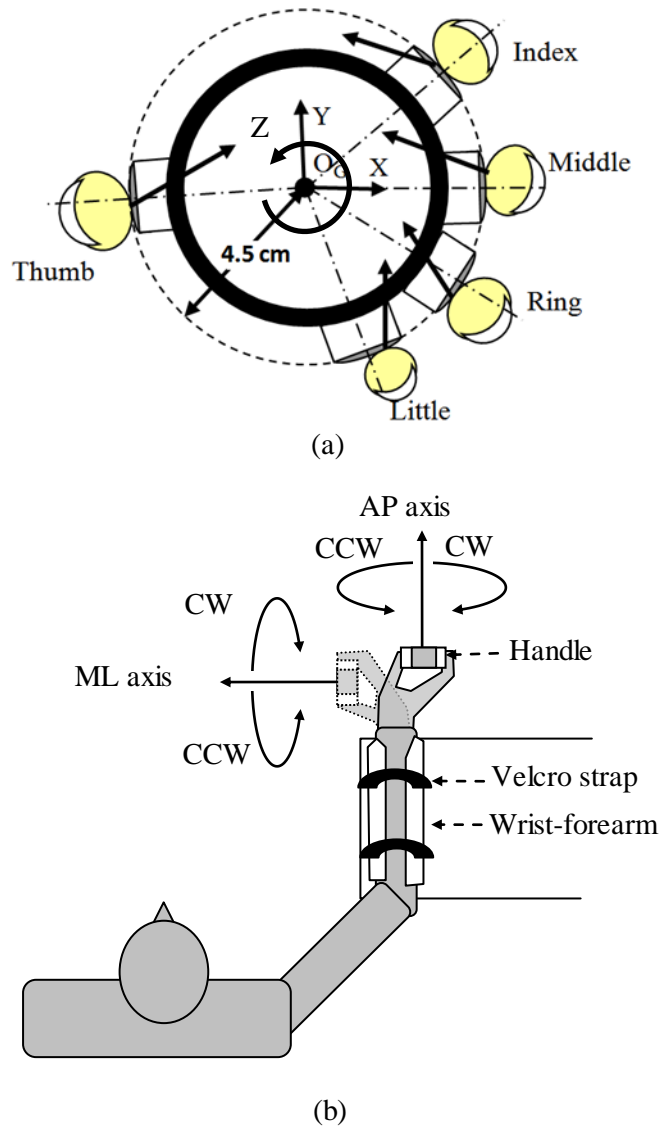


Fig. 5-1 The schematic diagram of the handle. Global reference frame is defined as X: pointing to the right side of subjects; Y: upward; Z: pointing towards subjects. (a) The plane shown here is referred to as “grasp plane” in this study. (b) Subject watch the visual feedback while manipulating the handle on their right hands.

For clarity in later discussion, the transition phase was further divided into T1 and T2 phases according to the moment the torque template equaled zero,  $t_0$  (Figure 5-2). Therefore, T1 (from  $t_1$  to  $t_0$ ) was the torque decrease phase, and T2 (from  $t_0$  to  $t_2$ ) was the torque increase phase. At the end, subjects held the torque constant for another 4 seconds (S2 phase). Two representative

torque profiles can be seen in Figure 5-2. Twelve trials were performed for each condition, preceded by three practice trials. The conditions were block-randomly tested. Two minutes of rest were given between each block.

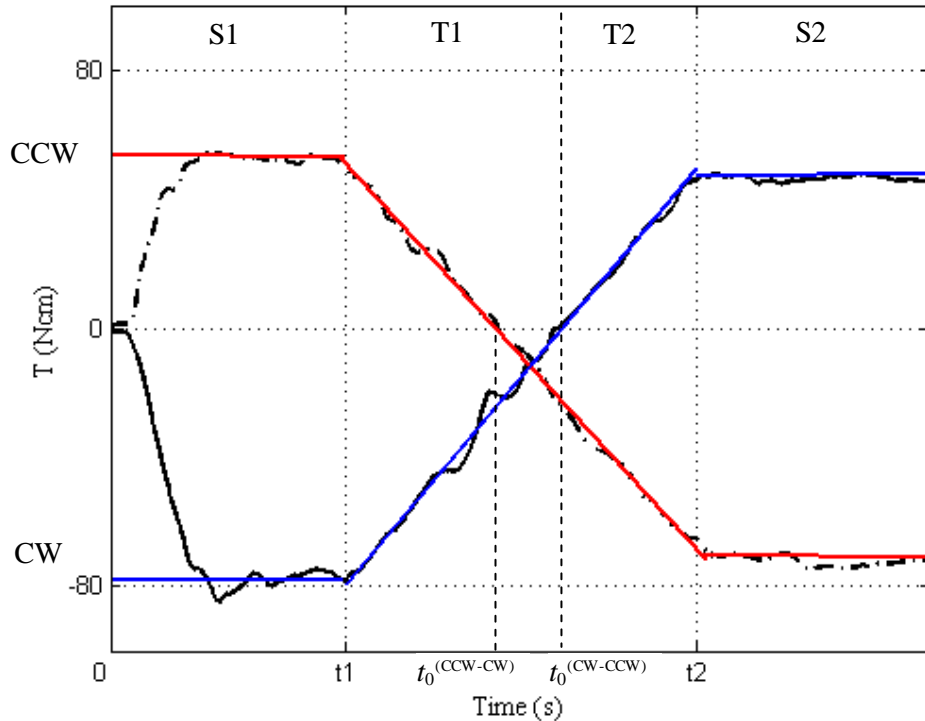


Fig. 5-2 Samples of torque profile. Blue line and black solid line was the template and the actual torque from a trial in CW-CCW condition; while red line and black dash line was from a trial in CCW-CW condition. The four phases labeled were for CW-CCW condition (blue) based on  $t_0$ .  $t_1$  and  $t_2$  indicated the initiation and the termination of the transition phase.

### 5.2.4 Data processing

Individual digit force and torque data was processed with a customized Matlab program (Mathworks, Netick, MA). A zero-phaseshift Butterworth filter was used to remove any noise above 25Hz (Winter 1989). Because the data was recorded on the local centers of top surface of the sensors ( $O_L$ ), a coordinate transformation was performed to compute the actual forces and



torques at the points of application of forces. According to the “soft finger” assumption (Arimoto, Tahara 2001; Mason and Salisbury 1985; Nguyen and Arimoto 2002; Shimoga and Goldenberg 1996), a free moment about the direction of a normal force exists due to the friction between the digit tip and the contact surface (see Figure 5-3). However, we did not consider this component because it did not contribute to the task torque about the Z-axis and the magnitude of this component recorded was ignorable. Therefore, the torque by tangential force is the sole source of output torque, and it equaled the torque by local force  $f_x$  subtracted by the free moment  $m_y$  according to the principle of parallelism.

$$M_Z^{(j)} = f_x^{(j)} d - m_y^{(j)} = F_t^{(j)} r \quad (0.1)$$

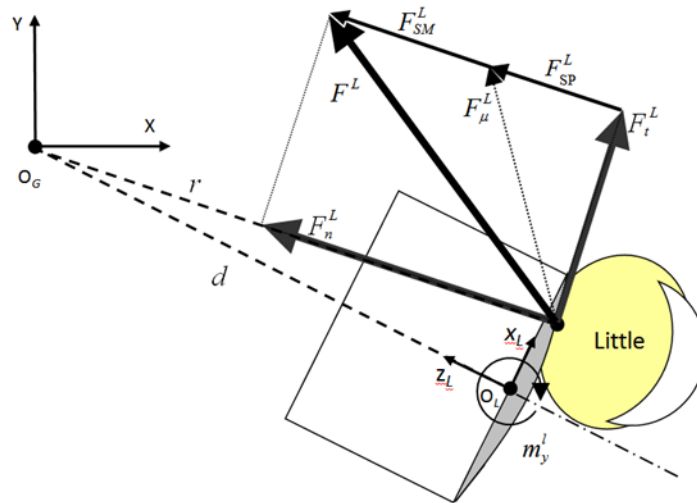


Fig. 5-3 An example of labeling notion in this study. Lowercase letters indicate variables in local reference frame, and capital letters indicate variables in global reference frame.  $r$  is the radius of the circular contour (4.5cm) and  $d$  is the distance from the center of the handle to the center of top surface of any sensor (about 4.3cm).  $j$  represents a specific digit, L for little finger.  $F_n^L$ ,  $F_t^L$ ,  $F^L$ ,  $F_{SP}^L$ ,  $F_\mu^L$ ,  $F_{SM}^L$  represents normal force, tangential force, total force, critical normal force, critical total force and safety margin of the little finger, respectively.

The tangential force  $F_t^{(j)}$  and normal force  $F_n^{(j)}$  of digit  $j$  was computed by

$$F_t^{(j)} = (f_x^{(j)}d - m_y^{(j)}) / r \quad (5-1)$$

$$F_n^{(j)} = \sqrt{(F_x^{(j)})^2 + (F_z^{(j)})^2 - (F_t^{(j)})^2} \quad (5-2)$$

The time profile of constant error (CE) was calculated as the discrepancy of total tangential force to the template averaged across trials.

$$CE = \frac{1}{N} \sum_{i=1}^N (F_{t,i} - F_t^{(template)}) \quad (5-3)$$

$N$  is the total number of trials.  $i$  is the actual trial number.

Uncontrolled manifold (UCM) method was used to analyze the trial-by-trial variability of tangential forces. According to UCM hypothesis, in a redundant system, the central nervous system constrains the variability in the task performance variable (or variables), in the mean time has no control on the rest degrees of freedom (Scholz and Schoner 1999; Scholz, Danion 2002). The two manifolds (mathematical concept for subspaces), UCM space and orthogonal (ORT) space, are orthogonal to each other. The performance variable is associated with elemental variables via a Jacobian matrix. In this study, the performance variable (the total torque) is the summation of elemental variables (the tangential forces of individual digits) multiplied by the radius of the handle. For simplification, the radius was removed from the Jacobian matrix without affecting the result,

$$J = [1 \ 1 \ 1 \ 1 \ 1]^T \quad (5-4)$$

In the above equation, T represents the transpose of a matrix. ORT and UCM space correspond to the kernel and null space with dimension of one and four, respectively.

Assuming that the basis for UCM space are  $e_{\parallel}$ , we can compute the projection of  $F$  (a centralized force vector by removing means across trials from individual digit force) onto them separately.

$$F_{\parallel} = e_{\parallel} e_{\parallel}^T F \quad (5-5)$$

$$F_{\perp} = F - F_{\parallel} \quad (5-6)$$

The variability of elemental variables can subsequently be computed as the sum of two components,  $V_{\text{ORT}}$  and  $V_{\text{UCM}}$ .

$$V_{\text{UCM}} = \text{Var}(F_{\parallel}) \quad (5-7)$$

$$V_{\text{ORT}} = \text{Var}(F_{\perp}) \quad (5-8)$$

Delta variance, an index used to study motor synergy, is the difference between  $V_{\text{UCM}}$  and  $V_{\text{ORT}}$  per degree of freedom. To compare over subjects of different strength, it is usually normalized by the total variability.

$$DV = \frac{V_{\text{UCM}} / d_{\text{UCM}} - V_{\text{ORTH}} / d_{\text{ORTH}}}{V_{\text{UCM}} + V_{\text{ORTH}}} \quad (5-9)$$

$d_{\text{UCM}}$  and  $d_{\text{ORTH}}$  are 4 and 1, respectively. In this study, DV represents the capacity of individual digit to compensate the error of each other. In other words, a positive DV indicates a negative covariation, while a negative DV indicates a positive covariation among tangential forces.

1-second window of CE and DV was averaged for right before (S1) and after (S2) phases as well as the maximum CE and minimum DV during the transition phase. The results were applied to statistical analysis.

### 5.2.5 Statistical analysis

Repeated measure ANOVA was performed for between-subject factor: wrist position (*Axis*) and torque direction (*Direction*). *Direction* has two levels, i.e. CW-CCW and CCW-CW, indicating

the sequence of torque direction in one trial. Another factor PHASE (four levels: S1, T1, T2, and S2) was added when comparing CE and DV. The level of significance was set at  $p = 0.05$ . The Kolmogorov-Smirnov test and Shapiro-Wilks test were used to test violation of the normal distribution assumption, and Levene's homogeneity test was used to test the assumption of variance homogeneity. Means and standard errors are shown.

## 5.3 Results

### 5.3.1 Total normal force and total tangential force

Tangential force was used in this study instead of torque as one of the dependent variables, because the other source of torque, i.e. free moment of force perpendicular to the grasp plane, was neglectable due to the "soft-finger" model. The averaged time profiles of total normal force and total tangential force over 12 trials from a representative subject are shown below under four different conditions.

The minimum normal force across conditions was  $13.6 \pm 2.7$  N. The time instant was denoted as  $t_n$ . When the initial torque direction was CW (CW-CCW conditions),  $t_n$  proceeded  $t_0$  (zero torque) by  $0.77 \pm 0.32$  and  $1.11 \pm 0.38$  second for ML and AP conditions, respectively. The tangential force at the moment was on average  $-2.4 \pm 0.8$  N. In contrast, when the initial torque direction was CCW (CCW-CW conditions),  $t_n$  occurred around  $t_0$  with a difference of  $0.23 \pm 0.22$  and  $0.05 \pm 0.14$  second, respectively. The average tangential force was  $0.37 \pm 0.42$  N. The timing difference was also confirmed by two-way repeated measure ANOVA (*Direction*:  $F(1,8) = 12.8$ ,  $p < 0.01$ , *Axis*: not significant).

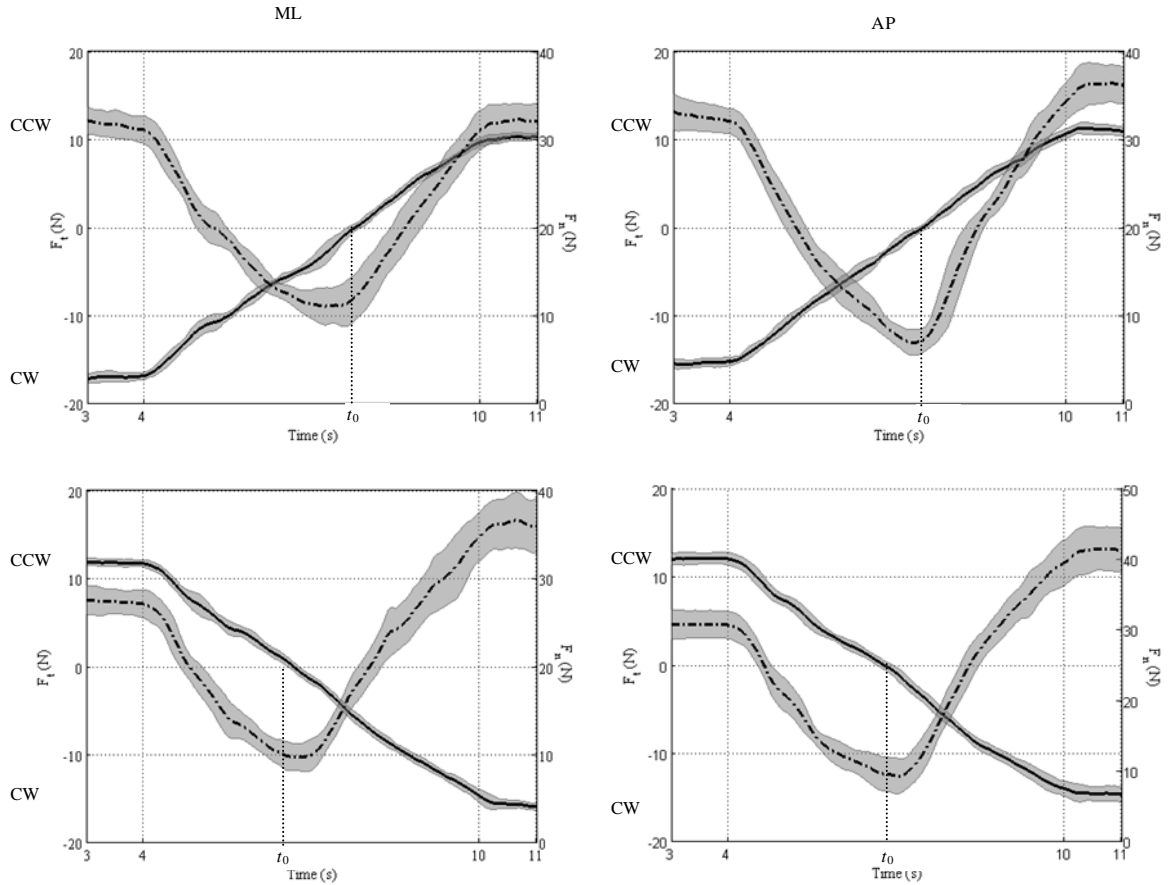


Fig. 5-4 Tangential force (solid line) and normal force (dashed line) from a typical subject in 12 trials when the wrist was in ML position (left) and in AP position (right). The initial torque direction is CW for the top two panels and CCW for the bottom two panels. Shaded areas represent one standard error. Transitions occurred between 4~10s.

To analyze the relationship between total normal force and total tangential force quantitatively,  $t_n$  was used to slice the transition into two phases: decrease and increase phases (see Figure 5-5(a)). The linear regression coefficients were compared with a three-way ANOVA, including *Axis*, *Direction*, and *Phase* (two levels: decreasing and increasing). Both *Axis* and *Phase* showed significant effects (*Axis*:  $F(1,9) = 17.77, p = 0.002$ ; *Phase*:  $F(1,9) = 5.43, p = 0.045$ ). Paired *t*-test showed significant effect of *Phase* in CW-CCW conditions ( $p = 0.02$  and  $0.009$ , respectively) but not in the CCW-CW conditions. On average, the ratio of normal force vs. tangential force was

1.68 in decrease phase and 2.18 in increase phase, 1.72 in ML axis and 2.14 in AP axis. The initial torque direction, however, was not significant.

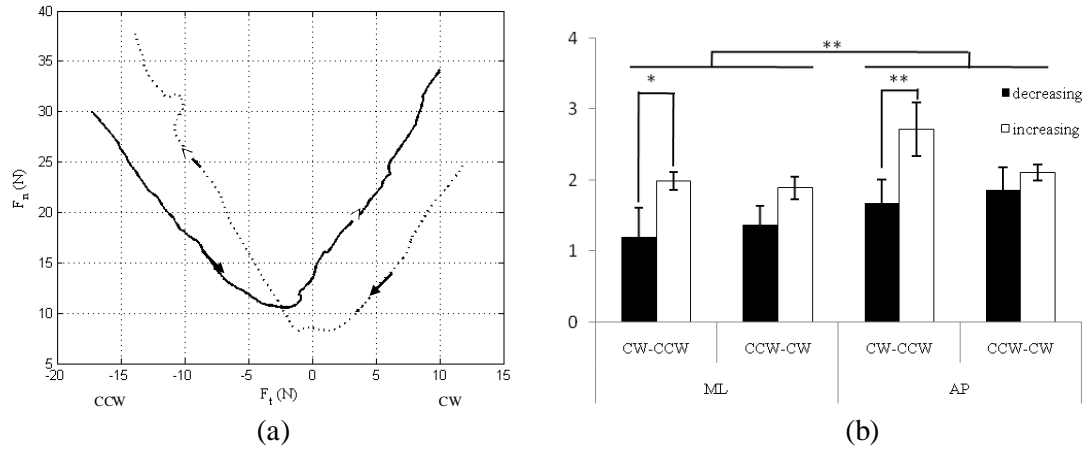


Fig. 5-5 Linear regressions for decreasing and increasing phases. (a) Demonstration of normal force vs. tangential force in two trials with opposite initial directions. The solid line represents the CCW-CW condition, and the dotted line represents the CW-CCW condition. Black arrows represent the decreasing phases, and white arrows represent the increasing phases; (b) the ratio of normal force vs. tangential force (significance level was set at 0.05 for \*, 0.01 for \*\*).

### 5.3.2 Constant error of tangential force

Constant error reflects the deviation of the total tangential force with respect to the template on the screen over time. It was found that maximum constant error in a whole trial occurred during the TRANSITION phase. Figure 5-6 showed one-second window of constant error extracted from S1 and S2 phases, and around  $t_0$ , normalized by the overall total tangential force (e.g. 20% x ( $F_{CW}^t + F_{CCW}^t$ )) for either wrist position). Except the last condition, the constant error was greater at  $t_0$ , when tangential force was zero, than S1 and S2, when tangential force was 20% of  $F_{CW}^t$  or  $F_{CCW}^t$ .

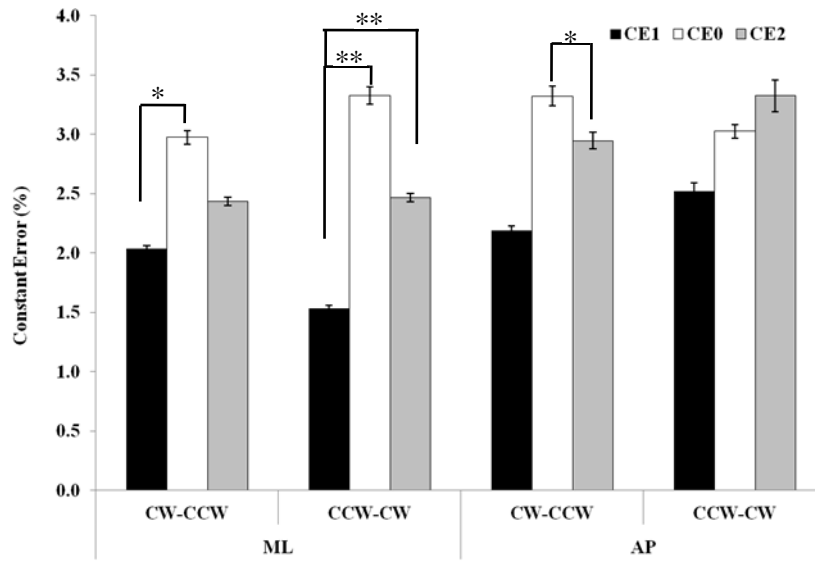


Fig. 5-6 One-second time window average of CE during S1, S2, and  $t_0$ . Paired  $t$ -test results within each *Axis x Direction* condition are also shown.

Repeated ANOVA with three factors (*Axis*, *Direction*, and *Phase*: CE1, CE0, and CE2) showed significant effects of *Phase* ( $CE1 < CE2 \approx CE0$ ,  $F(2,8) = 7.65$ ,  $p = 0.014$ ) and *Axis* ( $CE_{ML} < CE_{AP}$ ,  $F(1,9) = 5.54$ ,  $p = 0.045$ ) but no effect of *Direction* or any interaction. On average, CE along AP axis was 16% greater than along ML axis. CE0 and CE2 were larger than the initial CE1 by 52% and 33%, respectively, although the difference between CE0 and CE2 was not significant.

### 5.3.3 Tangential force variance in UCM and ORT spaces

The variance of tangential force across trials was shown in Figure 5-7 for ORT and UCM space separately.  $V_{ORT}$  represents the performance variability which individual digit tangential forces should work together to control, while  $V_{UCM}$  is the “free” variability allowed among the forces. Both had been normalized by their own degrees of freedom, i.e.  $d_{ORT} = 1$  and  $d_{UCM} = 4$ . As in previous analysis, three-way ANOVA was performed with *Axis*, *Direction*, and *Phase* (S1, T1, T2, and S2).

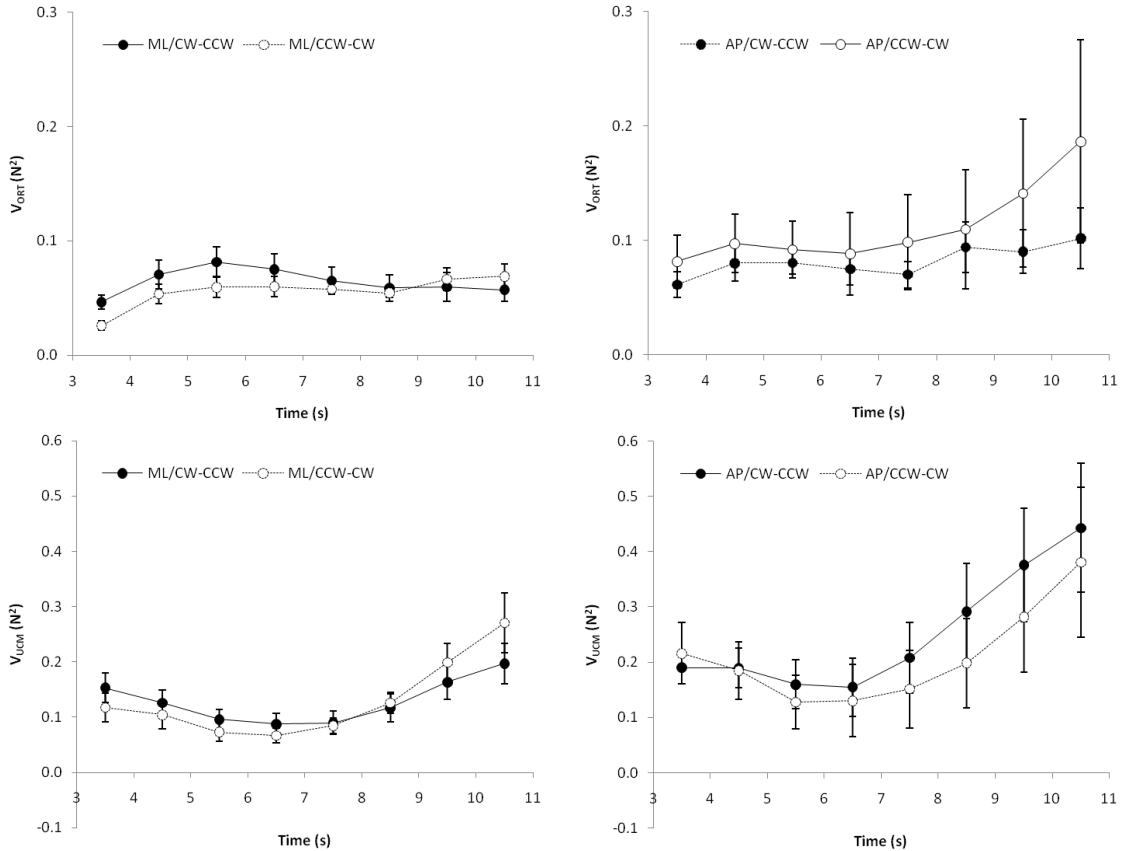


Fig. 5-7 Variance in ORT (top) and UCM (bottom) subspace. One-second window averages are drawn from one second before to one second after the transition phase, i.e. [3~11s]. The two conditions from the same wrist position are shown together.

On average,  $V_{UCM}$  was 1.59 times more than  $V_{ORT}$ . This was within our expectation because subjects performed the task well across all conditions. For  $V_{ORT}$ , the only significant effect was the interaction between *Axis* and *Phase* ( $F(3,7) = 5.86, p = 0.025$ ). More specifically, when the wrist was in ML position, the variance increased about 80% in T1 and maintained relatively stable throughout the task; when the wrist was in AP position, however, the variance rose until the torque changed direction.

$V_{UCM}$  exhibited a “U”-shape pattern with smaller values during the transition phase. The main effects of *Axis* and *Phase* were significant (*Axis*:  $F(1,9) = 5.88, p = 0.038$ ; *Phase*:  $F(3,7) = 20.54$ ,



$p = 0.001$ ). In particular, AP ( $0.26N^2$ ) had almost twice the variance of ML ( $0.15N^2$ ). And the variance in different phases followed the order:  $S2 > S1 = T2 > T1$ . No other effect was found.

Delta variance (DV) was calculated as the difference between  $V_{UCM}$  and  $V_{ORT}$ , normalized by the total variance (see equation 5-10). DV was positive before the transition, indicating a tangential force stabilizing synergy among individual digits to maintain a constant total tangential force. During the transition, DV decreased and sometimes became negative (DVmin), suggesting the synergy was partially weakened/deconstructed. After the transition, DV returned to positive again and maintained throughout the trial.

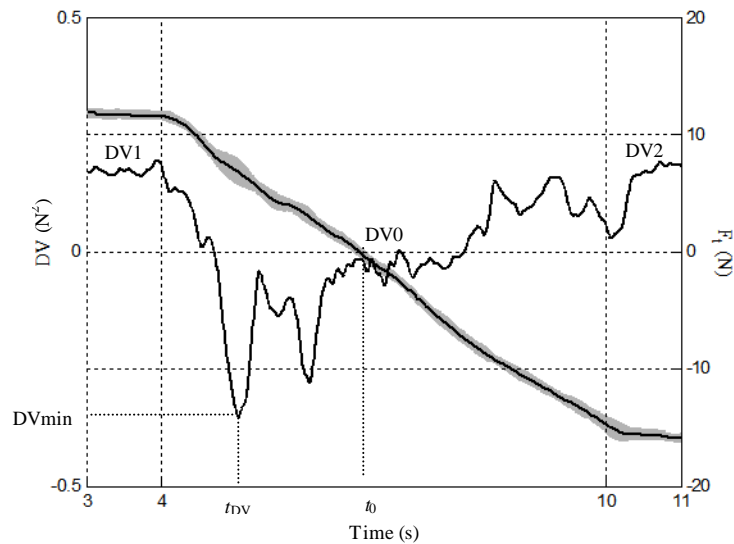


Fig. 5-8 Delta variance from a representative subject in ML/CCW-CW condition. Mean and one SD of tangential force from the 12 trials were shown on the secondary axis.

There was no difference between DV1 and DV2. However, DV at  $t_0$  was significantly smaller than both and approximately zero (on average  $0.019 \pm 0.036$ ) except in the AP/CW-CCW condition (see Figure 5-9). DVmin occurred during the transition. However, no significant main effect or interaction was found.

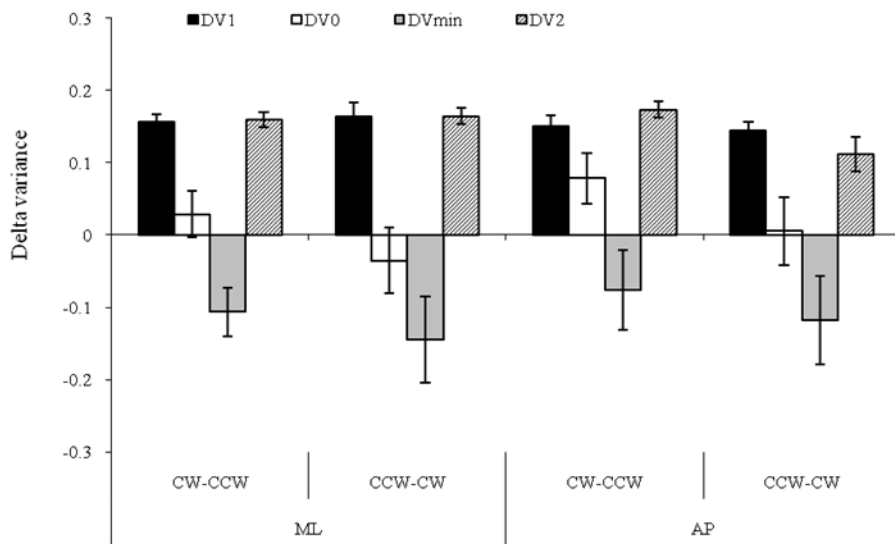


Fig.5-9 Delta variance at S1,  $t_0$ , and S2 as well as DVmin.

### 5.3.4 The relations of time variables

The time instants of CEmax and DVmin ( $t_{CE}$  and  $t_{DV}$ ), were compared with the moment of torque changing direction ( $t_0$ ). A positive value indicated it took place before  $t_0$  and in the torque decreasing (T1) phase, while a negative value indicated it occurred after  $t_0$  and in the torque increasing (T2) phase.

On average, CEmax (black columns in the figure below) occurred before  $t_0$  ( $414 \pm 274$ ms) in CW-CCW conditions and after  $t_0$  ( $-600 \pm 238$ ms) in CCW-CW conditions. The effect of *Direction* was supported by ANOVA ( $F(1,9) = 6.01, p = 0.037$ ). The effect of *Axis* or its interaction with *Direction* was not significant.

On contrast, minimum DV (see the white columns in Figure 5-10) all occurred before  $t_0$ , except in the AP/CCW-CW condition which was about the same time as  $t_0$  ( $-172 \pm 544$ ms). Statistics showed significantly greater values in CW-CCW conditions, meaning that it occurred earlier with

respect to  $t_0$ . The interaction between *Axis* and *Direction* was not significant by our criteria ( $F(1,9) = 4.224, p = 0.07$ ).

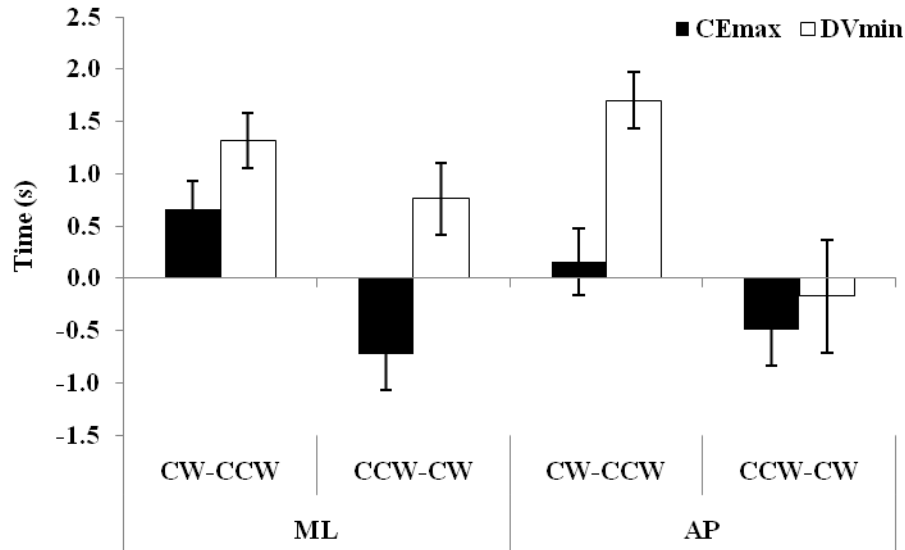


Fig. 5-10 Temporal relationship of CEmax and DVmin with respect to  $t_0$ . A positive value means an earlier occurrence, and a negative value means a later occurrence.

## 5.4 Discussion

In this study, subject performed five-digit submaximal static torque production on a circular handle. Wrist positions and direction of torque change was systematically varied. Since the torque in this study can be translated to the total tangential force, it would be attempted to compare the results to one of previous studies (Shim, Olafsdottir 2005). In that experiment, subjects pressed digits on sensors and generated a total normal force of “ramp-up, maintain, ramp-down” paradigm. However, they are different in two ways. First, in the previous study, the digits were pressed on sensors in a flat surface; the thumb acted in parallel with all fingers. In the current study they were placed around a circular contour. The difference in hand configuration should be taken into account when the results are examined. For example, from the aspect of biomechanics,

all digit tangential forces in circular manipulation have equal moment arms, therefore no mechanical advantage exists (Zatsiosky 2002). A second difference is that the previous study used a pressing task, i.e. the target variable was the total normal force, while in the current study, the handle was fixed and normal force was only required to prevent digits from slipping on the contact surface, and it was the total tangential force contributing to the explicit goal. The discussion will continue with these two facts in mind.

#### **5.4.1 Modulation of the direction of tangential force change**

The current study found a strong coupling between normal force and tangential force in both directions of tangential force (CW and CCW) as well as both directions of tangential force change (decrease and increase). In particular, within a single task, the ratio of normal force to tangential force was smaller in force decrease phase (T1) than that in force increase phase (T2). For the same direction of tangential force, the ratio was smaller in force decrease direction than that in force increase direction. For example, subjects produced continuous CCW tangential force during both T1 phase in CCW-CW condition and T2 phase in CW-CCW condition. Yet the ratio in the force increase T2 phase was greater than in the force decrease T1 phase. This can be also seen in Figure 5-5(a). Either segment with white arrows (tangential force increase direction) has a larger slope than those with black arrows (tangential force decrease direction).

The ratio of normal force to tangential force is equal to the ratio of normal force rate to tangential force rate (by “rate” we mean the first derivative of time). Since tangential force rate is the same for both directions, this result implies that increase phase is associated with a greater normal force rate. The finding is consistent with those studies about external perturbation in precision grip. In one experiment, subjects lifted and held the object with the thumb and index finger, with an unexpected increase or decrease of the tangential force (Mrotek, Hart et al. 2004). An increase in tangential force elicits a faster, larger response in normal force adjustment with a shorter latency;

while a decrease in tangential force causes a declination of normal force with a longer latency. Hager-Ross and colleagues found that this adjustment in normal force is more prominent if the sudden increase of tangential force is to pull the object out of the hand, especially toward the gravity (Hager-Ross, Cole 1996). The authors hypothesized that the increase direction in load perturbation is regarded “more dangerous” and treated with higher priority (Johansson, Hager et al. 1992; Winstein, Abbs et al. 1991).

For predictive grasp, our study provides the first evidence that the direction of tangential force change influences normal force. Our theory is that human are more experienced with tangential force increase direction, therefore develop normal force quickly, while in tangential decrease direction, a slower reduction of normal force allows handling the object with greater care to prevent it from slipping, e.g. pick up a glass object from a table and put it back down. An interesting case is when manipulating a fragile device when normal force is restrained from exceeding the critical force. It was found the ratio is significantly lower than with a normal object (Gorniak, Zatsiorsky 2010). The conjuncture is that similar results will be obtained when performing the current experiment with the fragile device, i.e. faster normal force development and shorter duration in the direction tangential force increase.

#### **5.4.2 Multi-digit synergy**

As expected, a multi-digit synergy stabilizing the total tangential force emerged in both pre- and post-transition phases. For some subjects, this synergy disappears during the transition while for the others, it remained active throughout a trial (16/40 conditions from all subjects). Still, the extent of the synergy here is partially weakened during the transition, as evident from a minimum DV. It indicates a weak error compensation or even positive covariation of digit tangential forces. In the finger pressing study mentioned in the Introduction section (Shim, Olafsdottir 2005), once ramp down phase started, the DV was reduced to negative values within a few hundred

milliseconds and force synergy disappeared for all subjects. The difference can be understood by examining the stage of ramp-down phase in the two tasks. In our study, ramp-down (T1) phase was ahead of ramp-up (T2) phase. Subjects might be making adjustments to prepare for the subsequent ramp-up phase in the opposite direction. In contrast, the ramp-down phase in the finger pressing study was at the end of one trial, therefore a quick break down of synergy was more advantageous. Another reason might originate from the difference in the two tasks as mentioned at the beginning of the Discussion section. The synergy we investigated in this study was to stabilize the total tangential force. Due to the prehension posture with all fingers abducted, tangential force can easily arise during grasping action and hence, extra tangential force synergy is required. In the last study, we found that when asked to grasp the same circular handle with minimum rotation force, subjects produced small amount of tangential forces from each digit. These forces were not neglectable, although the total sum was close to zero. It means that a tangential force synergy exists while grasping even when the total tangential force is zero. That explains why for some people, tangential force synergy remained during the transition.

Variability in UCM space is sometimes informally called as “good variability” because it does not affect the performance variable. It is suggested that the central nervous system utilizes this variability to achieve greater flexibility in a redundant motor system. In this study  $V_{UCM}$  showed a V shape profile, similar to the magnitude of the total tangential force. A hypothesis based on Gutman’s model of motor variability (Gutman, Latash 1993) argues the  $V_{UCM}$  is the result of imprecise modulation of force magnitude by individual fingers (Latash, Scholz 2002). Therefore it increases with individual digit forces, as well as the total force. In contrast,  $V_{ORT}$  is the variability of the performance variable and reflects the timing errors among individual finger forces. It is therefore strongly affected by the force rate. Since the force rate was not altered in any condition (always finish in 6 seconds),  $V_{ORT}$  remained constant most of the time.

### 5.4.3 Force error in accurate torque production

Performance error in this study is quantified by both constant error (CE) and  $V_{ORT}$ , the first-order and second-order of tangential force error with respect to the template. The maximum CE occurred in the transition phase and was about twice as large as that at  $t_0$ , while  $V_{ORT}$  was mostly constant throughout an entire trial (Figure 5-8). As expected, our experiment supports the idea that performance error in multi-digit task is not directly associated with force level, because tangential force at the transition phase was smaller than at the two stable phases. This increase in force error might be related to the reduced/deconstructed synergy we saw in the Result section.

It should be noted that since the maximal torque in CW direction is larger than in CCW direction (statistics not shown here), the timing for the torque to change direction also occurs later in CW-CCW conditions (see Figure 5-2 for illustration), i.e.  $t_0^{(CW-CCW)}$  lags behind  $t_0^{(CCW-CW)}$ . For CW-CCW task,  $t_{CE}$  is earlier than  $t_0^{(CW-CCW)}$ , while for CCW-CW task,  $t_{CE}$  is later than  $t_0^{(CCW-CW)}$ . This implies that  $t_{CE}$  is located within the time interval  $[t_0^{(CCW-CW)}, t_0^{(CW-CCW)}]$ , i.e. maximum CE always occurs at the moment when producing torque in CW direction (supination or ulnar deviation). However, since the time interval varies for wrist positions, we could not test the effect of *Axis* in this study.

## 5.5 Conclusion

This study investigated multi-digit synergy in a ramp-down, then ramp-up submaximum torque production task on a circular object. We found that: (1) the magnitude of force ratio (normal force vs. tangential force) is similar during ramp-down phase than ramp-up phase; (2) delta variance of torque is reduced during transition and recovers after; (3) constant error is greater during transition than before and after; the greatest constant error occurs in supination/ulnar deviation.

## Chapter 6

### Multi-digit coordination in a repetitive rotating task on a circular object

#### Abstract

Repetitive manipulation is an important task in human prehension. This study investigated multi-digit coordination in a dynamic cyclic torque production task on a circular object. The aim was to identify the roles of movement frequency and moment of inertia in several aspects, including normal/tangential force coupling, force variability and regularity. During the experiment, subjects grasped a customized circular handle and produced oscillating angular movement with one of the three frequencies. The moment of inertia of the handle was varied by changing the distances of two symmetrical mass relative to the vertical rotation axis. Individual digit normal and tangential forces were recorded by miniature six component force sensors. The results include: (1) both modulation gain and offset of normal force by tangential force were positively associated with frequency and moment of inertia; (2) within-cycle similarity of normal and tangential force, characterized by hysteresis index, was not affected by frequency; (3) between-cycle regularity of normal and tangential force, characterized by approximate entropy, decreased with moment of inertia; (4) multi-digit torque synergy was negative and remained constant across conditions.

Keywords: *circular object; torque; synergy; hysteresis; approximate entropy*



## 6.1 Introduction

A significant amount of human prehension tasks are associated with repetitive movements of hands and digits, such as tapping on computer keyboards, writing cursive letters, playing musical instruments, or using tools like screwdrivers. Understanding the coordination of individual digit forces can improve our knowledge about how the central nervous system controls repetitive movements. On the other hand, hand and wrist studies received great attention in both industry environments and sports activities because of common injuries on these sites caused by bone fracture, tendinous tear, or muscle fatigue etc. (Ciriello, Webster et al. 2002; Dumont, Popovic et al. 2006; Liang, Takahashi et al. 2007; Wei, Huang 2003).

The modulation of normal force on tangential force has been studied in abundance, both in discrete and cyclic tasks (see Flanagan 2006 for a review). Regression analysis revealed the relationship between normal force and tangential force in discrete movements is associated with various task properties, such as surface smoothness, memory representation, and object density, *etc.* (Cole and Beck 1994; Salimi, Hollender et al. 2000; Zhang, Gordon et al. 2010). On the other hand, increasing the movement frequency was shown to reduce the modulation effect (Danion, Descoins et al. 2009; Flanagan and Wing 1995; Uygur, de Freitas et al. 2010; Zatsiorsky, Gao et al. 2005). The authors suggested that the modulation gain and offset are under high level motor command.

The structure of motor variability can be characterized by approximate entropy (ApEn) (Kuznetsov and Riley 2010; Pincus 1991). A smaller value indicates a more regular motor output. During isometric index finger abduction, ApEn was independent of the amount of variability at low force level ( $< 5\text{N}$ ) (Sosnoff, Valentine et al. 2006). In the full force range, however, ApEn decreased linearly with the force level (Hong, Lee 2007). On the other hand, the two task-irrelevant tangential force components showed an increased in ApEn. Therefore it would be interesting to determine how ApEn of tangential force (task-relevant) and normal force (task-

irrelevant) look in a cyclic task. The force level was modified in this study by adjusting moment of inertia (MOI) of the device or the movement frequency. We expected to see a decrease of ApEn for tangential force and an increase of ApEn for normal force when the force level is raised by either factor.

Recently, the framework of multi-digit synergy has been formalized. It is hypothesized that the central controller exploits the coordination of multiple effectors to constrain the variability that impacts the performance goal, and to allow the variability that does not affect the task (Latash and Zatsiorsky 2009). Two task-specific kinetic synergies have been proposed separately: force-stabilizing synergy and torque-stabilizing synergy (Gorniak, Zatsiorsky 2009; Li, Latash 1998; Rearick and Santello 2002; Santello and Soechting 2000; Shim, Latash 2005). It is suggested that the force-stabilizing synergy has to be explicitly specified; while the torque-stabilizing synergy is implicitly implemented due to daily activities requiring constraint of the wrist at a neutral position (Latash, Li et al. 2002; Zhang, Zatsiorsky et al. 2007). The computation of torque in these studies was task-specific. In the four-finger pressing task, the torque is calculated by individual finger normal forces multiplied by the distance of each finger to the longitudinal line passing through the midpoint between middle and ring fingers. In the prismatic prehension task, i.e. the thumb in opposition to the fingers, the torque is the summation of two components, i.e. torque by normal forces and torque by tangential forces (Shim, Latash 2005). The moment arms are usually different for each finger. In a circular grasp, however, all digits are placed around a circular contour. Moment arms are equal for individual digit tangential forces. Our previous experiment on static torque production revealed a torque synergy among individual tangential forces during the constant phase and for some subjects, during the slow, smooth torque transition phase as well. We hypothesize that the same torque-stabilizing synergy might exist in the repetitive task.

In this study, repetitive torque production on a circular object was investigated with variations of two factors. MOI was varied by changing the distance between loads and the axis of rotation.

Three frequencies (0.5Hz, 0.75Hz, and 1Hz) were tested. By manipulating the two factors, we expected that the variability and regularity of force output will be systematically changed.

## **6.2 Methods**

### **6.2.1 Subjects**

Six subjects (male,  $21 \pm 1.2$  years old,  $176.2 \pm 6.9$ cm,  $69.1 \pm 2.2$ cm) were recruited to participate in the study. They were right handed determined by Edinburgh Handedness Inventory (Oldfield 1971). None of the subjects had any history of neuropathological disease or trauma with either side of upper extremity. Subjects were given consent form prior to the experiment according to Institutional Research Board in University of Maryland.

Before the experiment, subjects were asked to grasp a wooden circular handle with a radius of 4.5cm with all digits. The preferred angular positions of four fingers relative to the thumb ( $0^\circ$ ) were averaged across subjects for later experiment setup.

### **6.2.2 Equipment**

Five 6D sensors (NANO-17, ATI Industrial Automation, Garner, NC, USA) was mounted around the circumference of a customized aluminum circular handle. The radius of the handle after installment of the sensors was 4.5cm. A spherical rubber cap was mounted on top of each sensor to conform to the circular contour (see Figure 6-1a). Sandpaper (110-grit, static coefficient of friction, 1.5, as measured in (Zatsiosky 2002)) was used to cover the caps to increase the friction between fingertips and contact surface.

An aluminum beam (length = 69.8cm) was attached to the center bottom of the handle at its midpoint. A vertical Plexiglas plate fixed to a wire was attached perpendicular to the bottom of

the aluminum beam below the center of the handle. At the bottom of the wire a three dimensional magnetic sensor (Polhemus, Colchester, VT) was mounted to provide online feedback about the angular position of the handle about the axis of rotation. Two masses (each 262.5g) are attached to the aluminum beam, each an equal distance in a transverse plane. The masses can be mounted at seven different distances from the handle, 0, 5, 10, 15, 20, 25, and 30cm, resulting in different moments of inertia with respect to the vertical axis of rotation.

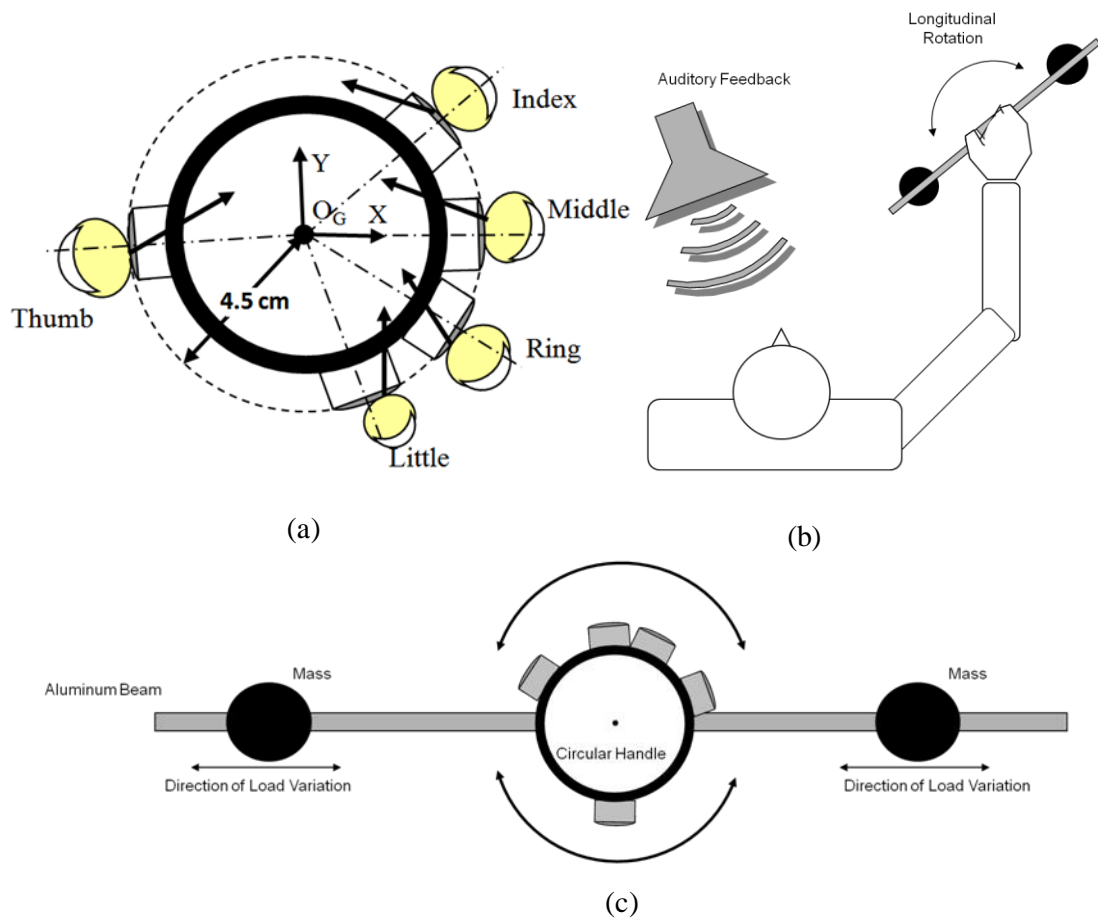


Fig. 6-1 Schematic view of the handle. Global reference frame is defined as X: pointing to the right side of subjects; Y: upward; Z: pointing towards the palm. The plane shown here is called “grasp plane” in this study. (b) subject rotated the handle on their right hands under auditory signal paced by a metronome. Each beep was accompanied by a 45 ° deviation of the wrist to radial or ulnar direction. (c) the structure of the handle, the beam and two masses.

The exact values of MOI were acquired by mounting the handle on a frame and taking the measurement of the whole system as a pendulum.

$$\text{MOI} = \left( \frac{\tau}{2\pi} \right)^2 mgl_{CM} \quad (6-1)$$

$\tau$  is the oscillation period of the pendulum.  $m$  is the mass of the system.  $g$  is the acceleration of gravity.  $l_{CM}$  is the relative distance from center of mass of the system to the axis of rotation. The difference between the system with a given load locations and the empty frame gives the MOI of the handle. The resulting MOIs are listed in Table 6-1.

Table 6-1 Moment of inertia corresponding to different load locations

Load location (cm)	0	5	10	15	20	25	30
MOI (kgm <sup>2</sup> )	0.0164	0.0179	0.0216	0.0280	0.0373	0.0486	0.0629

30 channels of data (local force and torque components in 3D space from each sensor) as well 6 channels of kinematic data and 1 channel of metronome signal were routed through signal amplifiers and digitized with two analog-digital converters (PCI-6031 and PCI-6033, National Instrument, Austin, TX). A customized Labview program (National Instrument) was written to collect the data. Sampling frequency for 6D force/torque sensor was set as 100Hz. Sampling frequency for the magnetic sensor was 80Hz.

### 6.2.3 Procedure

Before the experiment, subjects washed their hands with warm water and soap to normalized skin condition. Subjects stood in front of a monitor screen and grasped the circular handle with the right hand (Figure 6-1b). The wrist was extended so that the plane with all five digit tips (grasp plane) was parallel to the transverse plane and the aluminum beam was in horizontal position.

The experimenter chose one of the seven locations (see Table 6-1) for the two masses. Subjects grasped the handle and stayed still. After a tone, subjects started to follow the metronome by rotating the handle in the transverse plane from 45 ° in pronation direction to 45 ° in supination direction. The angle of the aluminum beam was captured and displayed on the computer screen as a red pointer in a gauge. The two end positions were also labeled. Subjects were free to start the rotation in either direction. Three preset frequencies were chosen for the metronome (60bpm, 90bpm, 120 bpm), corresponding to 0.5Hz, 0.75Hz, and 1Hz. At least 20 complete cycles were recorded before the experimenter stopped the trial and gave subjects 1 minute of rest. A total of 21 conditions (7 load locations by 3 frequencies) were tested in random sequence. Subjects completed a few practice trials before each condition.

## 6.2.4 Data processing

Individual digit force and torque data was processed with a customized Matlab program (Mathworks, Netick, MA). A zero-phaseshift Butterworth filter was used to remove any noise above 25Hz (Winter 1989).

### 6.2.4.1 Coordinate transformation

Because the data was recorded on the local centers of top surface of the sensors ( $O_L$ ), a transformation was performed to compute the actual forces and torques at the points of application of forces. According to the “soft finger” assumption (Arimoto, Tahara 2001; Mason and Salisbury 1985; Nguyen and Arimoto 2002; Shimoga and Goldenberg 1996), fingertips can deform under pressure, but no free torque in the Z direction (Figure 4-2). Therefore, the torque by tangential force was the sole source of output torque, and it equaled the torque by local force  $f_x$  subtracted by the free moment  $m_y$ .

$$M_Z^{(j)} = f_x^{(j)} d - m_y^{(j)} = F_t^{(j)} r \quad (6-2)$$

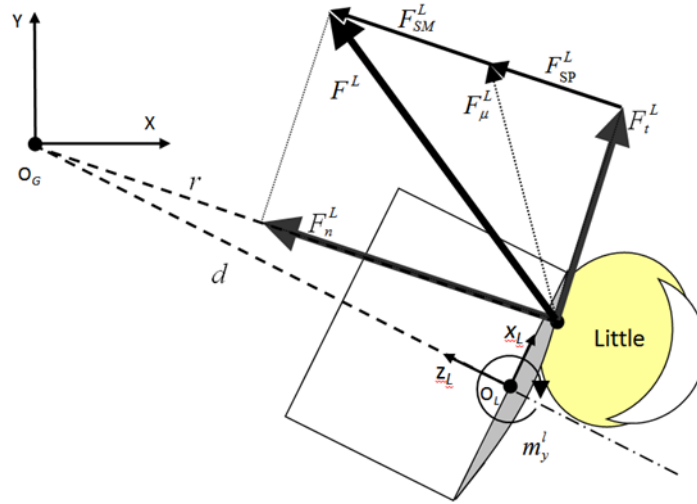


Fig. 6-2 An example of labeling notion in this study. Lowercase letters indicate variables in local reference frame, and capital letters indicate variables in global reference frame.  $r$  is the radius of the circular contour (4.5cm) and  $d$  is the distance from the center of the handle to the center of top surface of any sensor (about 4.3cm).  $j$  represents a specific digit, L for little finger.  $F_n^L$ ,  $F_t^L$ ,  $F^L$ ,  $F_{SP}^L$ ,  $F_\mu^L$ ,  $F_{SM}^L$  represents normal force, tangential force, total force, critical normal force, critical total force and safety margin of the little finger, respectively.

The tangential force  $F_t^{(j)}$  and normal force  $F_n^{(j)}$  of digit  $j$  was computed by

$$F_t^{(j)} = (f_x^{(j)} d - m_y^{(j)}) / r \quad (6-3)$$

$$F_n^{(j)} = \sqrt{(F_x^{(j)})^2 + (F_z^{(j)})^2 - (F_t^{(j)})^2} \quad (6-4)$$

#### 6.2.4.2 Segmentation and resampling

Trial data was truncated into epochs of equal length. Each cycle started with a local maximum angle of the circular handle (the pronation position), went to a local minimum (the supination position), then returned to the pronation position (Figure 6-3). Since all subjects finished at least 20 cycles each trial, 15 cycles starting from the 6<sup>th</sup> cycle were extracted and resampled to 100 Hz. Therefore each force/angle point represented a value in an interval of 1% of each cycle period.

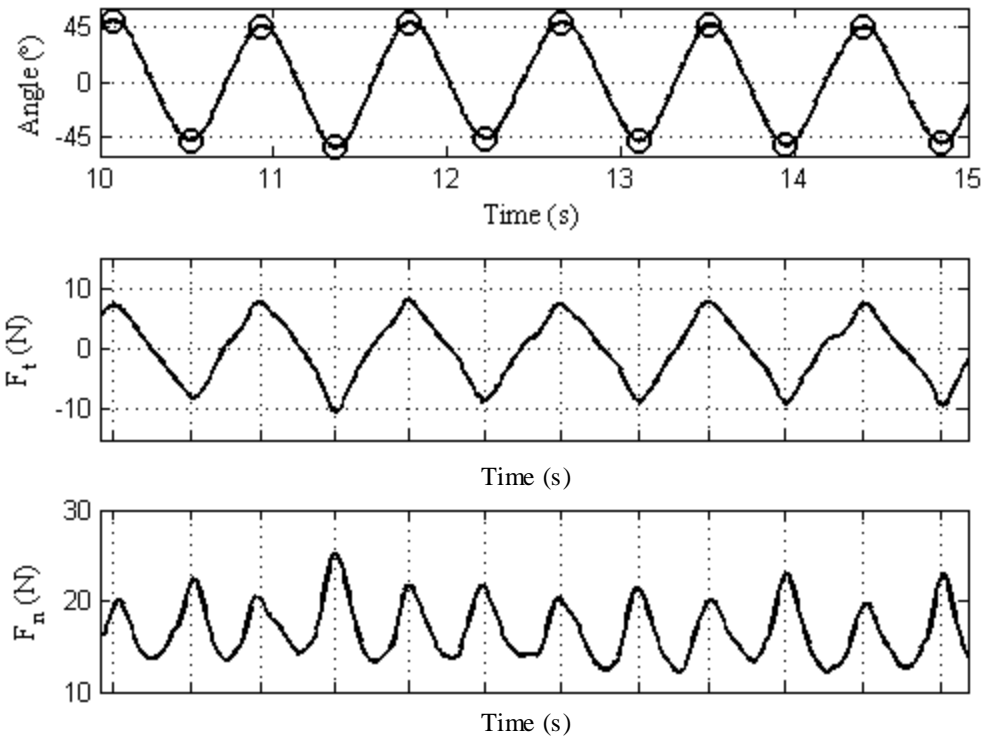


Fig. 6-3 A section of angle, total tangential force, and total normal force from a representative subject. The task frequency was 120bpm (1Hz). The circles in the top figure showed the end positions of the oscillation movement. Their timing was used to slice the tangential force and normal force into epochs, as shown by the dashed vertical lines in the lower two figures.

### 6.2.4.3 Approximate Entropy

The regularity of total normal force and tangential force was quantified by approximate entropy, ApEn (Lodha, Naik et al. 2010; Slifkin and Newell 2000; Vaillancourt and Russell 2002). The lower ApEn is, the more regular the variability-structure of the signal has. Therefore, a sinusoidal signal has ApEn close to 0, while a white Gaussian noise has ApEn almost 2. ApEn was calculated by (Pincus 1991):

$$\text{ApEn}(X, m, r) = \ln\left[\frac{C_m(r)}{C_{m+1}(r)}\right] \quad (6-5)$$



where  $r$  is the similarity measure,  $C_m$  represents the number of occurrence of a window of length  $m$  within  $r$  of the standard deviation of the time series  $X$ . In the current study,  $r$  was set at 0.5 and  $m$  was 2.

#### 6.2.4.4 UCM analysis

Uncontrolled manifold (UCM) method was used to analyze the trial-by-trial variability of tangential forces. According to UCM hypothesis, in a redundant system, the central nervous system constrains the variability in the task performance variable (or variables), in the mean time has no control on the rest degrees of freedom (Scholz and Schoner 1999; Scholz, Danion 2002). The two manifolds (mathematical concept for subspace), UCM space and orthogonal (ORT) space, are orthogonal to each other. The performance variable is associated with elemental variables via a Jacobian matrix. In this study, the performance variable (the total torque) is the summation of elemental variables (the tangential forces of individual digits) multiplied by the radius of the handle. For simplification, the radius was removed from the Jacobian matrix without affecting the result,

$$J = [1 \quad 1 \quad 1 \quad 1 \quad 1]^T \quad (6-6)$$

In the above equation, T represents the transpose of a matrix. ORT and UCM space correspond to the kernel and null space with dimension of one and four, respectively.

Assume that the basis for UCM space are  $e_{\parallel}$ , we can compute the projection of  $F$  (a centralized force vector by removing means across trials from individual digit force) onto them separately.

$$F_{\parallel} = e_{\parallel} e_{\parallel}^T F \quad (6-7)$$

$$F_{\perp} = F - F_{\parallel} \quad (6-8)$$

The variability of elemental variables can subsequently be computed as the sum of two components,  $V_{ORT}$  and  $V_{UCM}$ .

$$V_{UCM} = \text{Var}(F_{\parallel}) \quad (6-9)$$

$$V_{\text{ORT}} = \text{Var}(F_{\perp}) \quad (6-10)$$

Delta variance, an index used to study motor synergy, is the difference between  $V_{\text{UCM}}$  and  $V_{\text{ORT}}$  per degree of freedom. And to compare over subjects of different strength, it is usually normalized by the total variability.

$$DV = \frac{V_{\text{UCM}} / d_{\text{UCM}} - V_{\text{ORTH}} / d_{\text{ORTH}}}{V_{\text{UCM}} + V_{\text{ORTH}}} \quad (6-11)$$

$d_{\text{UCM}}$  and  $d_{\text{ORTH}}$  are 4 and 1, respectively.

### 6.2.5 Statistical analysis

Repeated measure ANOVAs were performed for the between-subject factor: frequency (*Freq*, 3 levels: 0.5Hz, 0.75Hz, and 1Hz) and moment of inertia (MOI, 7 levels). The level of significance was set at  $p = 0.05$ . The Kolmogorov-Smirnov test and the Shapiro-Wilks test were used to test violation of the normal distribution assumption, and Levene's homogeneity test was used to test the assumption of variance homogeneity. Huynh-Feldt stats were applied if the sphericity hypothesis for ANOVA was violated. Statistics were shown as means and standard deviations.

### 6.3 Results

Although there were two sets of tangential forces (the horizontal tangential force and the vertical tangential force), only the horizontal tangential forces in the grasp plane contributed to the rotational movement. The role of the vertical tangential forces was to balance against the gravitational force. The sum of them roughly equaled the weight of the handle, with small deviation due to the tilt movement unconstrained during the experiment. To avoid confusion, they are not discussed further. "Tangential force" in the following sections refers to the horizontal tangential force only.

### 6.3.1 The relationship between handle angle, normal and tangential force

Subjects tended to excurse past the angular boundaries, specifically  $47.1 \pm 1.6^\circ$  for pronation and  $47.4 \pm 1.6^\circ$  for supination, following a sinusoid pattern. Figure 6-4 showed an averaged time profile of handle angle, total tangential force, and total normal force after segmentation and resampling. Both normal force and tangential force were greater at the two ends of the movement range (0%, 50%, and 100%) compared to the wrist neutral position (25%, 75%). For normal force, its frequency doubled and it was always positive as the prerequisite for grasping, i.e. sufficient to prevent slipping. Tangential force was positive for pronation and negative for supination, and exhibited an in-phase relationship as the handle angle.

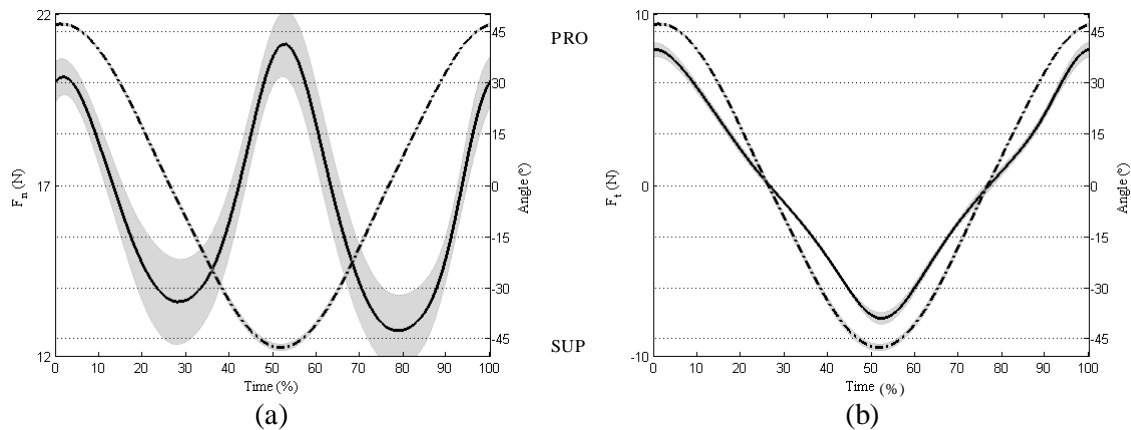


Fig. 6-4 (a) Normal force and (b) tangential force over time averaged across subjects ( $Freq$ : 0.5Hz,  $MOI$ : 7). The time profile of handle angle was superposed on each figure as dashed lines and labeled on the right.

Maximal normal force ( $F_n^{\max}$ ) and tangential force ( $F_t^{\max}$ ) were correlated with both movement frequency and moment of inertia (MOI) (Figure 6-5). Both  $F_n^{\max}$  and  $F_t^{\max}$  showed significant effects of  $Freq$ , MOI, and the interaction of the two factors. Similar effects were also found for  $F_n^{\min}$  and  $(F_n^{\max} - F_n^{\min})$  as well. For the same MOI,  $F_n^{\max}$  was more affected by frequency than

$F_t^{\max}$ . For instance, when MOI was  $0.0629\text{N}\cdot\text{m}^2$  (two masses 30cm apart),  $F_n^{\max}$  increased from 21.15N to 93.1N (4.4times), while  $F_t^{\max}$  from 7.93N to 28.75N (3.62 times).

Linear regression was performed between the time profile of  $F_t(t)$  and  $F_n(t)$ . For the current bidirectional tasks, one line was obtained for pronation and supination positions respectively. The average of slopes and offsets were shown in Figure 6-5(c) and (d). When the frequency was 0.5Hz, a more varied relationship existed between the slope and MOI. Otherwise, both slope and offset showed a linear association with MOI and increased with the frequency.

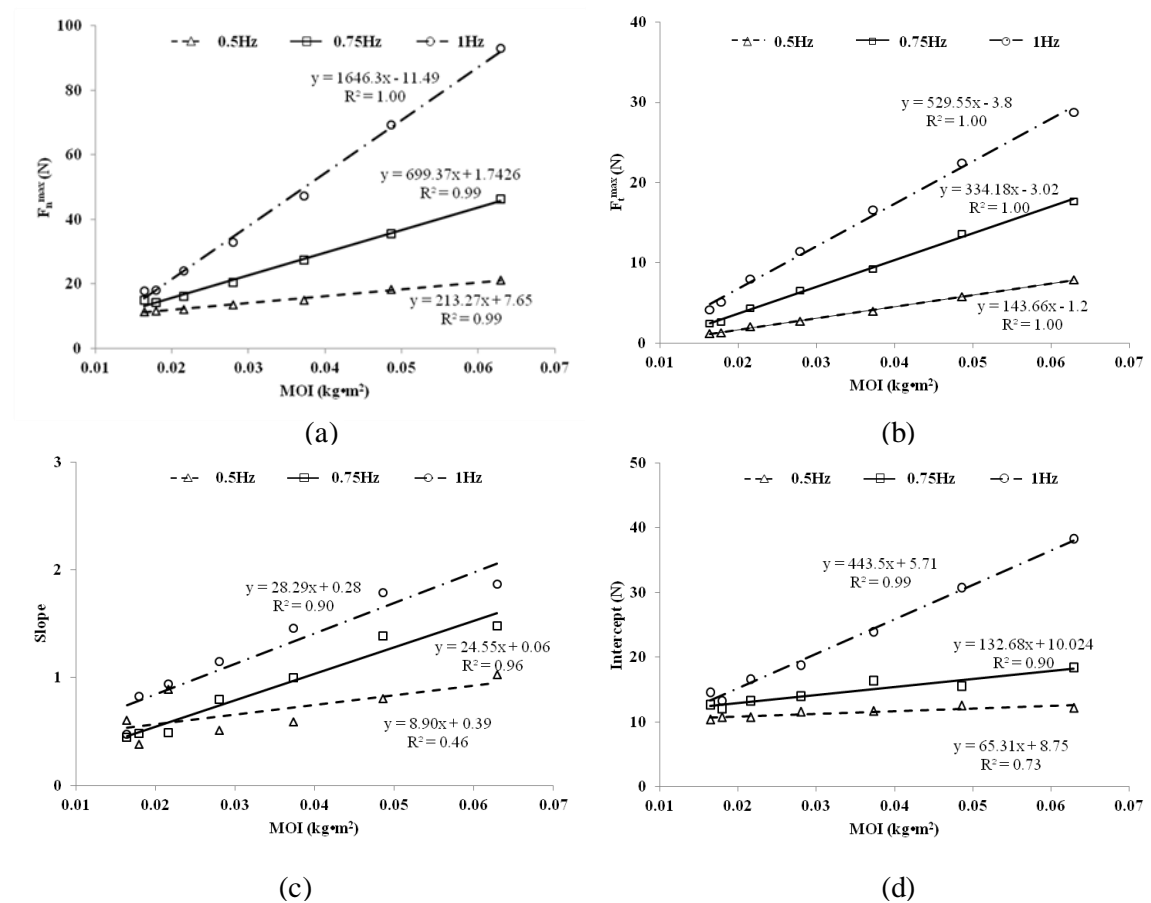


Fig. 6-5 (a) maximal normal forces, (b) maximal tangential forces, (c) slopes, and (d) intercepts of linear regression versus MOI at three frequencies. The standard deviations were too small compared to the force magnitude and thereby omitted.

### 6.3.2 Force hysteresis of normal and tangential force

Despite the synchronized-like behavior of both force components with handle angle in Figure 6-4, a closer look could reveal subtle difference within-cycle. An example of the relationship between normal/tangential force and handle angle is illustrated in Figure 6-6. For a full PRO-SUP-PRO cycle, there were minima of different timing and magnitude in normal force and a hysteresis loop in tangential force. To quantify the phenomenon, the average integral of force-angle curve in cycles was calculated. For normal force, the integral stands for the difference between the areas of two enclosed shapes; for tangential force, the integral represents the area in the hysterical loop. Therefore, this variable reflects the imbalance between the two PRO-SUP and SUP-PRO half-cycles. The smaller it is, the more similar the corresponding force-angle curve will be.

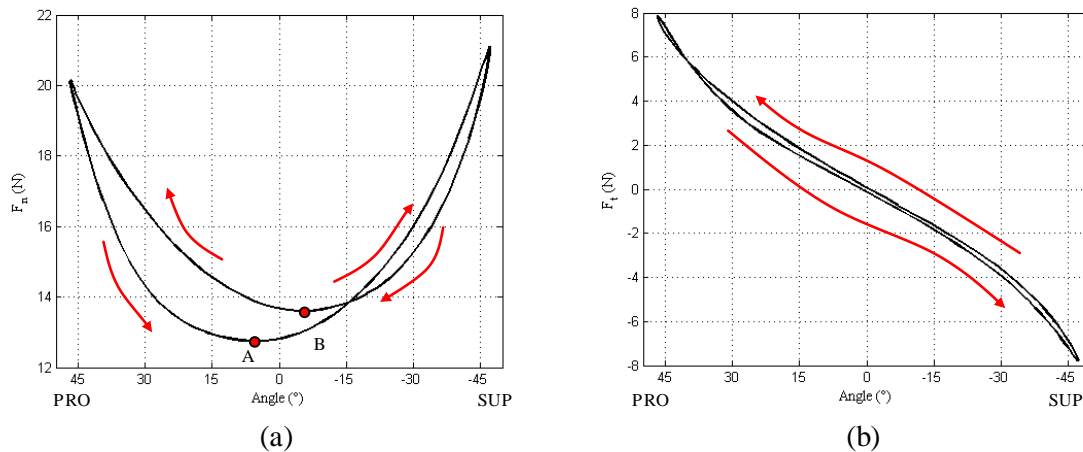


Fig. 6-6 (a) Normal force and (b) tangential force versus handle angle averaged across subjects (the same condition as in Figure 6-4, only the averaged trajectories are shown). Red arrows indicate the direction of  $F_n$  and  $F_t$  in a cycle. A and B are the minima of  $F_n$  in the direction of PRO-SUP and SUP-PRO respectively.

Figure 6-7 shows the hysteresis of normal force and tangential force. Hysteresis of normal force was associated with MOI ( $F(6,30) = 41.05, p = 0.001$ ) and the interaction of  $Freq \times MOI$  ( $F(12, 60) = 5.57, p = 0.18$ ).  $Freq$  was not significant. In contrast, hysteresis of tangential force was

dependent on  $Freq$  ( $F(2,10) = 22.3, p = 0.000$ ), but not on MOI or their interaction. Although maximal tangential force increased with MOI, the enclosed loop by the two sub-phases (Figure 6-6(b)) was stretched in the force dimension, it was compressed in the angle dimension. Therefore, the integral hysteresis remained nearly constant.

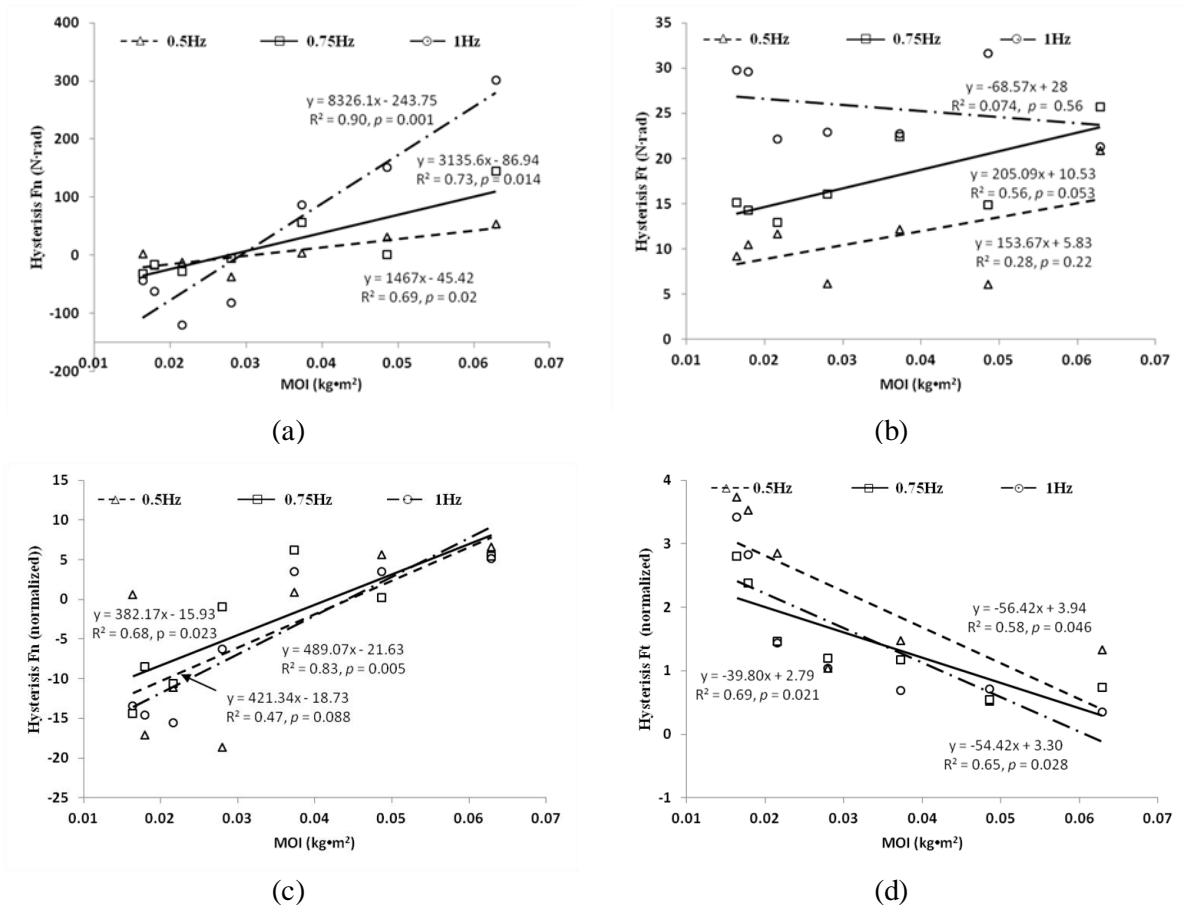


Fig. 6-7 Hysteresis of normal force (a) and tangential force (b) versus MOI, normalized hysteresis of normal force (c) and tangential force (d). Regression lines are shown for three frequencies with equations and goodness of fit. The rest of the chapter will use the same pattern to present the results.

The bottom two panels of Figure 6-7 show the hysteresis of normal force and tangential force after normalized by their  $|F_i^{\max} - F_i^{\min}|$  ( $i = t$  or  $n$ ), respectively. For both force components, the

three regression lines were identical based on the algorithm (Neter, Kutner et al. 1996) but had opposite dependency on MOI.

### 6.3.3 Approximate entropy of normal and tangential force

In contrast to the hysteresis index which characterizes the imbalance within cycle, approximate entropy (ApEn) from information theory was computed to quantify the regularity of force between cycles. A smaller value of ApEn indicates a more periodic signal, thereby easier to predict based on the information available; while a larger value means a pattern less-likely to repeat in the future. For instance, a total random signal would have an ApEn value of 2. Overall, ApEns from both force components were small ( $<0.01$  for most conditions), suggesting a quite regular force output. However, ApEn of normal force was about twice as large as tangential force (see Figure 6-7 and the sample data in Figure 6-3). This result was not unexpected because normal force was not explicitly controlled during the task, and therefore allowed more variation than tangential force.

For normal force, ApEn increased with frequency and in general decreased with MOI (see Figure 6-8(a)). One exception was when the two masses were 10cm away from the rotating axis (MOI = 3 and 4), ApEn showed a dip for all three frequencies, suggesting that normal force was more repeatable when the two masses were placed around this distance range. ANOVA analysis demonstrated significant effects of *Freq* ( $F(2,10) = 11.98, p = 0.001$ ) and MOI ( $F(6,30) = 6.57, p = 0.000$ ) without interaction.

In contrast, ApEn for tangential force did not change with frequency ( $F(2,10) = 3.37, p = 0.076$ ), but decreased with MOI ( $F(6,30) = 47.78, p = 0.000$ ). Tasks of slower movements with smaller MOI had larger ApEns. However, when MOI increased, the difference by frequency was largely diminished (except when the two masses were 25cm apart, MOI =  $0.0486\text{N}\cdot\text{m}^2$ ).

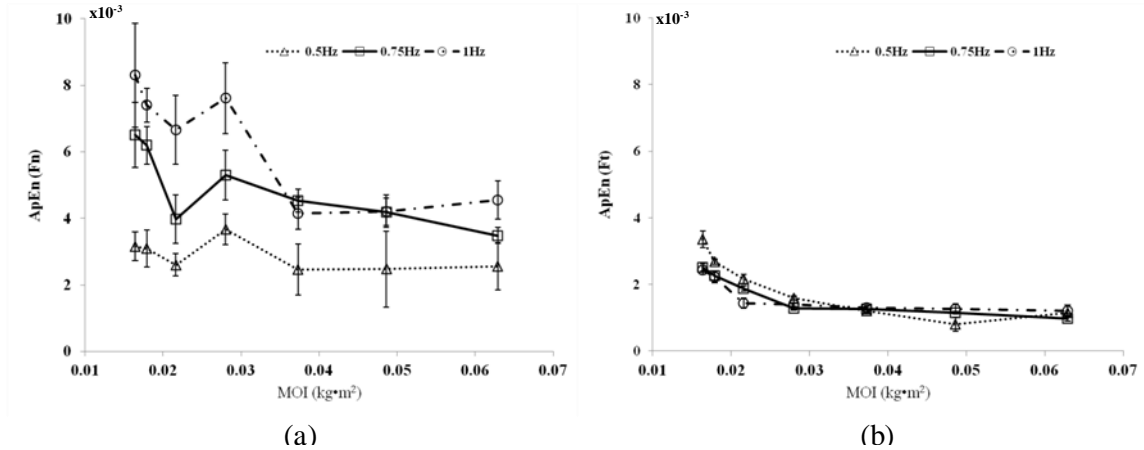


Fig. 6-8 Approximate entropy (ApEn) of (a) total normal force and (b) total tangential force versus MOI.

### 6.3.4 Force variability in UCM and ORT space

Strictly speaking, the decomposition of normal force into UCM and ORT spaces was not appropriate because there was no explicit goal that normal forces from individual digits had to achieve. Here we chose total normal force for the UCM computation on the consideration of safety margin (Johansson and Cole 1994), i.e. for a given total tangential force, total normal force must be large enough to prevent the handle from slipping out of hand.

Variances in UCM and ORT space presented in this section were divided by the degree of freedom of each space, i.e. 4 and 1, respectively and normalized by their maximum forces squared. The values for tangential force exhibited an exponential dependency on MOI. For the purpose of clear demonstration, a natural logarithm was applied to  $V_{UCM}$  and  $V_{ORT}$  when plotting the figures. The same procedure was used for the variances of normal force as well for consistency.

Overall the variability in UCM space was smaller than that in ORT space for both normal force and tangential force, indicating a negative delta variance (DV) and positive co-variation among digit forces.  $V_{UCM}$  and  $V_{ORT}$  for normal force were smaller than those for tangential force by an



order of one to three. However, it was due to the normalization with larger  $(F_n^{\max})^2$ . The actual values were within  $[0, 2 N^2]$  (UCM) and  $[0, 10 N^2]$  (ORT) for normal force, and  $[0, 0.5 N^2]$  (UCM) and  $[0, 1.2 N^2]$  (ORT) for tangential force.

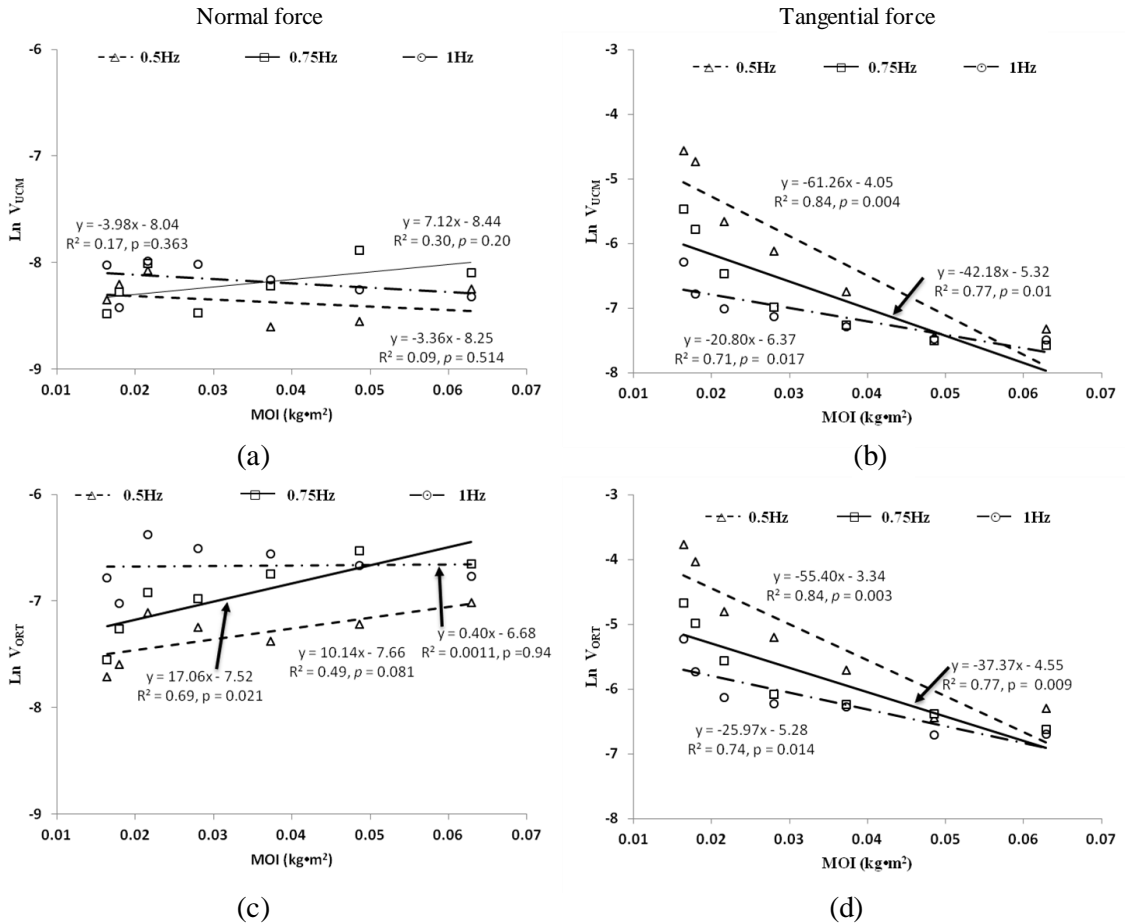


Fig. 6-9 The variability of normal and tangential force in UCM and ORT space. The values were normalized by  $(F_n^{\max})^2$  and  $(F_t^{\max})^2$ , followed by a natural logarithm. Note that the actual variances were smaller than 1 after normalization, therefore were negative on the ordinate.

For normal force, the effect of *Freq* was significant for both UCM ( $F(2,10) = 6.36$ ,  $p = 0.018$ ) and ORT ( $0.5\text{Hz} < 0.75\text{Hz} < 1\text{Hz}$ ,  $F(2,10) = 57.5$ ,  $p = 0.000$ ) variability. The two MOI conditions (0cm and 5cm) had smaller  $V_{\text{ORT}}$  than the other MOI conditions in 0.5Hz and 0.75Hz cases, resulting a significant effect of MOI in  $V_{\text{ORT}}$  ( $F(10,30) = 14.07$ ,  $p = 0.000$ ).

For tangential force, both  $V_{UCM}$  and  $V_{ORT}$  showed qualitatively similar dependency on  $Freq$  and MOI. All the main effects and interaction were significant. When the movement frequency increased or the two masses were separated further away, variances in both spaces reduced with quite analogous rate, resulting in a relative constant DV (see Figure 6-10b).

Delta variance (DV) from equation (6-11) was calculated using the non-normalized  $V_{UCM}$  and  $V_{ORT}$ . For normal force, DV was affected by both  $Freq$  ( $0.5\text{Hz} > 0.75\text{Hz} > 1\text{Hz}$ ,  $F(2,10) = 39.47$ ,  $p = 0.000$ ) and MOI ( $F(6,30) = 20.59$ ,  $p = 0.000$ ), but not by their interaction. For tangential force, MOI was the only significant effect ( $F(6,30) = 3.70$ ,  $p = 0.029$ ), however no pairwise comparison showed considerable difference.

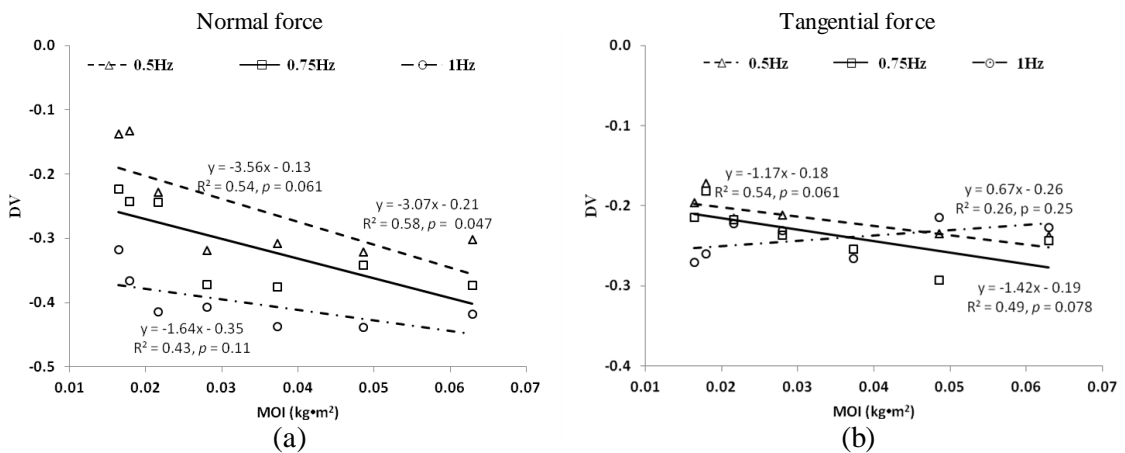


Fig. 6-10 Delta variance for normal force (a) and tangential force (b).

## 6.4 Discussion

This study investigated the multi-digit force production in a dynamic cyclic torque task. In contrast to other finger studies which used cyclic force pressing tasks (Friedman, Skm 2009; Latash, Scholz 2002), our experiment asked subjects to generate torque with both the hand and the forearm. Normal force was not specified by the experimenter except “grasping the handle as comfortably as you feel”. During the task, they did not contribute to the torque as in some

prehension tasks (Gao, Latash et al. 2005; Kinoshita, Kawai et al. 1996; Shim, Latash 2005). The only constraint of normal force came from safety margin, i.e. it should be large enough to prevent the handle from slipping. Instead, tangential force was the only variable producing the torque. As expected for inertia loads, total tangential force exhibited an in-phase behavior as the handle angle and  $F_t^{\max}$  increased with both frequency and moment of inertia.

#### **6.4.1 The effect of movement frequency on modulation of normal and tangential force in a cyclic movement**

As seen in precision grip tasks such as reach-and-grasp or lifting, there was a strong coupling between normal force and tangential force in timing and magnitude. For instance, both maximal normal force and tangential force occurred at the two angular boundaries, and showed linear dependency on moment of inertia (see Figure 6-4). This result matches the well-documented grip force (GF) – load force (LF) coupling. The coupling was originally studied in discrete tasks like lifting, has also been found in repetitive static and dynamic grasp tasks (Danion, Descoins 2009; Uygur, de Freitas 2010). In an isometric task, Uygur and colleagues asked subjects to produce oscillatory tangential force on a rectangular handle. They found that both slope and intercept decreased with movement frequency. In our experiment, however, both variables increased significantly with movement frequency. This difference might rise from the different “motor drive”, and therefore two sets of control policies, for the two tasks. In the first experiment, subjects needed to produce tangential force, predominantly with muscles for digits. When frequency increased, the digit joints needed to “loosen up” by reducing normal force. In contrast, the current experiment asked subjects to grasp and rotate the handle. The purpose of normal force was to secure the grasp. Therefore, when torque increased as a result of frequency, more normal force was required to “tighten down”. Another possible reason is that the direct goal shown to the subjects in the current study was a kinematic variable (the handle angle). Therefore the displacement of individual digits was strictly confined. In contrast, the direct goal in the first

study was total tangential force, allowing some freedom in digit displacement. A comparison of the displacement of center of pressure for individual digit on the contact surface can verify the hypothesis.

#### **6.4.2 Force-angle relationship**

Force-angle relationship was examined in our study both within-cycle by hysteresis, and between-cycle by approximate entropy. Hysteresis index has been used in some studies for biomechanical modeling of quasi-static stiffness of the ankle joint (Bach, Chapman et al. 1983; Gao, Ren 2011). It is thought to be associated with the viscoelastic property of the joint (Kubo, Kanehisa et al. 2001). However, it has not received much attention in cyclic arm movement.

In this study, we found that normalized hysteresis for normal and tangential force changed monotonically with MOI, and showed no difference on movement frequency. Specifically, if MOI increased, hence the maximal tangential force increased, the hysteresis loop narrowed in the handle angle dimension, i.e. the two half-cycles became homogenized. However, the narrowing was absent if the increase was caused by frequency, indicating the hysteresis was specific to the angular position of the wrist. A conclusion we can draw is that the viscosity property of the wrist for rotating movement is affected by force level, but not by movement frequency. In contrast, hysteresis for normal force was determined by the difference of the magnitude and angular position of  $F_n^{\min}$  in two half-cycles. When MOI was large (see Figure 6-6a as an example), hysteresis originated from the magnitude difference; when MOI was small, it was mainly due to the asymmetric angular position of the two  $F_n^{\min}$ . More specifically, the  $F_n^{\min}$  in the second half-cycle (supination to pronation) tended to occur after the neutral position while it stayed around the neutral position in the first half-cycle. Similar to that of tangential force, this result seemed to be related to the wrist angle in pronation/supination plane and was not affected by frequency.

Approximate entropy (ApEn) is an index to characterize the structure of variability in motor output (Ofori, Samson et al. 2010; Pincus 1991; Slifkin and Newell 2000; Vaillancourt, Slifkin et al. 2002). We expected that it would increase with movement frequency and the force level. The results showed that ApEn of normal force and tangential force decreased with MOI. This can be explained by the adjustment of contribution from intrinsic and extrinsic muscles to the force output. Rotating the handle with larger MOI required recruitment of extrinsic muscles, whose moment arms are less affected by the wrist movement than intrinsic muscles are. Therefore, the force output was more stable. On the other hand, significant effect of frequency on ApEn of tangential force was not found, either directly by causing more error or indirectly by modifying the force level. One possible explanation is that the frequencies used in this experiment were within a reasonable limit, allowing subjects to obtain a satisfactory performance with ease. Further study can push the frequency higher to 3Hz, a condition used by many cyclic finger pressing studies. Also the coordination between individual digits might compensate the error of each other and make the total tangential force more regular. ApEn of normal force, on the other hand, were greater for faster movement probably because subjects paid more attention to match the target with increased frequency.

#### **6.4.3 The dependence of multi-digit synergy on frequency**

As in previous chapters, variability of tangential force was decomposed into UCM space and ORT space using uncontrolled manifold analysis. Variability in ORT space,  $V_{ORT}$ , was greater than variability in UCM space,  $V_{UCM}$ , for all conditions, indicating an absence of negative compensation among individual digit tangential forces. The lack of multi-digit synergy in torque production was unexpected. Although we assumed that for fast frequency, individual digit forces may get more synchronized, slower movement, especially with large MOI, was expected to show a negative covariation among individual digit forces, as in finger-pressing studies. The frequencies we used in this study were below the preferred frequency (about 2Hz) of finger force

production (Latash, Scholz 2002). In fact, this “preferred frequency” is probably overestimated. In order to allow multi-digit synergy to emerge, frequencies equal to and below 1.33 Hz were recommended by the authors in a four finger cyclic force production task (Friedman, Skm 2009). Moreover, tangential force instead of normal force was used here. The viscoelastic and compliance properties of finger pad are different for contact and shear force, i.e. force in orthogonal and tangential direction (Nakazawa, Ikeura 2000; Serina, Mote et al. 1997). Moreover, mechanoreceptors respond to each type of force differently and have different sensitivity to the two types of forces (Pare, Carnahan et al. 2002; Wheat, Salo et al. 2009). The difference in sensory feedback may make it difficult to implement error compensation in the current study. Another explanation is related to the use of the wrist in this study. The whole forearm was free to rotate in the study, therefore the possibility existed that subjects just held the circular handle tight and relied on the wrist rotation to complete the task. According to “minimum intervention principle” (Todorov 2004), the central nervous system fixes the sharing pattern of individual digit tangential forces and controls only the resultant force.

## **6.5 Conclusion**

This study investigated the multi-digit coordination in repetitive oscillation task on a circular object. It was found: (1) both modulation gain and intercept of normal force by tangential force are positively associated with frequency and moment of inertia; (2) within-cycle similarity of normal and tangential force, characterized by hysteresis index, is not affected by frequency; (3) between-cycle regularity of normal and tangential force, characterized by approximate entropy, decreases with moment of inertia; (4) multi-digit synergy is negative and remains constant across conditions.

## Chapter 7

### Conclusion

#### 7.1 Summary

This section summarizes important findings in each study and discusses the significance of the results. Connections among findings between studies are explained.

- Study I (MVT, Chapter 3) investigated human's maximum voluntary isometric torque with different wrist positions and torque directions. It was found that torque in CW (closing) direction was greater than in CCW (opening) direction. The result provided ergonomics suggestion on jar lid direction design. Under the maximum torque, the sharing pattern of tangential forces was not affected by the either factor, while the sharing pattern of normal force was affected by wrist position. This task also served as a preparatory step for the second and the third experiment.
- Study II (Ramp, Chapter 4) examined the sharing pattern of individual normal and tangential forces as well as their relation, described by safety margin in submaximal torque production task. The sharing pattern of normal force was affected by wrist position only in GRASP (normal force producing) subtask, not in HOLD (torque producing) subtask. The discrepancy might be caused by the task-specific dependency of the coupling between normal force and tangential force. For MVT task, the coupling was automatic; while for submaximal torque task, the coupling of two force components was loose, resulting in a decoupled control. It was also found that initial normal force changed the dynamic process of safety margin so that a larger force led to a slower transition of safety margin and a higher safety margin in the stable torque producing phase. At last, fingers were grouped into radial (index and middle fingers)

and ulnar (ring and little fingers, which had opposite preferred torque direction in both normal force production (GRASP) phase and torque production (HOLD) phase.

- Study III (Ramp-Down-Ramp-Up, Chapter 5) investigated the multi-digit synergy in static torque production task. It was found that the modulation gain of normal force by tangential force was greater in torque increase direction than in torque decrease direction. The multi-digit synergy was diminished, and destroyed in some subjects, during the ramp down phase and was restored in the ramp up phase. Maximal constant error of torque and minimal delta variance occurred during the transition.
- Study IV (oscillation, Chapter 6) inspected the multi-digit coordination in a dynamic oscillation task. The maximal normal and tangential force increased with movement frequency and moment of inertia. Within-cycle regularity of normal force and tangential force showed opposite dependency on moment of inertia and neither was affected by frequency. Between-cycle regularity decreased with moment of inertia, but only that of normal force was affected by frequency. Multi-digit synergy was not present in any of the conditions.

## **7.2 Future research**

Despite the finding presented here, this dissertation also leaves a lot of questions open and raises even more to ask. For example, what is the optimal normal force in a torque production task? How will change the number of digits affect the multi-finger synergy? Will the results apply to manipulation of objects with other geometric shapes or sizes? How does the nervous system organize multi-digit synergy? In the future, a few research directions might be explored with the knowledge gained in the dissertation.

- (1) Combine kinetic measurement with kinematic and electromyography data. There are many studies trying to build the link between the output of end effector and individual muscles by solving the inverse dynamic problem (Johnston, Bobich 2010; Leijnse, Campbell-Kyureghyan et



al. 2008; Valero-Cuevas 2005) However, the researches on multi-digit synergy have so far been conducted at computational level. Although it would be challenge to establish a model for the entire musculoskeletal structure of hand and forearm, the goal may be approached with the combination of all the techniques.

(2) Multi-digit synergy is said to have a higher origin as the neural representation of individual digit is widely distributed in primary motor cortex (Schieber 2001). Several theories exist that acclaim, instead of specifying commands to each muscle, the brain encodes other targets such as force direction (Georgopoulos, Pellizzer et al. 1999) or grasp trajectory (Saleh, Takahashi et al. 2010). It is also likely that some parameter in manipulation is programmed in this area. For example, a previous study using magnetoencephalography (MEG) showed that there is a correlation between force rate and one principal component (poster in SFN2008).

(3) The deterioration of hand function cause unnecessary stress, fatigue or injury. Many factors can be involved, both central (Beck, Houdayer et al. 2009; Lang and Schieber 2003) and peripheral (such as swan neck deformity and trigger finger), developmental (Shim, Oliveira et al. 2007) or aging (Shinohara, Li et al. 2003). It would be beneficial not only to apply manipulative skill tests for hand evaluation, but also to develop rehabilitation protocols to help patients for a partial or full recovery.

## Bibliography

- [1] Adams, S.K. and Peterson, P.J. Maximum voluntary hand grip torque for circular electrical connectors. *Hum Factors*, 1988. **30**. **30**(6. 6): p. 733-45.
- [2] Addamo, P.K., Farrow, M., *et al.* The effects of age and attention on motor overflow production--A review. *Brain Res Rev*, 2007. **54**(1): p. 189-204.
- [3] Amis, A.A. Variation of finger forces in maximal isometric grasp tests on a range of cylinder diameters. *J Biomed Eng*, 1987. **9**(4): p. 313-20.
- [4] Andre, T., Lefevre, P., and Thonnard, J.L. Fingertip moisture is optimally modulated during object manipulation. *J Neurophysiol*, 2010. **103**(1): p. 402-8.
- [5] Aoki, T., Francis, P., and Kinoshita, H. Differences in the abilities of individual fingers during the performance of fast, repetitive tapping movements. *Experimental Brain Research*, 2003. **152**(2): p. 270.
- [6] Arimoto, S., Tahara, K., *et al.*, *Principles of superposition for controlling pinch motions by means of robot fingers with soft tips*. 2001, Cambridge University Press. p. 21-28.
- [7] Armstrong, T.J., Fine, L.J., *et al.* Ergonomic considerations in hand and wrist tendinitis. *Journal of Hand Surgery*, 1987. **12A**: p. 830-837.
- [8] Ayoub, M.M. and Presti, P.L. The determination of an optimum size cylindrical handle by use of electromyography. *Ergonomics*, 1971. **14**(4): p. 509-18.
- [9] Bach, T.M., Chapman, A.E., and Calvert, T.W. Mechanical resonance of the human body during voluntary oscillations about the ankle joint. *J Biomech*, 1983. **16**(1): p. 85-90.
- [10] Balasubramaniam, R., Riley, M.A., and Turvey, M.T. Specificity of postural sway to the demands of a precision task. *Gait Posture*, 2000. **11**(1): p. 12-24.
- [11] Baud-Bovy, G. and Soechting, J.F. Factors influencing variability in load forces in a tripod grasp. *Exp Brain Res*, 2002. **143**(1): p. 57-66.
- [12] Beck, S., Houdayer, E., *et al.* The role of inhibition from the left dorsal premotor cortex in right-sided focal hand dystonia. *Brain Stimul*, 2009. **2**(4): p. 208-14.
- [13] Bernstein, N., *The co-ordination and regulation of movements*. 1967: Pergamon, Oxford.
- [14] Blau, P.J., *Friction science and technology*. 1996, New York: Marcel Dekker, Inc. 27-38.
- [15] Brand, P. and Hollister, A., *Clinical Biomechanics of the Hand*. 3 ed. 1999, Chicago, IL: Mosby.
- [16] Buchanan, T.S., Moniz, M.J., *et al.* Estimation of muscle forces about the wrist joint during isometric tasks using an EMG coefficient method. *J Biomech*, 1993. **26**(4-5): p. 547-60.
- [17] Burstedt, M.K., Edin, B.B., and Johansson, R.S. Coordination of fingertip forces during human manipulation can emerge from independent neural networks controlling each engaged digit. *Exp Brain Res*, 1997. **117**(1): p. 67-79.
- [18] Burstedt, M.K., Flanagan, J.R., and Johansson, R.S. Control of grasp stability in humans under different frictional conditions during multidigit manipulation. *Journal of neurophysiology*, 1999. **82**(5): p. 2393.

- [19] Carlton, L. and Newell, K., Force variability and characteristics of force production, in *Variability and Motor Control*, N. KM and C. DM, Editors. 1993, Human Kinetics: Champaign, IL. p. 15-36.
- [20] Christou, E.A., Grossman, M., and Carlton, L.G. Modeling variability of force during isometric contractions of the quadriceps femoris. *J Mot Behav*, 2002. **34**(1): p. 67-81.
- [21] Ciriello, V.M., Webster, B.S., and Dempsey, P.G. Maximal acceptable torques of highly repetitive screw driving, ulnar deviation, and handgrip tasks for 7-hour workdays. *AIHA J (Fairfax, Va)*, 2002. **63**(5): p. 594-604.
- [22] Cole, K. and Beck, C. The stability of precision grip force in older adults. *Journal of Motor Behavior*, 1994. **26**: p. 171-177.
- [23] Cole, K.J. and Johansson, R.S. Friction at the digit-object interface scales the sensorimotor transformation for grip responses to pulling loads. *Exp Brain Res*, 1993. **95**(3): p. 523-32.
- [24] Cutkosky, M.R. and Howe, R.D., *Dextrous Robot Hands*. 1990, New York: Springer Verlag.
- [25] d'Avella, A., Saltiel, P., and Bizzi, E. Combinations of muscle synergies in the construction of a natural motor behavior. *Nat Neurosci*, 2003. **6**(3): p. 300-8.
- [26] Danion, F., Latash, M.L., *et al*. The effect of a fatiguing exercise by the index finger on single- and multi-finger force production tasks. *Exp Brain Res*, 2001. **138**(3): p. 322-9.
- [27] Danion, F., Li, S., *et al*. Relations between surface EMG of extrinsic flexors and individual finger forces support the notion of muscle compartments. *Eur J Appl Physiol*, 2002. **88**(1-2): p. 185-8.
- [28] Danion, F., Schoner, G., *et al*. A mode hypothesis for finger interaction during multi-finger force-production tasks. *Biol Cybern*, 2003. **88**(2): p. 91-8.
- [29] Danion, F., Descoins, M., and Bootsma, R.J. When the fingers need to act faster than the arm: coordination between grip force and load force during oscillation of a hand-held object. *Exp Brain Res*, 2009. **193**(1): p. 85-94.
- [30] Dimitriou, M. and Edin, B.B. Discharges in human muscle receptor afferents during block grasping. *J Neurosci*, 2008. **28**(48): p. 12632-42.
- [31] Dumont, C.E., Popovic, M.R., *et al*. Dynamic force-sharing in multi-digit task. *Clin Biomech (Bristol, Avon)*, 2006. **21**(2): p. 138-46.
- [32] Edin, B.B., Westling, G., and Johansson, R.S. Independent control of human finger-tip forces at individual digits during precision lifting. *J Physiol*, 1992. **450**: p. 547-64.
- [33] Effenbein, D.H. and Rettig, M.E. The digital extensor mechanism of the hand. *Bull Hosp Jt Dis*, 2000. **59**(4): p. 183-8.
- [34] Fellows, S.J., Kronenburger, M., *et al*. The effect of subthalamic nucleus deep brain stimulation on precision grip abnormalities in Parkinson's disease. *Parkinsonism Relat Disord*, 2006. **12**(3): p. 149-54.
- [35] Flanagan, J.R. and Wing, A.M. The stability of precision grip forces during cyclic arm movements with a hand-held load. *Exp Brain Res*, 1995. **105**(3): p. 455-64.
- [36] Flanagan, J.R., Burstedt, M.K., and Johansson, R.S. Control of fingertip forces in multidigit manipulation. *Journal of neurophysiology*, 1999. **81**(4): p. 1706.

- [37] Flanagan, J.R. and Beltzner, M.A. Independence of perceptual and sensorimotor predictions in the size-weight illusion. *Nat Neurosci*, 2000. **3**(7): p. 737-41.
- [38] Fong, P.W. and Ng, G.Y. Effect of wrist positioning on the repeatability and strength of power grip. *Am J Occup Ther*, 2001. **55**(2): p. 212-6.
- [39] Fowler, N.K. and Nicol, A.C. Measurement of external three-dimensional interphalangeal loads applied during activities of daily living. *Clin Biomech*, 1999. **14**. **14**(9. 9): p. 646-52.
- [40] Fowler, N.K. and Nicol, A.C. A biomechanical analysis of the rheumatoid index finger after joint arthroplasty. *Clin Biomech (Bristol, Avon)*, 2002. **17**(5): p. 400-5.
- [41] Freund, J., Toivonen, R., and Takala, E.P. Grip forces of the fingertips. *Clin Biomech (Bristol, Avon)*, 2002. **17**(7): p. 515-20.
- [42] Friden, J. Vibration damage to the hand: clinical presentation, prognosis and length and severity of vibration required. *J Hand Surg [Br]*, 2001. **26**(5): p. 471-4.
- [43] Friedman, J., Latash, M., and Zatsiorsky, V. Prehension synergies: a study of digit force adjustments to the continuously varied load force exerted on a partially constrained hand-held object. *Experimental Brain Research*, 2009. **197**(1): p. 1.
- [44] Friedman, J., Skm, V., *et al*. The sources of two components of variance: an example of multifinger cyclic force production tasks at different frequencies. *Experimental Brain Research*, 2009. **196**(2): p. 263.
- [45] Gao, F., Latash, M., and Zatsiorsky, V. Internal forces during object manipulation. *Experimental Brain Research*, 2005. **165**(1): p. 69.
- [46] Gao, F., Latash, M.L., and Zatsiorsky, V.M. Internal forces during object manipulation. *Exp Brain Res*, 2005. **165**(1): p. 69-83.
- [47] Gao, F., Latash, M.L., and Zatsiorsky, V.M. Control of finger force direction in the flexion-extension plane. *Exp Brain Res*, 2005. **161**(3): p. 307-15.
- [48] Gao, F., Ren, Y., *et al*. Effects of repeated ankle stretching on calf muscle-tendon and ankle biomechanical properties in stroke survivors. *Clin Biomech (Bristol, Avon)*, 2011. **26**(5): p. 516-22.
- [49] Garcia-Elias, M., An, K.N., *et al*. Extensor mechanism of the fingers. II. Tensile properties of components. *J Hand Surg [Am]*, 1991. **16**(6): p. 1136-40.
- [50] Gentilucci, M., Caselli, L., and Secchi, C. Finger control in the tripod grasp. *Experimental Brain Research*, 2003. **149**(3): p. 351.
- [51] Georgopoulos, A.P., Pellizzer, G., *et al*. Neural coding of finger and wrist movements. *J Comput Neurosci*, 1999. **6**(3): p. 279-88.
- [52] Goodman, S.R. and Latash, M.L. Feed-forward control of a redundant motor system. *Biol Cybern*, 2006. **95**(3): p. 271-80.
- [53] Goodwin, A., Jenmalm, P., and Johansson, R. Control of grip force when tilting objects: effect of curvature of grasped surfaces and applied tangential torque. *J Neurosci*, 1998. **18**(24): p. 10724-34.
- [54] Gordon, A.M., Forssberg, H., *et al*. Visual size cues in the programming of manipulative forces during precision grip. *Exp Brain Res*, 1991. **83**(3): p. 477-82.

- [55] Gordon, A.M., Forssberg, H., *et al.* Development of human precision grip. III. Integration of visual size cues during the programming of isometric forces. *Exp Brain Res*, 1992. **90**(2): p. 399-403.
- [56] Gordon, A.M., Westling, G., *et al.* Memory representations underlying motor commands used during manipulation of common and novel objects. *J Neurophysiol*, 1993. **69**(6): p. 1789-96.
- [57] Gordon, A.M., Ingvarsson, P.E., and Forssberg, H. Anticipatory control of manipulative forces in Parkinson's disease. *Exp Neurol*, 1997. **145**(2 Pt 1): p. 477-88.
- [58] Gorniak, S., Zatsiorsky, V., and Latash, M. Hierarchical control of static prehension: II. Multi-digit synergies. *Experimental Brain Research*, 2009. **194**(1): p. 1.
- [59] Gorniak, S.L., Zatsiorsky, V.M., and Latash, M.L. Hierarchical control of static prehension: I. Biomechanics. *Exp Brain Res*, 2009. **193**(4): p. 615-31.
- [60] Gorniak, S.L., Zatsiorsky, V.M., and Latash, M.L. Manipulation of a fragile object. *Exp Brain Res*, 2010. **202**(2): p. 413-30.
- [61] Gracco, V.L. and Abbs, J.H. Variant and invariant characteristics of speech movements. *Exp Brain Res*, 1986. **65**(1): p. 156-66.
- [62] Gutman, S.R., Latash, M.L., *et al.* Kinematic description of variability of fast movements: analytical and experimental approaches. *Biol Cybern*, 1993. **69**(5-6): p. 485-92.
- [63] Hager-Ross, C., Cole, K.J., and Johansson, R.S. Grip-force responses to unanticipated object loading: load direction reveals body- and gravity-referenced intrinsic task variables. *Exp Brain Res*, 1996. **110**(1): p. 142-50.
- [64] Hager-Ross, C. and Schieber, M.H. Quantifying the independence of human finger movements: comparisons of digits, hands, and movement frequencies. *J Neurosci*, 2000. **20**(22): p. 8542-50.
- [65] Hatze, H. The inverse dynamics problem of neuromuscular control. *Biol Cybern*, 2000. **82**(2): p. 133-41.
- [66] Hazelton, F.T., Smidt, G.L., *et al.* The influence of wrist position on the force produced by the finger flexors. *J Biomech*, 1975. **8**(5): p. 301-6.
- [67] Hershkovitz, M., Tasch, U., and Teboulle, M. Toward a formulation of the human grasping quality sense. *J Robot Syst*, 1995. **12**(4): p. 249-256.
- [68] Hershkovitz, M., Tasch, U., *et al.* Experimental Validation of an Optimization Formulation of the Human Grasping Quality Sense. *Journal of Robotic Systems*, 1997. **14**(11): p. 753-766.
- [69] Hogan, N. An organizing principle for a class of voluntary movements. *J Neurosci*, 1984. **4**(11): p. 2745-54.
- [70] Hogan, N. and Sternad, D. On rhythmic and discrete movements: reflections, definitions and implications for motor control. *Exp Brain Res*, 2007. **181**(1): p. 13-30.
- [71] Hong, S.L., Lee, M.H., and Newell, K.M. Magnitude and structure of isometric force variability: mechanical and neurophysiological influences. *Motor Control*, 2007. **11**(2): p. 119-35.
- [72] Hore, J., Watts, S., *et al.* Control of finger grip forces in overarm throws made by skilled throwers. *J Neurophysiol*, 2001. **86**(6): p. 2678-89.

- [73] Ingram, J.N., Kording, K.P., *et al.* The statistics of natural hand movements. *Exp Brain Res*, 2008. **188**(2): p. 223-36.
- [74] Jindrich, D., Zhou, Y., *et al.* Non-linear viscoelastic models predict fingertip pulp force-displacement characteristics during voluntary tapping. *Journal of Biomechanics*, 2003. **36**(4): p. 497.
- [75] Jinji, T. and Sakurai, S. Direction of spin axis and spin rate of the pitched baseball. *Sports Biomech*, 2006. **5**(2): p. 197-214.
- [76] Johansson, R.S. and Westling, G. Roles of glabrous skin receptors and sensorimotor memory in automatic control of precision grip when lifting rougher or more slippery objects. *Exp Brain Res*, 1984. **56**(3): p. 550-64.
- [77] Johansson, R.S. and Cole, K.J. Sensory-motor coordination during grasping and manipulative actions. *Curr Opin Neurobiol*, 1992. **2**(6): p. 815-23.
- [78] Johansson, R.S., Hager, C., and Riso, R. Somatosensory control of precision grip during unpredictable pulling loads. II. Changes in load force rate. *Exp Brain Res*, 1992. **89**(1): p. 192-203.
- [79] Johansson, R.S. and Cole, K.J. Grasp stability during manipulative actions. *Can J Physiol Pharmacol*, 1994. **72**(5): p. 511-24.
- [80] Johansson, R.S. and Flanagan, J.R. Coding and use of tactile signals from the fingertips in object manipulation tasks. *Nat Rev Neurosci*, 2009. **10**(5): p. 345-59.
- [81] Johnston, J.A., Bobich, L.R., and Santello, M. Coordination of intrinsic and extrinsic hand muscle activity as a function of wrist joint angle during two-digit grasping. *Neurosci Lett*, 2010. **474**(2): p. 104-8.
- [82] Jung, M.C. and Hallbeck, M.S. The Effect of Wrist Position, Angular Velocity, and Exertion Direction on Simultaneous Maximal Grip Force and Wrist Torque Under the Isokinetic Conditions. *International Journal of Industrial Ergonomics*, 2002. **29**(3): p. 133-143.
- [83] Kao, S.Y. Carpal tunnel syndrome as an occupational disease. *J Am Board Fam Pract*, 2003. **16**(6): p. 533-42.
- [84] Kapandji, A. Biomechanics of pronation and supination of the forearm. *Hand Clin*, 2001. **17**(1): p. 111-22, vii.
- [85] Karol, S., Kim, Y.S., *et al.* Multi-finger pressing synergies change with the level of extra degrees of freedom. *Exp Brain Res*, 2010. **208**(3): p. 359-67.
- [86] Keen, D. and Fuglevand, A. Distribution of motor unit force in human extensor digitorum assessed by spike-triggered averaging and intraneural microstimulation. *Journal of neurophysiology*, 2004. **91**(6): p. 2515.
- [87] Kilbreath, S. and Gandevia, S. Independent control of the digits: changes in perceived heaviness over a wide range of force. *Exp Brain Res*, 1992. **91**(3): p. 539-42.
- [88] Kinoshita, H., Kawai, S., *et al.* Individual finger forces acting on a grasped object during shaking actions. *Ergonomics*, 1996. **39**(2): p. 243-56.
- [89] Kinoshita, H., Murase, T., and Bandou, T. Grip posture and forces during holding cylindrical objects with circular grips. *Ergonomics*, 1996. **39**(9): p. 1163-1176.
- [90] Kinoshita, H., Murase, T., and Bandou, T. Grip posture and forces during holding cylindrical objects with circular grips. *Ergonomics*, 1996. **39**(9): p. 1163-76.

- [91] Kinoshita, H., Backstrom, L., *et al.* Tangential torque effects on the control of grip forces when holding objects with a precision grip. *J Neurophysiol*, 1997. **78**(3): p. 1619-30.
- [92] Kleinholdermann, U., Brenner, E., *et al.* Grasping trapezoidal objects. *Exp Brain Res*, 2007. **180**(3): p. 415-20.
- [93] Kong, Y.K., Lowe, B.D., *et al.* Evaluation of handle design characteristics in a maximum screwdriving torque task. *Ergonomics*, 2007. **50**(9): p. 1404-18.
- [94] Kruger, E.S., Hoopes, J.A., *et al.* Error compensation during finger force production after one- and four-finger voluntarily fatiguing exercise. *Exp Brain Res*, 2007. **181**(3): p. 461-8.
- [95] Kubo, K., Kanehisa, H., *et al.* Influence of static stretching on viscoelastic properties of human tendon structures in vivo. *J Appl Physiol*, 2001. **90**(2): p. 520-7.
- [96] Kuo, L.C., Chang, J.H., *et al.* Jar-opening challenges. Part 2: estimating the force-generating capacity of thumb muscles in healthy young adults during jar-opening tasks. *Proc Inst Mech Eng H*, 2009. **223**(5): p. 577-88.
- [97] Kutluhan, S., Akhan, G., *et al.* Carpal tunnel syndrome in carpet workers. *Int Arch Occup Environ Health*, 2001. **74**(6): p. 454-7.
- [98] Kuznetsov, N.A. and Riley, M.A. Spatial resolution of visual feedback affects variability and structure of isometric force. *Neurosci Lett*, 2010. **470**(2): p. 121-5.
- [99] Landsmeer, J.M. and Long, C. The mechanism of finger control, based on electromyograms and location analysis. *Acta Anat (Basel)*, 1965. **60**(3): p. 330-47.
- [100] Lang, C. and Schieber, M. Differential impairment of individuated finger movements in humans after damage to the motor cortex or the corticospinal tract. *Journal of neurophysiology*, 2003. **90**(2): p. 1160.
- [101] Latash, M. There is no motor redundancy in human movements. There is motor abundance. *Motor Control*, 2000. **4**(3): p. 259-60.
- [102] Latash, M., Synergy. 1 ed. 2008: Oxford University Press.
- [103] Latash, M. and Zatsiorsky, V. Multi-finger prehension: control of a redundant mechanical system. *Advances in Experimental Medicine and Biology*, 2009.
- [104] Latash, M.L., Scholz, J.F., *et al.* Structure of motor variability in marginally redundant multifinger force production tasks. *Experimental Brain Research*, 2001. **141**(2): p. 153.
- [105] Latash, M.L., Li, S., *et al.* Central mechanisms of finger interaction during one- and two-hand force production at distal and proximal phalanges. *Brain Res*, 2002. **924**(2): p. 198-208.
- [106] Latash, M.L., Scholz, J.F., *et al.* Finger coordination during discrete and oscillatory force production tasks. *Exp Brain Res*, 2002. **146**(4): p. 419-32.
- [107] Latash, M.L., Scholz, J.P., and Schoner, G. Motor control strategies revealed in the structure of motor variability. *Exerc Sport Sci Rev*, 2002. **30**(1): p. 26-31.
- [108] Latash, M.L., Shim, J.K., *et al.* Rotational equilibrium during multi-digit pressing and prehension. *Motor Control*, 2004. **8**(4): p. 392-404.
- [109] Latash, M.L., Shim, J.K., *et al.* A central back-coupling hypothesis on the organization of motor synergies: a physical metaphor and a neural model. *Biol Cybern*, 2005. **92**(3): p. 186-91.

- [110] Latash, M.L. and Zatsiorsky, V.M. Multi-finger prehension: control of a redundant mechanical system. *Adv Exp Med Biol*, 2009. **629**: p. 597-618.
- [111] Lee, J.W. and Rim, K. Measurement of finger joint angles and maximum finger forces during cylinder grip activity. *Journal of Biomedical Engineering*, 1991. **13**(2): p. 152-62.
- [112] Leijnse, J.N., Campbell-Kyureghyan, N.H., *et al.* Assessment of individual finger muscle activity in the extensor digitorum communis by surface EMG. *J Neurophysiol*, 2008. **100**(6): p. 3225-35.
- [113] Li, Z.M., Latash, M.L., *et al.* Motor redundancy during maximal voluntary contraction in four-finger tasks. *Exp Brain Res*, 1998. **122**(1): p. 71-8.
- [114] Li, Z.M., Latash, M.L., and Zatsiorsky, V.M. Force sharing among fingers as a model of the redundancy problem. *Exp Brain Res*, 1998. **119**(3): p. 276-86.
- [115] Li, Z.M., Zatsiorsky, V.M., and Latash, M.L. Contribution of the extrinsic and intrinsic hand muscles to the moments in finger joints. *Clinical Biomechanics*, 2000. **15**(3): p. 203-11.
- [116] Li, Z.M. The influence of wrist position on individual finger forces during forceful grip. *J Hand Surg [Am]*, 2002. **27**(5): p. 886-96.
- [117] Li, Z.M. The influence of wrist position on individual finger forces during forceful grip. *J Hand Surg Am*, 2002. **27**(5): p. 886-96.
- [118] Liang, N., Takahashi, M., *et al.* Effects of intermanual transfer induced by repetitive precision grip on input-output properties of untrained contralateral limb muscles. *Exp Brain Res*, 2007. **182**(4): p. 459-67.
- [119] Lin, J.H. and McGorry, R.W. Predicting subjective perceptions of powered tool torque reactions. *Appl Ergon*, 2009. **40**(1): p. 47-55.
- [120] Lodha, N., Naik, S.K., *et al.* Force control and degree of motor impairments in chronic stroke. *Clin Neurophysiol*, 2010. **121**(11): p. 1952-61.
- [121] Long, C., Conrad, P.W., *et al.* Intrinsic-extrinsic muscle control of the hand in power grip and precision handling. *Journal of Bone and Joint Surgery*, 1970. **52-A**: p. 853-867.
- [122] Lukos, J., Ansuini, C., and Santello, M. Choice of contact points during multidigit grasping: effect of predictability of object center of mass location. *J Neurosci*, 2007. **27**(14): p. 3894-903.
- [123] Macefield, V.G., Hagerross, C., and Johansson, R.S. Control of Grip Force During Restraint of an Object Held Between Finger and Thumb: Responses of Cutaneous Afferents From the Digits. *Experimental Brain Research*, 1996. **108**(1): p. 155-171.
- [124] Macefield, V.G. and Johansson, R.S. Control of grip force during restraint of an object held between finger and thumb: responses of muscle and joint afferents from the digits. *Exp Brain Res*, 1996. **108**(1): p. 172-84.
- [125] Mason, M.T. and Salisbury, K.J., *Robot Hands and the Mechanics of Manipulation (Artificial Intelligence)*. 1985, Cambridge, MA: MIT Press.
- [126] McIsaac, T. and Fuglevand, A. Motor-unit synchrony within and across compartments of the human flexor digitorum superficialis. *Journal of neurophysiology*, 2007. **97**(1): p. 550.
- [127] Mogk, J.P. and Keir, P.J. The effects of posture on forearm muscle loading during gripping. *Ergonomics*, 2003. **46**(9): p. 956-75.



- [128] Mrotek, L.A., Hart, B.A., *et al.* Grip responses to object load perturbations are stimulus and phase sensitive. *Exp Brain Res*, 2004. **155**(4): p. 413-20.
- [129] Muratori, L., McIsaac, T., *et al.* Impaired anticipatory control of force sharing patterns during whole-hand grasping in Parkinson's disease. *Experimental Brain Research*, 2008. **185**(1): p. 41.
- [130] Mussa Ivaldi, F.A., Morasso, P., and Zaccaria, R. Kinematic networks. A distributed model for representing and regularizing motor redundancy. *Biol Cybern*, 1988. **60**(1): p. 1-16.
- [131] Naiper, J.R. The prehensile movements of the human hand. *J Bone Joint Surg*, 1956. **38B**(4): p. 902-913.
- [132] Nakazawa, N., Ikeura, R., and Inooka, H. Characteristics of human fingertips in the shearing direction. *Biol Cybern*, 2000. **8**(3): p. 207-14.
- [133] Nelson, W.L. Physical principles for economies of skilled movements. *Biol Cybern*, 1983. **46**(2): p. 135-47.
- [134] Neter, J., Kutner, M., *et al.*, Applied linear statistical models. 1996.
- [135] Newell, K., Carlton, L., and Hancock, P. A kinetic analysis of response variability. *Psychological Bulletin*, 1984. **96**: p. 133-151.
- [136] Newell, K. and Carlton, L. Force variability in isometric responses. *Journal of Experimental Psychology: Human Perception and Performance*, 1988. **14**: p. 37-44.
- [137] Nguyen, P.T.A. and Arimoto, S., *Dexterous manipulation of an object by means of multi-DOF robotic fingers with soft tips*. 2002. p. 349-362.
- [138] Niu, X., Latash, M., and Zatsiorsky, V. Effects of grasping force magnitude on the coordination of digit forces in multi-finger prehension. *Experimental Brain Research*, 2009. **194**(1): p. 115.
- [139] Nowak, D.A. and Hermsdorfer, J. Selective deficits of grip force control during object manipulation in patients with reduced sensibility of the grasping digits. *Neurosci Res*, 2003. **47**(1): p. 65-72.
- [140] Nowak, D.A., Topka, H., *et al.* The beneficial effects of subthalamic nucleus stimulation on manipulative finger force control in Parkinson's disease. *Exp Neurol*, 2005. **193**(2): p. 427-36.
- [141] Ofori, E., Samson, J.M., and Sosnoff, J.J. Age-related differences in force variability and visual display. *Exp Brain Res*, 2010. **203**(2): p. 299-306.
- [142] Olafsdottir, H., Zatsiorsky, V., and Latash, M. Is the thumb a fifth finger? A study of digit interaction during force production tasks. *Experimental Brain Research*, 2005. **160**(2): p. 203.
- [143] Olafsdottir, H., Zatsiorsky, V.M., and Latash, M.L. Is the thumb a fifth finger? A study of digit interaction during force production tasks. *Exp Brain Res*, 2005. **160**(2): p. 203-13.
- [144] Oldfield, R.C. The assessment and analysis of handedness: the Edinburgh inventory. *Neuropsychologia*, 1971. **9**(1): p. 97-113.
- [145] Pare, M., Carnahan, H., and Smith, A.M. Magnitude Estimation of Tangential Force Applied to the Fingerpad. *Experimental Brain Research*, 2002. **142**(3): p. 342-348.

- [146] Pataky, T., Latash, M., and Zatsiorsky, V. Tangential load sharing among fingers during prehension. *Ergonomics*, 2004. **47**(8): p. 876-89.
- [147] Pataky, T. Soft tissue strain energy minimization: a candidate control scheme for intra-finger normal-tangential force coordination. *Journal of Biomechanics*, 2005. **38**(8): p. 1723.
- [148] Pataky, T.C., Latash, M.L., and Zatsiorsky, V.M. Prehension synergies during nonvertical grasping, I: experimental observations. *Biol Cybern*, 2004. **91**(3): p. 148-58.
- [149] Pataky, T.C., Latash, M.L., and Zatsiorsky, V.M. Prehension synergies during nonvertical grasping, II: Modeling and optimization. *Biol Cybern*, 2004. **91**(4): p. 231-42.
- [150] Pataky, T.C., Slota, G.P., *et al.* Radial force distribution changes associated with tangential force production in cylindrical grasping, and the importance of anatomical registration. *J Biomech*, 2012. **45**(2): p. 218-24.
- [151] Penfield, W. and Boldrey, E. Somatic motor and sensory representation in the cerebral cortex of man as studied by electrical stimulation. *Brain*, 1937. **60**: p. 389-443.
- [152] Penfield, W. and Flanigin, H. Surgical therapy of temporal lobe seizures. *AMA Arch Neurol Psychiatry*, 1950. **64**(4): p. 491-500.
- [153] Pincus, S.M. Approximate entropy as a measure of system complexity. *Proc Natl Acad Sci U S A*, 1991. **88**(6): p. 2297-301.
- [154] Poston, B., Danna-Dos Santos, A., *et al.* Force-independent distribution of correlated neural inputs to hand muscles during three-digit grasping. *J Neurophysiol*, 2010.
- [155] Pouydebat, E., Gorce, P., *et al.* Biomechanical study of grasping according to the volume of the object: human versus non-human primates. *J Biomech*, 2009. **42**(3): p. 266-72.
- [156] Radhakrishnan, S. and Nagaravindra, M. Analysis of hand forces in health and disease during maximum isometric grasping of cylinders. *Med Biol Eng Comput*, 1993. **31**(4): p. 372-6.
- [157] Rao, J.S. and Sengupta, A., Topics in circular statistics. 2001, River Edge, NJ: World Scientific Publishers.
- [158] Rearick, M.P. and Santello, M. Force synergies for multifingered grasping: effect of predictability in object center of mass and handedness. *Exp Brain Res*, 2002. **144**(1): p. 38-49.
- [159] Reilly, K., Nordstrom, M., and Schieber, M. Short-term synchronization between motor units in different functional subdivisions of the human flexor digitorum profundus muscle. *Journal of neurophysiology*, 2004. **92**(2): p. 734.
- [160] Reilly, K.T. and Hammond, G.R. Independence of force production by digits of the human hand. *Neurosci Lett*, 2000. **290**(1): p. 53-6.
- [161] Saleh, M., Takahashi, K., *et al.* Encoding of coordinated grasp trajectories in primary motor cortex. *J Neurosci*, 2010. **30**(50): p. 17079-90.
- [162] Salimi, I., Hollender, I., *et al.* Specificity of internal representations underlying grasping. *J Neurophysiol*, 2000. **84**(5): p. 2390-7.
- [163] Sancho-Bru, J.L., Perez-Gonzalez, A., *et al.* A 3D biomechanical model of the hand for power grip. *J Biomech Eng*, 2003. **125**(1): p. 78-83.

- [164] Santello, M. and Soechting, J.F. Gradual molding of the hand to object contours. *J Neurophysiol*, 1998. **79**(3): p. 1307-20.
- [165] Santello, M. and Soechting, J.F. Force synergies for multifingered grasping. *Exp Brain Res*, 2000. **133**(4): p. 457-67.
- [166] Schieber, M. Individuated finger movements of rhesus monkeys: a means of quantifying the independence of the digits. *J Neurophysiol*, 1991. **65**(6): p. 1381-91.
- [167] Schieber, M. and Santello, M. Hand function: peripheral and central constraints on performance. *Journal of applied physiology*, 2004. **96**(6): p. 2293.
- [168] Schieber, M.H. and Hibbard, L.S. How somatotopic is the motor cortex hand area? *Science*, 1993. **261**(5120): p. 489-92.
- [169] Schieber, M.H. Constraints on somatotopic organization in the primary motor cortex. *J Neurophysiol*, 2001. **86**(5): p. 2125-43.
- [170] Scholz, J.P. and Schoner, G. The uncontrolled manifold concept: identifying control variables for a functional task. *Exp Brain Res*, 1999. **126**(3): p. 289-306.
- [171] Scholz, J.P., Danion, F., *et al.* Understanding finger coordination through analysis of the structure of force variability. *Biol Cybern*, 2002. **86**(1): p. 29-39.
- [172] Schoner, G. and Kelso, J.A. Dynamic pattern generation in behavioral and neural systems. *Science*, 1988. **239**(4847): p. 1513-20.
- [173] Seo, N.J., Armstrong, T.J., *et al.* The effect of torque direction and cylindrical handle diameter on the coupling between the hand and a cylindrical handle. *J Biomech*, 2007. **40**(14): p. 3236-43.
- [174] Seo, N.J. and Armstrong, T.J. Investigation of grip force, normal force, contact area, hand size, and handle size for cylindrical handles. *Hum Factors*, 2008. **50**(5): p. 734-44.
- [175] Seo, N.J. Dependence of safety margins in grip force on isometric push force levels in lateral pinch. *Ergonomics*, 2009. **52**(7): p. 840-7.
- [176] Serina, E.R., Mote, C.D., Jr., and Rempel, D. Force response of the fingertip pulp to repeated compression--effects of loading rate, loading angle and anthropometry. *J Biomech*, 1997. **30**(10): p. 1035-40.
- [177] Shih, Y.C. and Wang, M.J. The influence of gloves during maximum volitional torque exertion of supination. *Ergonomics*, 1997. **40**(4): p. 465-75.
- [178] Shim, J., Latash, M., and Zatsiorsky, V. Finger coordination during moment production on a mechanically fixed object. *Experimental Brain Research*, 2004. **157**(4): p. 457.
- [179] Shim, J., Latash, M., and Zatsiorsky, V. Prehension synergies: trial-to-trial variability and principle of superposition during static prehension in three dimensions. *Journal of neurophysiology*, 2005. **93**(6): p. 3649.
- [180] Shim, J., Latash, M., and Zatsiorsky, V. Prehension synergies in three dimensions. *Journal of neurophysiology*, 2005. **93**(2): p. 766.
- [181] Shim, J. and Park, J. Prehension synergies: principle of superposition and hierarchical organization in circular object prehension. *Experimental Brain Research*, 2007. **180**(3): p. 541.

- [182] Shim, J.K., Latash, M.L., and Zatsiorsky, V.M. Prehension synergies: trial-to-trial variability and hierarchical organization of stable performance. *Exp Brain Res*, 2003. **152**: p. 173-184.
- [183] Shim, J.K., Latash, M.L., and Zatsiorsky, V.M. The human central nervous system needs time to organize task-specific covariation of finger forces. *Neurosci Lett*, 2003. **353**(1): p. 72-4.
- [184] Shim, J.K., Latash, M.L., and Zatsiorsky, V.M. Finger coordination during moment production on a mechanically fixed object. *Exp Brain Res*, 2004. **157**(4): p. 457-67.
- [185] Shim, J.K., Lay, B.S., *et al.* Age-related changes in finger coordination in static prehension tasks. *J Appl Physiol*, 2004.
- [186] Shim, J.K., Latash, M.L., and Zatsiorsky, V.M. Prehension synergies in three dimensions. *J Neurophysiol*, 2005. **93**(2): p. 766-76.
- [187] Shim, J.K., Latash, M.L., and Zatsiorsky, V.M. Prehension synergies: trial-to-trial variability and principle of superposition during static prehension in three dimensions. *J Neurophysiol*, 2005. **93**(6): p. 3649-58.
- [188] Shim, J.K., Olafsdottir, H., *et al.* The emergence and disappearance of multi-digit synergies during force-production tasks. *Exp Brain Res*, 2005. **164**(2): p. 260-70.
- [189] Shim, J.K., Huang, J., *et al.* Multi-digit maximum voluntary torque production on a circular object. *Ergonomics*, 2007. **50**(5): p. 660-75.
- [190] Shim, J.K., Oliveira, M.A., *et al.* Hand digit control in children: age-related changes in hand digit force interactions during maximum flexion and extension force production tasks. *Exp Brain Res*, 2007. **176**(2): p. 374-86.
- [191] Shim, J.K., Hsu, J., *et al.* Strength training increases training-specific multifinger coordination in humans. *Motor Control*, 2008. **12**(4): p. 311-29.
- [192] Shim, J.K., Karol, S., *et al.* Hand digit control in children: motor overflow in multi-finger pressing force vector space during maximum voluntary force production. *Exp Brain Res*, 2008. **186**(3): p. 443-56.
- [193] Shimoga, K.B. and Goldenberg, A.A., *Soft Robotic Fingertips: Part II: Modeling and Impedance Regulation*. 1996. p. 335-350.
- [194] Shinohara, M., Li, S., *et al.* Effects of age and gender on finger coordination in MVC and submaximal force-matching tasks. *J Appl Physiol*, 2003. **94**(1): p. 259-70.
- [195] Silverstein, B.A., Fine, L.G., and Armstrong, T.J. Hand wrist cumulative trauma disorders in industry. *British Journal of Industrial Medicine*, 1986. **43**: p. 779-784.
- [196] Sitburana, O., Wu, L.J., *et al.* Motor overflow and mirror dystonia. *Parkinsonism Relat Disord*, 2009. **15**(10): p. 758-61.
- [197] Slifkin, A.B. and Newell, K.M. Variability and Noise in Continuous Force Production. *J Mot Behav*, 2000. **32**. **32**(2. 2): p. 141-150.
- [198] Smeets, J.B. and Brenner, E. A new view on grasping. *Motor control*, 1999. **3**(3): p. 237.
- [199] Smeets, J.B. and Brenner, E. Independent movements of the digits in grasping. *Exp Brain Res*, 2001. **139**(1): p. 92-100.
- [200] Sosnoff, J.J., Valantine, A.D., and Newell, K.M. Independence between the amount and structure of variability at low force levels. *Neurosci Lett*, 2006. **392**(3): p. 165-9.

- [201] Sternad, D., Dean, W.J., and Newell, K.M. Force and timing variability in rhythmic unimanual tapping. *J Mot Behav*, 2000. **32**(3): p. 249-67.
- [202] Sternad, D., Wei, K., *et al.* Intermanual interactions during initiation and production of rhythmic and discrete movements in individuals lacking a corpus callosum. *Exp Brain Res*, 2007. **176**(4): p. 559-74.
- [203] Tanaka, T., Amadio, P.C., *et al.* Flexor digitorum profundus tendon tension during finger manipulation. *J Hand Ther*, 2005. **18**(3): p. 330-8; quiz 338.
- [204] Todorov, E. and Jordan, M.I. Optimal feedback control as a theory of motor coordination. *Nat Neurosci*, 2002. **5**(11): p. 1226-35.
- [205] Todorov, E. Optimality principles in sensorimotor control. *Nat Neurosci*, 2004. **7**(9): p. 907-15.
- [206] Uno, Y., Kawato, M., and Suzuki, R. Formation and control of optimal trajectory in human multijoint arm movement. Minimum torque-change model. *Biol Cybern*, 1989. **61**(2): p. 89-101.
- [207] Uygur, M., de Freitas, P.B., and Jaric, S. Effects of varying the load force range and frequency on force coordination in static manipulation. *Neurosci Lett*, 2010. **475**(2): p. 115-9.
- [208] Vaillancourt, D.E. and Russell, D.M. Temporal capacity of short-term visuomotor memory in continuous force production. *Exp Brain Res*, 2002. **145**(3): p. 275-85.
- [209] Vaillancourt, D.E., Slifkin, A.B., and Newell, K.M. Inter-digit Individuation and Force Variability in the Precision Grip of Young, Elderly, and Parkinson's Disease Participants. *Motor Control*, 2002. **6**(2): p. 113-28.
- [210] Valero-Cuevas, F. An integrative approach to the biomechanical function and neuromuscular control of the fingers. *Journal of Biomechanics*, 2005. **38**(4): p. 673.
- [211] Van Doren, C.L. Grasp stiffness as a function of grasp force and finger span. *Motor control*, 1998. **2**(4): p. 352.
- [212] Vereijken, B., Whiting, H.T., and Beek, W.J. A dynamical systems approach to skill acquisition. *Q J Exp Psychol A*, 1992. **45**(2): p. 323-44.
- [213] Voorbij, A.I. and Steenbekkers, L.P. The twisting force of aged consumers when opening a jar. *Appl Ergon*, 2002. **33**(1): p. 105-9.
- [214] Wei, S.H., Huang, S., *et al.* Wrist kinematic characterization of wheelchair propulsion in various seating positions: implication to wrist pain. *Clin Biomech (Bristol, Avon)*, 2003. **18**(6): p. S46-52.
- [215] Werner, D., Kozin, S.H., *et al.* The biomechanical properties of the finger metacarpophalangeal joints to varus and valgus stress. *J Hand Surg Am*, 2003. **28**(6): p. 1044-51.
- [216] Werremeyer, M. and Cole, K. Wrist action affects precision grip force. *J Neurophysiol*, 1997. **78**(1): p. 271-80.
- [217] Westling, G. and Johansson, R.S. Factors influencing the force control during precision grip. *Exp Brain Res*, 1984. **53**(2): p. 277-84.
- [218] Wheat, H., Salo, L., and Goodwin, A. Cutaneous afferents from the monkeys fingers: responses to tangential and normal forces. *Journal of neurophysiology*, 2009.

- [219] Winges, S., Eonta, S., *et al.* Effects of object compliance on three-digit grasping. *Journal of neurophysiology*, 2009. **101**(5): p. 2447.
- [220] Winges, S.A., Soechting, J.F., and Flanders, M. Multidigit control of contact forces during transport of handheld objects. *J Neurophysiol*, 2007. **98**(2): p. 851-60.
- [221] Winstein, C.J., Abbs, J.H., and Petashnick, D. Influences of object weight and instruction on grip force adjustments. *Exp Brain Res*, 1991. **87**(2): p. 465-9.
- [222] Winter, D.A., Coordination of motor tasks in human gait, in *Perspectives on the Coordination of Movement*, S.A. Wallace, Editor. 1989, Elsevier: Amsterdam. p. 329-363.
- [223] Wolpert, D.M. and Ghahramani, Z. Computational principles of movement neuroscience. *Nat Neurosci*, 2000. **3 Suppl**: p. 1212-7.
- [224] Zatsiorsky, V., *Kinetics of Human Motion*. 2002, Champaign, IL: Human Kinetics.
- [225] Zatsiorsky, V., Gao, F., and Latash, M. Motor control goes beyond physics: differential effects of gravity and inertia on finger forces during manipulation of hand-held objects. *Experimental Brain Research*, 2005. **162**(3): p. 300.
- [226] Zatsiorsky, V.M., Li, Z.M., and Latash, M.L. Coordinated force production in multi-finger tasks: finger interaction and neural network modeling. *Biol Cybern*, 1998. **79**(2): p. 139-50.
- [227] Zatsiorsky, V.M., Gregory, R.W., and Latash, M.L. Force and torque production in static multifinger prehension: biomechanics and control. I. Biomechanics. *Biol Cybern*, 2002. **87**(1): p. 50-7.
- [228] Zatsiorsky, V.M. *Kinetics of Human Motion*. Champaign, IL: Human Kinetics, 2002.
- [229] Zhang, W., Zatsiorsky, V., and Latash, M. Accurate production of time-varying patterns of the moment of force in multi-finger tasks. *Experimental Brain Research*, 2006. **175**(1): p. 68.
- [230] Zhang, W., Zatsiorsky, V., and Latash, M. Finger synergies during multi-finger cyclic production of moment of force. *Experimental Brain Research*, 2007. **177**(2): p. 243.
- [231] Zhang, W., Gordon, A.M., *et al.* Manipulation after object rotation reveals independent sensorimotor memory representations of digit positions and forces. *J Neurophysiol*, 2010. **103**(6): p. 2953-64.